

CHAPTER ONE

INTRODUCTION

1.1 BACKGROUND OF THE STUDY

In recent years, there has been an increasing demand in mobile communication services with limited spectrum bandwidth. Wide-band Code Division Multiple Access (W-CDMA) is a spread spectrum technique that allows a large number of users to share access to a single communication channel by encoding their data with a special pseudo noise (PN) code for each channel [1], W-CDMA cellular systems use a form of direct sequence CDMA (DS-CDMA).

W-CDMA offers many advantages which include jam resistance, privacy and flexibility. CDMA has been considered and recognized as a viable alternative to both FDMA and TDMA[2]. W-CDMA schemes have many advantages over FDMA and TDMA but these advantages are hindered by the increasing interference caused by other active terminals, since all signals in the W-CDMA system share the same transmission bandwidth. Blocking occurs when the tolerance limit to interference is exceeded, hence in W-CDMA, the level of interference is a limiting factor [2]. Consider a receiver and two terminals (transmitters) with one closer to the receiver and the other farther away. If they transmit simultaneously at equal powers, then the receiver will receive more power from the nearest transmitter. Since one's transmitted signal is the other's noise, the signal-to-noise ratio(SNR) for the farther transmitter is much lower. If the nearest transmitter transmits a signal of magnitude higher than the farther transmitter, then the SNR for the latter may be below detection and may as well not transmit. This effectively distorts the communication channel.

This problem is commonly solved by dynamic modulation and dynamic output power adjustment of the transmitters [2]. That is, the nearest

transmitter uses less power and higher order modulation techniques so that the SNR for all transmitters at the receiver is roughly the same. This sometimes can have a noticeable impact on hand set battery life, which varies depending on distance from the base station.

In high-noise situations, closer transmitters may boost their output power, which forces distance transmitters to boost their output to maintain a good SNR, and other transmitter react to the rising noise floor by increasing their output. This process continues, and eventually, distant transmitters lose their ability to maintain a useable SNR and drop from the network. If there are optimum numbers of active terminals, when noise and out-of-cell interference are negligible, the transmitter power levels should be controlled to achieve power balancing. Throughput, which is the rate of average message delivery over a communication channels, is affected by this near far problem. With power balancing, all signals arrive at the base station with equal power. On the other hand, when noise and interference from other cells are not negligible, the power optimization problem is more complicated. The optimum set of transmitter powers depends on the maximum achievable SNR of the terminals, say N , and the optimum received power levels are unequal. In the research work [3], observe that in order to reduce base station bit error rate with any power control algorithm, the number of active transmitters, N , should be limited to $N \leq N^*$, where N^* is a property of the frame success function. It maintains the systems bit error rate when the signals of the transmitting terminals arrive at the receiver with equal power.

The specific form of the frame success function depends on the details of the W-CDMA transmission system parameters which include the bandwidth, packet size, modem configuration, channel coding, antennas, modulation and radio propagation details. To enhance the quality of the system, there is a need to maintain the throughput and the bit error rate W-

CDMA of a network by finding the transmitter power level and Modulation techniques given a number of terminals transmitting simultaneously. This can be achieved through study of Network Spectrum management such as: Total transmit power, Received Signal Strength (RSS), Antenna tilt, Antenna height, Total bandwidth, individual quality of service requirement, transmitter power control and adaptive modulation which is the goal of the study. Imo State is used for the real testing environment with MTN Nigeria; an adopted or simplified approach for throughput and bit error rate problem is to assume continuous rate and power assignments, at the expense of an approximate solution [4]. This method is valid because throughput and bit error rate is continuously distributed over time and improves with continuous power assignments. The benchmark of what a system is capable of doing or its maximum performance is what the user or designer is interested in. Bit error rate and throughput are the performance metrics and a key measure of the quality of wireless data link. Throughput is the average rate of successful message delivery over a communication channel and one would naturally like this quality to be high as possible when browsing or downloading large files. This research will help to improve the quality of services of W-CDMA network operators in Nigeria [4]. Again theoretical analysis is a very important key to ensuring correct implementation in any system. This research will go a long way to ensure easy and correct implementation of future generation systems (as W-CDMA has been accepted as a key component of worldwide 3G systems).

1.2 PROBLEM STATEMENT

This dissertation examines the benefits of using adaptive modulation in terms of spectral efficiency and probability of bit error in a real radio networks environment. In channels that fluctuate dynamically over time, systems that are based upon the conventional methods of fixed modulation formats do not perform well. Adaptive modulation provides many parameters that can be adjusted relative to the channel fading, including data rate, transmit power, instantaneous BER, symbol rate, and channel code rate or scheme. In this thesis, a systematic study on the increase in spectral efficiency obtained by optimally varying combinations of the modulation formats for a real radio environment is provided. It has been assumed, that the transmitter has a correct knowledge of the channel conditions and the resulting adaptive modulation system is subject to an average BER constraint. Simulations show how adaptively changing the modulation schemes improve the performance of the system by meeting a BER constraint over a range of SNR.

1.3 OBJECTIVES OF THE RESEARCH

To enhance the quality of a communication system, there is a need to keep the bit error of a W- CDMA network at threshold value by finding the modulation techniques, transmitter power Levels, given that a number of terminals are transmitting simultaneously and by changing the modulation techniques simultaneously as well.

The specific objectives of the research are:

- (1) To characterize the radio environment under study (Test bed) using Received Signal Strength and then developing a mathematical model of the Environment.
- (2) To use the results/ Models obtained to modify the most widely deployed Hata Model for the test Environment.
- (3) To Evaluate the effects of noise on the bit error rate and throughput on a W- CDMA network.
- (4) To evaluation the Bit Error rate of QAM and QPSK system versus signal to noise ratio (SNR) and use the results to evaluate system for adaptive modulation.

1.4 SIGNIFICANCE OF STUDY

Due to the growing demand for high bandwidth and high speed information transfer in the communication industry, it becomes inevitable that a network that will be fast to meet to an extent the demand of different communication traffics and services is desirable. This has raised up research issues of adaptive modulation for the achievement of this purpose. This dissertation examines the benefits of using adaptive modulation in terms of spectral efficiency and probability of bit error in a real radio networks environment. In channels that fluctuate dynamically over time, systems that are based upon the conventional methods of fixed modulation formats do not perform well. Adaptive modulation provides many parameters that can be adjusted relative to the channel fading, including data rate, transmit power, instantaneous BER, symbol rate, and channel code rate or scheme.

1.5 SCOPE OF WORK

There is need for cellular systems to be equipped with mechanisms that can adapt themselves according to channel or link conditions, which will enable better utilization of the scheduled resources in a mobile environment. The existing spectrum allocations shows that to satisfy the ever increasing demand for high speed data services under resource constraints, it is essential to push the spectral efficiency to the extreme. Therefore, instead of designing systems to work in the worst or average link conditions, it is better to apply link adaptation techniques for the better utilization of the instantaneously varying link capacity. Besides improving spectral utility, they also aid in meeting the diverse QoS guarantees. Therefore, this study focuses mainly on two link adaptation mechanisms namely; adaptive modulation and power control. Later by integrating them,

the interdependency among them has been exploited to further enhance the spectral efficiency largely.

There are many wireless networks but this work is limited to wideband code division multiple access (W-CDMA) network. CDMA is a spread spectrum system and these systems have two categories : frequency hopping(FH), direct sequence (DS) etc. This work will be based on DS-CDMA network. The two modulation techniques QPSK and QAM techniques are chosen in this thesis, because these are the primary technique that will deliver higher data rate for High Speed Downlink Packet Access (HSDPA), an extension of 3G networks

1.6 THE ORGANIZATION OF THE DISSERTATION

The Dissertation is divided into six chapters. Chapter 1 introduces the content of the report by elaborating the background to investigation, Problem statement ,objectives, limitations and scope of the work. Chapter 2 reviews the literature so as to establish the background theory of the dissertation. A summary of the existing method on bit error rate and throughput parameters is also provided. Chapter 3 shows Field Measurement tools, Map, Terrain and the route to different base stations Chapter 4 Examines the performance and analysis of the results obtained in Chapter 3. Chapter 5 provides the parameters obtained at MTN classical Software Node for simulation purpose, then chapter 6 Presents the conclusion, recommendation, contribution to knowledge and future work.

CHAPTER TWO

LITERATURE REVIEW

2.1 Fixed and Adaptive modulation in wireless Communication system

This thesis focuses on the idea and concepts of adaptive modulation, which can be used in Real radio networks environment to achieve an efficient means of communication. Conventional wireless communication systems based upon fixed modulation schemes do not perform well in channels whose coefficients fluctuate randomly. By adaptively altering the modulation schemes for transmission in a radio system, a higher throughput, an acceptable Bit-Error rate, and a better quality of service can be achieved by dynamically changing channel conditions. Although rapid variations in channel conditions with respect to time pose challenges to the appropriate functioning of adaptive modulation based system, researchers believed that they are at least a step above the traditional systems based on fixed modulation formats. Figure 2.1 shows adaptive modulation in operation, nearer transmitter uses less power and higher order modulation scheme and farther transmitter uses high power and lower modulation techniques so that the SNR for all transmitters at the receiver is roughly the same. This sometimes can have a noticeable impact on hand set battery life, which varies depending on distance from the base station.

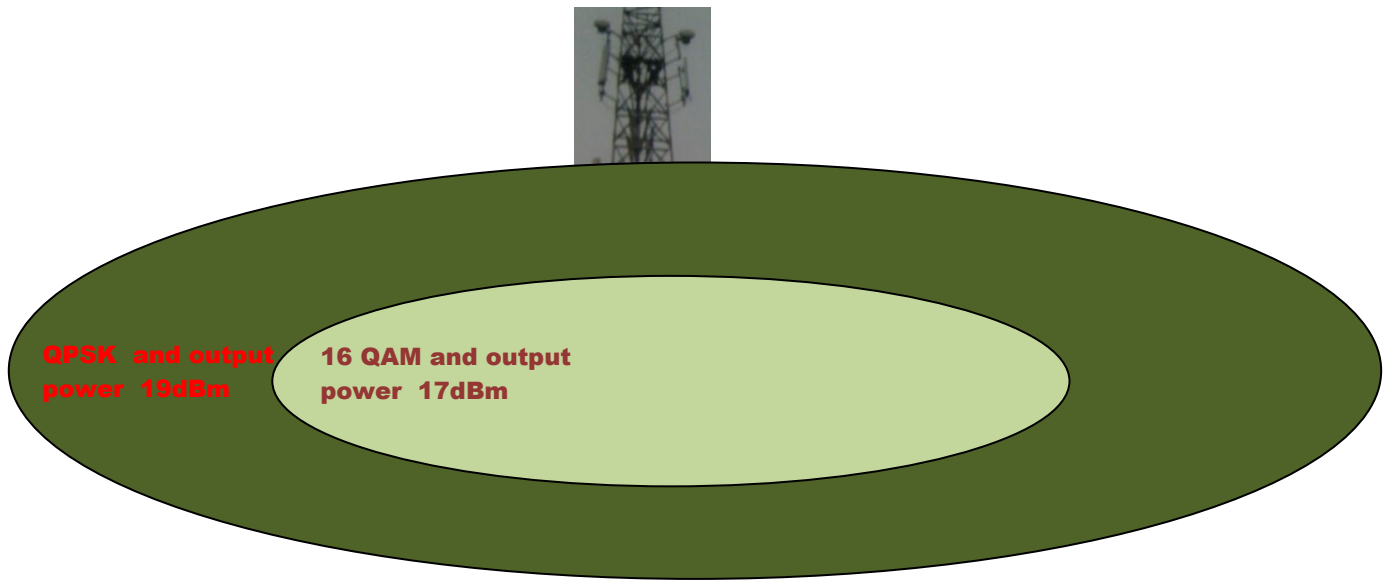


Fig 2.1 Adaptive Modulation and Coding in Operation

2.2 MOBILE WIRELESS COMMUNICATION SYSTEM

In [5], their work explained that a data source generates packets of length L bits at each terminal of a CDMA system. A forward error correction (FEC) encoder, if present and a cyclic redundancy check (CRC) encoder together expand the packet size to M bits at each terminal of a CDMA system. The data rate of the coded packet is R_s b/s. The digital modulator spreads the signal to produce R_c chips/s. The CDMA processing gain is [5]

$$G = W/R_s \text{ -----(2.1)}$$

Where W (Hz) is the system bandwidth

R_s is the data rate of the coded packets

Terminal i also contains a radio modulator and a transmitter radiating power p_i watt. The path gain from transmitter i to the base station is g_i and the signal from terminal i arrives at the base station at a received power level of [5]

$$Q_i = P_i g_i (W) \text{-----}(2.2)$$

Where P_i is the radiating power

g_i is the path gain from transmitter i to base station

The base station also receives noise and out-of-cell interference with a total power of Q^2W . The base station has N receivers, each containing a demodulator, a correlator for de-spreading the received signal, and a cyclic redundancy check decoder. Each receiver also has a channel decoder if the transmitter includes forward error correction.

In this analysis, the details of the transmission system are embodied in a mathematical function $f(y)$, which is the probability that a packet arrive at the CRC decoder without errors. The dependent variable (y) is the received SINR. For terminal i ,

$$\gamma_i = G \frac{p_i g_i}{\sum_{\substack{j=1 \\ j \neq i}}^N p_j g_j + \sigma^2} \text{-----} (2.3)$$

Substituting equation 2.2 into 2.3, obtain

$$\gamma_i = G \frac{Q_i}{\sum_{\substack{j=1 \\ j \neq i}}^N Q_j + \sigma^2} \text{-----} (2.4)$$

Messages acknowledged from the receiver inform the transmitter of errors detected at the CRC decoder that have not been corrected by the channel decoder. The transmitter employs selective-repeat retransmission of packets received in error. It is assumed in parts of this analysis that intra-cell interference dominates the total distortion and study of system performance when $\sigma^2 = 0$. When $\sigma^2 > 0$, the signal-to-noise ratio of the receiver is defined as

$$s_i = Q_i / \sigma^2 \text{-----}(2.5)$$

Substituting equation (2.5) into (2.4) gives

$$\gamma_i = G \frac{s_i}{\sum_{\substack{j=1 \\ j \neq i}}^N s_j + 1} \text{-----} (2.6)$$

If the probability of undetected error at the CRC decoder is negligible, the throughput of signal i , defined as the number of information bits per second received without error is

$$T_i = \frac{L}{M} R_s \cdot f(\gamma) \text{ b/s} \text{-----} (2.7)$$

where T_i is the throughput of terminal i (b/s)

L is the packet length (bit)

M is the packet size expanded by both FEC encoder and the CRC encoder (bit)

R_s is the packet data rate (b/s)

$f(\gamma)$ is the probability function that a packet arrives at the CRC decoder without errors.

The aggregate throughput, T_{total} , is the sum of the N individual throughput measures. Assuming that L , M , and R_s are system constants, the normalized throughput, U , is analyzed and defined

$$U = \frac{M}{LR_s} T_{total} = \sum_{i=1}^N f(\gamma_i) \text{-----} (2.8)$$

Where U is dimensionless and bounded by $0 \leq U \leq N$,

2.3 THE BIT ERROR RATE AND DATA TRANSMISSION

Bit error rate (BER) is a performance indicator that specifies the number of bits corrupted or destroyed as they are transmitted from the source to the destination

The work of [6] proved that the probability of correct decision at the receiver in the transmission of M-ary (not to be confused with the total number of bits in a frame) orthogonal equal energy signal over an AWGN channel, which are envelope detected at the receiver is given by [6]:

$$p_c = \sum_{n=0}^{M-1} (-1)^n \binom{M-1}{n} \frac{1}{n+1} \exp \left[\frac{-n\xi_s}{(n+1)N_0} \right] \text{-----} (2.9)$$

Where

ξ_{s/N_0} is the SNR per symbol. Then, the probability of a symbol error, which is $PM = 1 - PC$ becomes

$$p_c = \sum_{n=1}^{M-1} (-1)^{n-1} \binom{M-1}{n} \frac{1}{n-1} \exp \left[\frac{-n\xi_s}{(n-1)N_0} \right] \text{-----} (2.10)$$

Where E_s/N_0 is the SNR. For binary orthogonal signals

($M = 2$), Equation (2.2) reduces to a very simple form and the probability of correct decision is given by

$$p_b = \frac{1}{2} e^{\frac{-\xi_s}{2N_0}} \text{-----} (2.11)$$

Relating Equation (2.3) to the BER (γ) in the section below, it will be assumed that the interference has the same effect as white Gaussian Noise (WGN) and therefore,

$$\gamma_i = \xi_{s/N_0} \quad \text{where } \xi_s \text{ is the received energy per bit at the receiver.}$$

2.3.1 BER Expressions for AWGN.

The mathematical expression for the BER performance of BPSK, QPSK and square 16-point QAM, assuming perfect clock and carrier recovery, in a Gaussian channel are given in [6] as

$$P_{BPSK}(\gamma) = Q(\sqrt{2\gamma}) \text{-----2.12}$$

$$P_{QPSK}(\gamma) = Q(\sqrt{\gamma}) \text{-----2.13}$$

$$P_{16QAM}(\gamma) = \frac{1}{4} Q\left[\left(\sqrt{\frac{\gamma}{5}}\right) + Q\left(3\sqrt{\frac{\gamma}{5}}\right)\right] + \frac{1}{2} Q\left(\frac{\gamma}{5}\right) \text{-----2.14}$$

In equation 2.12, 2.13 and 2.13, (γ) is the SNR and $Q(--)$ is the Q-function which is defined as

$$Q(x) = \frac{1}{\sqrt{2\pi}} \int_x^{\infty} \exp\left\{-\frac{x^2}{2}\right\} dx \text{-----2.15}$$

2.3.2 BER Expressions for Rayleigh Fading Channel.

The mathematical expression for the BER performance of BPSK, 4-QAM and square 16-point QAM over a Rayleigh fading channel are given [6] as

$$P_{BPSK}(\gamma) = \frac{1}{2} \left\{ 1 - \sqrt{\frac{\gamma}{1+\gamma}} \right\} \text{-----2.16}$$

$$P_{4-QAM}(\gamma) = \frac{1}{2} \left\{ 1 - \sqrt{\frac{\gamma}{2+\gamma}} \right\} \text{-----2.17}$$

$$P_{16-QAM}(\gamma) = \frac{1}{4} \left[\left\{ 1 - \sqrt{\frac{\gamma}{10+\gamma}} \right\} + \left\{ \frac{9\gamma}{10+9\gamma} \right\} \right] \text{-----2.18}$$

2.4 MULTIPLE ACCESS SCHEMES IN WIRELESS COMMUNICATION

With the rapid increasing demand of mobile phone services by cell phone users, wireless communication has become a very dynamic area of research due to the limited spectrum to accommodate many users. Multiple access schemes allow the network to maximize the number of users that can occupy a channel [7]. There are three multiple access schemes which are

- Frequency Division Multiple Access (FDMA), Time Division Multiple Access (TDMA) and Code Division Multiple Access (CDMA)

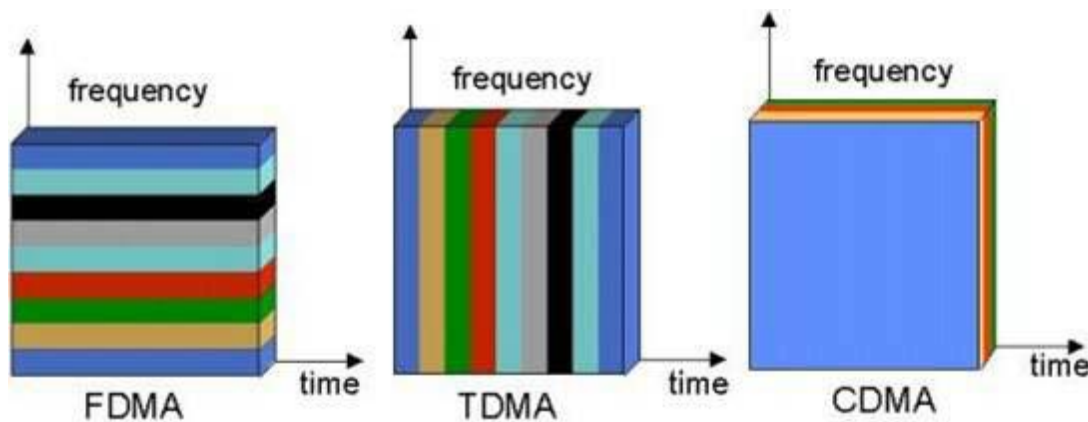


Figure 2.2 Comparison between FDMA, TDMA, and CDMA.

Each multiple access scheme aims at better use of the spread spectrum by allowing multiple users to share the same physical channel.

FDMA achieved this by assigning each user a frequency slot within the channel. This is the simplest multiple access scheme which needs no

synchronization. Its disadvantage is that unused bandwidth cannot be reassigned to other congested users which lead to insufficient use of the bandwidth. Hence, FDMA is more suitable for users with relatively constant data. TDMA does this by assigning unique time slots to each user within the channel where users take turns transmitting and receiving one after another. It is very efficient when the traffic is heavy because time slots are always filled. However, it has the disadvantage because it needs synchronization and central timing which makes it more complex. Users are also constrained to their time slots only. This is called fixed assignment TDMA [8]. Latest researches have shown that there is a new technique where the large number of subscribers can be accommodated called on-demand access TDMA. Borrowing from [9], each user is allocated a fixed percentage of bandwidth can be allocated to the user on demand. This technique guarantees quality of service because it saves a lot of bandwidth. However, it achieves this in the expense of propagation time delay. It is still more complex to implement due to its complex software and hardware. CDMA in contrast lets everyone transmit at the same time sharing the same frequency band. It is different from FDMA and TDMA because unlike them it is not constrained to frequency and time slots. It achieves multiple accesses by assigning each user a special code which is used to transform user's signal into spread spectrum coded signal. At the receiver the same

code that was used at the transmitter for coding is used to recover the user's signal.

Previous researchers have also shown DS- CDMA to have many benefits compared to TDMA and FDMA in many communications systems, which makes it the focus of our research.

2.5 THEORETICAL DSSS-CDMA SYSTEM AND CHANNEL MODELS

A. Transmitter Model

If BPSK modulation scheme is used in the W-CDMA system model, the transmitted signal of k_{th} user in reverse link (mobile to base station) can be represented as [10].

$$s_k = \sqrt{2p_k(t)}b_k a_k \cos(w_c + \theta_k) \text{-----}(2.19)$$

Where p_k represents transmitted signal power, $b_k(t)$ is data signal, $a_k(t)$ is spreading signal, w_c is carrier frequency and θ_k is carrier phase. The k_{th} user's data signal is a random process that is a rectangular waveform, taking values from with service rate, and is expressed as

$$b_k(t) = \sum_{j=-\infty}^{\infty} b_j^{(k)} p_T(t - jT) \text{-----}(2.20)$$

Where $p_T(t) = 1$, for $0 \leq t \leq T$, and $PT = 0$, otherwise. The j_{th} data bit of k_{th} user is denoted as $b_j^{(k)}$. Data source are assumed uniform, i.e.

$p_r\{b_j^{(k)} = +1\} = p_r\{b_j^{(k)} = -1\} = \frac{1}{2}$. The spreading signal $a_k(t)$ can be expressed as

$$a_k(t) = \sum_{j=-\infty}^{\infty} a_l^{(k)} \psi(t - jT) \text{-----} (2.21)$$

Where $\psi(t)$ is an arbitrary chip waveform that is time-limited to $(0, T_c)$ and T_c is chip duration. Chip waveform is assumed to be normalized according to $\int_0^{T_c} \psi^2(t) dt = T_c$. The l_{th} chip of the k_{th} user is denoted $a_l^{(k)}$, which assumes values from $\{-1, +1\}$. All signature sequences $\{a_k^{(k)}\}$ are assumed to be random in the following sense. Every chip polarity is determined by flipping an unbiased coin. Further justification for the random chip sequence assumption is provided in. There are N chips for one data symbol and the period of the signature sequence is N . We normalize the chip duration so that $T_c=1$ and, thus, $T=N$. Note that if the chip waveform is rectangular, i.e. $a_k(t) = \sum_{j=-\infty}^{\infty} a_j^{(k)} p_{T_c}(t - jT_c)$ the transmitted signal becomes the well known phased coded SS model. For QPSK modulation scheme, the transmitted signal of k_{th} user in the subsystem l is [11]

$$s_{ik}(t) = \sqrt{2p_i} b_{ik}^I(t) c_{ik}^I(t) \cos(w_c t + \theta_{ik}) \\ + \sqrt{2p_i} b_{ik}^Q(t) c_{ik}^Q(t) \cos(w_c t + \theta_{ik}) \text{-----} (2.22)$$

Where $b_{ik}^I(t)$ and $b_{ik}^Q(t)$ are the In-phase and Quadrature-phase signal.

B. Receiver Model

The received signal $r(t)$ at the input of the matched filter receiver is given by [11].

$$r(t) = \sum_{k=1}^K s_k * h_k(t) + n(t) = \sum_{k=1}^K \sqrt{2p_k} A_k b_k(t - \tau_k) a_k(t - \tau_k) \cos(w_c t + \phi_{ik}) + n(t). \quad (2.23)$$

Where $*$ denotes convolution and $\phi_k = \beta_k + \theta_k + w_c \tau_k$ is assumed a uniform random variable over $[0, 2\pi]$. The average received power of the k_{th} signal is $E[p^r] = E[A^2 k] P_k$.

C. Channel Model

• AWGN

The transmitted signal for BPSK modulation is subjected to AWGN process $n(t)$, that has two-sided power spectral density $\frac{N_0}{2}$ and $A_k = 1, k=1, \dots, K$. A_k is independent, Rayleigh distributed and account for the fading channel attenuation of all signal. The first order of probability density function (pdf) is given by [12]

$$p_{A_k}(a) = a e^{\frac{-a^2}{2}} I_{[0, \infty]}(a) \quad (2.24)$$

Due to the fact that Simplified Gaussian approximation (SGA) considers an average variance value for Multi Access Interference (MAI) or in other words, the first moment of ζ , the Improved Gaussian approximation (IGA) exploits knowledge of all moments of ζ . It was shown that the BER for an

AWGN channel obtained from IGA is significantly more accurate than the BER obtained from the SGA especially for small number of user, k . Thus by applying SIGA, overall BER can be represented as

$$p_e^{SIGA} \approx \frac{1}{3} \left[1 - \frac{N}{\sqrt{\mu\zeta + N^2}} \right] + \frac{1}{12} \left[1 - \frac{N}{\sqrt{\mu\zeta + \sqrt{3}\sigma_\zeta + N^2}} \right] + \frac{1}{12} \left[1 - \frac{N}{\sqrt{\mu\zeta - \sqrt{3}\sigma_\zeta + N^2}} \right] \dots$$

-----(2.25)

Where $\mu\zeta$ and σ_ζ^2 are given by

$$\mu_\zeta = \frac{2N}{3}(K - 1) \text{ -----(2.26)}$$

and

$$\sigma_\zeta^2 = (k - 1) \left[\frac{1}{45} (43N^2 + 18N - 18) + (k - 2) \cdot \frac{N-1}{9} \right] \text{ -----(2.27)}$$

Where this method is extended by applying first and second moment for the received power.

• Rayleigh Fading

The output of a low pass filter (LPF) of a synchronous system i.e. $\tau_1 = \tau_2 = \dots = \tau_K$ for user 1 can be represented as $y_1 = \int_0^T r(t) a_1 \cos(w_c t) dt = s_1 + I_1 + n_1$ ----- (2.28)

Where n_1 is a zero-mean Gaussian random variable with variance $\sigma_{n_1}^2 = N_o \frac{N}{4}$, s_1 is the signal component $s_1 = A_1 N$, and the interference term I_1 is given by [12]

$$I_1 = \sum_{K=2}^K A_k b_o^{(k)} \cos(\phi_k) \int_0^T A_k(t) a_1(t) dt \text{ ----- (2.29)}$$

Since a sum of independent Gaussian random variable has Gaussian distribution, it follows that I_1 is a Gaussian random variable with zero-mean and variance, by symmetry and using the independence I_1 and n_1 , one has

$$P_{e/A1}^{SSYNC} Q \left[\frac{A_1 N}{\sqrt{\frac{N_0 N}{4} + \sum_{K=2}^K N^2 \rho_{K1}^2}} \right] \text{ ----- (2.30)}$$

and averaging over the pdf of A_1 , BER for a Rayleigh-faded user is

$$P_e^{SYNC} = \frac{1}{2} \left[1 - \frac{1}{\sqrt{1 + \frac{N_0}{4N} + \sum_{K=2}^K \rho_{K1}^2}} \right] \text{ ----- (2.31)}$$

From the equation above, one sees that the interferers act like additional independent Gaussian background noise. This is because the MAI on the flat Rayleigh fading channel has a Gaussian first-order distribution assuming synchronous transmission. This implies that the optimum receiver that does not perform user-interference cancellation is a correlator detector. However, this is not the case of asynchronous transmission. For uniformity, uniform random signature sequences $E[\rho_{k1}^2] = \frac{1}{N}$ and

$$P_e^{SYNC} = \frac{1}{2} \left[1 - \frac{1}{\sqrt{1 + \frac{N_0}{4N} + \frac{k-1}{N}}} \right] \text{ ----- (2.32)}$$

2.6 Modulation Schemes in Wireless System

- **Quadrature Phase Shift Keying (QPSK) Modulation**

Quadrature Phase Shift Keying (QPSK) is the digital modulation technique. Quadrature Phase Shift Keying (QPSK) is a form of Phase Shift Keying in which two bits are modulated at once, selecting one of four possible carrier phase shifts (0 , $\pi/2$, π , and $3\pi/2$). QPSK perform by changing the phase of the In-phase (I) carrier from 0° to 180° and the Quadrature-phase (Q) carrier between 90° and 270° . This is used to indicate the four states of a 2-bit binary code. Each state of these carriers is referred to as a Symbol [13].

QPSK perform by changing the phase of the In-phase (I) carrier from 0° to 180° and the Quadrature-phase (Q) carrier between 90° and 270° . This is used to indicate the four states of a 2-bit binary code. Each state of these carriers is referred to as a Symbol. Quadrature Phase-shift Keying (QPSK) is a widely used method of transferring digital data by changing or modulating the phase of a carrier signal. In QPSK digital data is represented by 4 points around a circle which correspond to 4 phases of the carrier signal. These points are called symbols. Fig 2.3 shows this mapping.

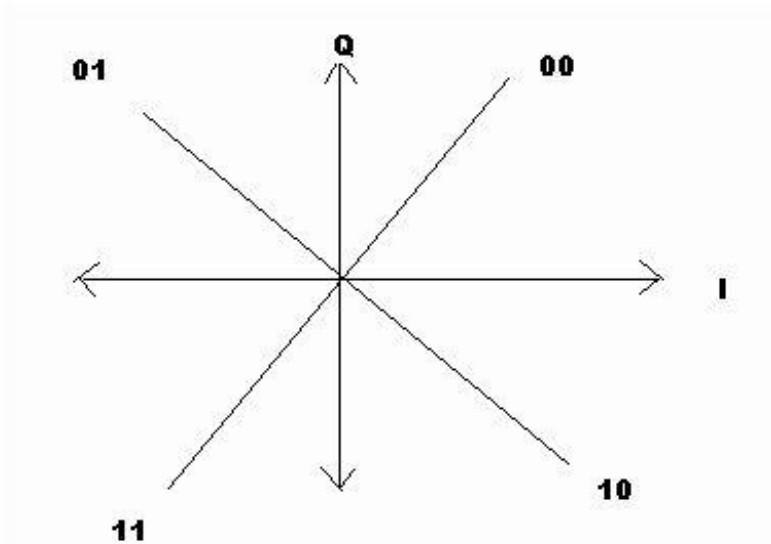


Fig2.3 : QPSK diagram showing how four different binary code transmitted

- **M-ary Quadrature Amplitude Modulation (QAM)**

The Modulation equation for QAM is a variation of the one used for PSK. The generalized PSK allows changing the Amplitude and the Phase. In PSK all points lie on a circle so the I and Q values are related to each other. PSK signals are constant envelop because of this; all points have the same amplitude. If we allow the phase and amplitude to change from symbol to symbol, then we get a modulation called quadrature amplitude modulation (QAM) .It can be considered a linear combination of two DSB-SC.so it is an AM and a PM modulation at same time.

$$s_m(t) = \sqrt{\frac{2E_s}{T_s}} \cos(\theta(t)) \cos(2\pi f_c t) - \sqrt{\frac{2E_s}{T_s}} \sin(\theta(t)) \sin(2\pi f_c t) \text{ -----2.33}$$

This equation can be used to create an hybrid type of modulation that varies both in amplitude and the phase. When M=16,we have 16 symbols, each representing a four bit word. We can lay these out in a circle but they would be too close and error rate is likely to be high.

In 16QAM, we vary not just the phase of the symbol but also the amplitude. In PSK, all symbols sat on a circle so they all had the same amplitude.

2.7 SUMMARY OF RELATED RESEARCH EFFORT

2.7.1 ADAPTIVE MODULATION AND DATA RATE

In [13], the author defines an Adaptive modulation in cognitive radio as: “an intelligent wireless communication system that is aware of its environment, and uses the understanding-by-building methodology to learn from the environment and adapt to statistical variations in the input stimuli ”.

2.7.2 Effectiveness of Packet Length and data rate:

In [14], their work presents a mathematical technique for determining the optimum transmission. The throughputs defined as the number of bits per second correctly received. and equations are derived for the optimal choice of the design variables. These parameters are SNR dependent and can be adapted dynamically in response to the mobility of a wireless data terminal. They also looked at the joint optimization problem involving all the design parameters together. They found that not all the three parameters (b , SNR, L) need to be adapted simultaneously: in the received SNR per symbol stays at some rate so that the received SNR per symbol stays at some preferred value.

They also varied received power by changing the distance between the transmitter and receiver. Finally, they gave a characterization of the optimal parameter values as functions of received SNR.

2.7.3 Rate management

The work of [15] considered a wireless multimedia code-division multiple-access system, in which the terminals transmit at different rates. They formulated the problem as a constrained optimization problem, with the objective of maximizing the total effective rate. An optimal power control strategy was derived. When the scale of the system is large, the optimal solution takes a simple form, which is easy to be applied practically.

In their literature, the control problem is usually formulated as an optimization problem which minimizes the transmit power subject to minimum signal-to-interference (SIR) requirement. This approach is very suitable for handling voice traffic. They showed that for some other multimedia applications, however, different objectives may be more appropriate. Thus, they proposed different power control schemes.

In their work, they took a different approach. They asked the following questions: how should they set the SIR for delay tolerant source? Such sources can potentially benefit from coding, which is obtained at the cost of delay. They also assumed that various sources differ only in their data rate. The main theme of their paper is to find an efficient way to allocate resources for delay tolerant sources. They showed that the coexistence of delay tolerant and delay-sensitivity sources in a system has no effect on their main result as the problem can be easily decoupled.

2.7.4 Resource Management:

In the work done by [16] reviewed the developments of distributed power control and related resource management problems in cellular wireless systems. They highlighted the feasibility issue in a power-controlled system, which enables us to push the system towards high efficiency, and prevent the system from collapsing at the same time. Considering the unique features of multimedia traffic to be supported in future wireless system.

They also review power and rate control schemes proposed for wireless data, and present a frame work for utility-based power control as a possible candidate for distributed power control of multimedia wireless systems.

The thesis work of [17] examined some of the variables affecting throughput and they include; packet size, transmission rate, received signal power, etc. he looked at the effect of transmission rate and packet size on

throughput. He also looked at how the transmission rate and packet size can optimize the throughput jointly.

His analysis involved forward error correction which theoretically should improve the throughput and also when there is no forward error correction. The analysis was also performed involving BCH codes for comparison of results to draw a more general conclusion, his work did not take any particular wireless system into account.

His result is a mathematical technique for determining the optimum transmission rate and packet size as a function of other variables. He also found out that the key to maximizing the throughput rate is maintaining the signal to noise at an optimum level.

An early work of [18], introduce variable rate QAM. The transmitter varies the signal constellation size from 1bit/symbol corresponding to BPSK, 2bits/symbol for QPSK and 6bits/symbol for 64-QAM. In a good quality channel, the constellation size is increased, and as the channel quality become worst, that is, as the receiver enters a deep fade, the constellation size is decreased to a value, which provides an acceptable BER. Two choices of implementation can be applied; to keep constant of one parameter and varying the other parameter. Specifying a required BER value leads to varying data throughput and vice versa. The work also highlights two different types of switching criteria to control the modulation modes, Received Signal Strength Indicator (RSSI) system and error detector switching system. RSSI system uses SNR values corresponding to the BER of interest as the switching thresholds while the later system use the channel coder to monitor the channel quality. Simulation results showed the performance improvement over fixed modulation and comparisons of the two switching systems. It is observed that RSSI typically offering a slightly higher number of bits/symbol at low SNRs for some BERs. This is due to the RSSI switching system's ability to select a

lower number of levels before any errors occurred. RSSI is also more attractive in term of implementation complexity because no additional BCH codec is needed.

According to [19], the author examined switching system as the channel state information (CSI) which specified the channel quality. SNR based CSI corresponding to RSSI system was compared with error-based CSI corresponding to error detector switching system. SNR based CSI adapts with a faster rate, but relies on the computation of adaptation or switching thresholds that may be inaccurate. Accuracy of the threshold mechanism increases by taking into account higher order statistics of SNR than just the mean. Studies on varying combination of parameters also attract a great interest. In the work of [20] produce trellis-coded adaptive MQAM. Analytical and simulation results shows that the new simple 4-state trellis-coded adaptive MQAM achieves 3-dB effective coding gain relative to uncoded adaptive M-QAM and 3.6 dB for 8-state trellis. Compared with traditional trellis codes and fixed-rate modulation, the new scheme shown more than 20 dB power savings.

2.8 RADIO PROPAGATION MODELS

2.8.1 Preview

Propagation models are mathematical attempts to model the real radio environment as closely as possible, propagation models are used extensively in network planning particularly for conducting feasibility studies and during initial deployment. These models can be broadly categorized into three types; empirical, deterministic and stochastic. Empirical models are those based on observations and measurements alone. The deterministic models make use of the laws governing electromagnetic wave propagation to determine the received signal power at a particular location. Deterministic models often require a complete 3-D

map of the propagation environment. An example of a deterministic model is a ray tracing model. Stochastic models, on the other hand, model the environment as a series of random variables.

Propagation models are useful for predicting signal attenuation or path loss which is the reduction in power of an electromagnetic wave as it propagates through space. It is a major component in analysis and design of link budget of a communication system. It depends on frequency, antenna height, receive terminal location relative to obstacles and reflectors, and link distance, among many other factors. Macro cells are generally large, providing a coverage range in kilometers and used for outdoor communication. Several empirical path loss models have been determined for Micro and macro cells. Among numerous propagation models, the following are the most significant ones, providing the foundation of mobile communication services. The models are

2.8.2 THE JOINT RADIO COMMITTEE METHOD (JRC)

This method was adopted in UK by the Joint Radio Committee and uses a computer-based topographic database, which provides height reference points at 0.5km intervals in a matrix of rows, columns and diagonal interpolations. For a given set of transmitter and receiver locations, a path profile reconstructed by the computer program, and heights and positions of the obstacles are then determined [21] . The computer then test for the existence of line of sight and Fresnel zone clearance over the entire path and the following scenarios can be separated.

- If there is clear line of sight and adequate Fresnel zone clearance, the larger of free space loss and plane earth loss is taken:

$$L = \max(L_f, L_p) \text{ -----2.34}$$

- If no line of sight or there is inadequate Fresnel zone clearance, the resulting diffraction loss is estimated and added to the larger of free space loss and plane earth loss:

$$L = \max(L_f, L_p) + L_d \text{ -----} 2.35$$

The JRC method has the limitation of being unable to account for trees and hence tends to underestimate the path loss [22].

2.8.3 THE LONGLEY-RICE METHOD

The Longley-Rice method [23] is based on well-established propagation theory and has been tested against thousands of measurement data. For the line of sight paths, the calculated reference is based on two-ray theory and an extrapolated value of diffraction attenuation and the forward scatter attenuation. The Longley-Rice method is a computer –oriented method that may be used either with profiles for actual paths or with profiles that are representative of median terrain characteristics for a given area. The method has been attractive for years and has drawn attention for many authors, who proposed its modified applications. Nevertheless, even including the use of computer, the method is not so simple and description of the calculation of the many parameters used is rather lengthy.

2.8.4 THE LEE'S MODEL

Lee's model became popular mainly because the parameters of the model can be easily adjusted to the local environment by additional field measurement .By doing so, greater accuracy of the model can be achieved [24]. In addition, the prediction algorithm is simple and fast. The model consists of two part . The first part, an area –to- area prediction, is used to predict a path loss over a general flat terrain taking into account the particular terrain configuration. The second part of lee's model uses the

area- area prediction as a basis and the develop a point – to- point prediction, thus resolving the problem.

The basic area-to- area model can be expressed in the following form:

$$L_{50} = L_o + y \log d + F_o \text{ dB} \text{ -----} 2.36$$

Where L_o is the median transmission loss at a range of 1km

Y is the slope of the path loss curve in dB/decade

Values of L_o and y are obtain from experiments.

F_o = is an adjustment factor and can be calculated as

$$F_o = F1 F2 F3 F4 \text{ -----} 2.37$$

2.8.5 FREE SPACE MODEL

In free space there are no obstacles. The propagated wave radiates freely to an infinite distance without being absorbed or reflected [25].

In radio wave propagation models, the free space model predicts that received power decays as a function of T-R separation distance, the path loss in dB for free space model when antenna gains are included is given by [25]

$$P_L \text{ (dB)} = -G_t - G_r + 32.44 + 20 \log(d) + 20 \log(f) \text{ -----} 2.38$$

Where;

G_t is the transmitter antenna gain in dB,

G_r is the receiver antenna gain in dB,

d is the T-R separation distance in kilometres and

f is the operating frequency in MHz

2.8.6 HATA OKUMURA MODEL

The Hata-Okumura model is an empirical formula for graphical path loss data provided by Yoshihisa Okumura, and is valid from 150 MHz to 1500

MHz. The Hata model is a set of equations based on measurements and extrapolations from curves derived by Okumura. Hata presented the urban area propagation loss as a standard formula, along with additional correction factors for application in other situations such as suburban, rural among others. The computation time is short and only four parameters are required in Hata model.

However, the model neglects terrain profile between transmitter and receiver, i.e. hills or other obstacles between transmitter and receiver are not considered.

- This is because both Hata and Okumura made the assumption that transmitter would normally be located on hills.

- **Okumura Hata Model**

The Okumura Hata Model for path loss prediction in different radio propagation environment is given as

➤ For Urban Area

$$P_{L(URBAN)} (dB) = A + B \log (d) \quad \text{-----2.39}$$

Where;

$P_{L(URBAN)} (dB)$ is the path loss for urban area in dB

d is distance between transmitter (Tx) and receiver (Rx) in kilometer,

'A' represents a fixed loss that depends on frequency of the signal.

These parameters are given by the empirical formula

$$A = 69.55 + 26.16 \log (f) - 13.82 \log (h_b) - a (h_m).$$

$$B = 44.9 - 6.55 \log (h_b).$$

Where,

f is the operation frequency measured in MHz,

h_b is height of the base station antenna in meters,

h_m is mobile antenna height in meters and

$a(h_m)$ is correction factor in dB

For effective mobile antenna height $a(h_m)$ is given by

➤ for small and medium size cities

$$a[h_m] = [1.1 \log(f) - 0.7] h_m - [1.56 \log(f) - 0.8],$$

➤ for large cities,

$$a[h_m] = 8.29[\log 1.54 h_m]^2 - 11, f \leq 200 \text{ MHz}$$

$$a[h_m] = 3.2[\log 11.75 h_m]^2 - 4.97, f \geq 400 \text{ MHz}$$

For Sub-Urban Area the path loss is given as

$$P_{L(\text{SUB-URBAN})}(\text{dB}) = P_{L(\text{URBAN})} - 2[\log(f/28)^2 - 5.4] \text{ Db} \quad \text{-----2.40}$$

For Rural Area the path loss is given as

$$P_{L(\text{RURAL})}(\text{dB}) = P_{L(\text{URBAN})} - 4.78 \log(f)^2 + 18.33 \log f - 40.94 \text{ dB} \quad \text{-----2.41}$$

The range of value for validity of Hata model is

$$150 \leq f \leq 1500 \text{ MHz}, 30 \leq h_b \leq 200 \text{ m}, 1 \leq h_m \leq 10 \text{ m and } 1 \leq d \leq 20 \text{ km}.$$

2.8.7 COST 231 MODEL

To extend Hata-Okumura- model for personal communication system (PCS) applications operating at 1800 to 2000 MHz, the European Co-operative for Scientific and Technical Research (COST) came up with

COST-231 model. This model is derived from Hata model and depends upon four parameters for prediction of propagation loss: frequency, height of received antenna, height of base station and distance between base station and received antenna.

The path loss in urban area is given in equation For Urban Area the path loss is given as [26]

$$P_L \text{ (dB)} = 46.33 + 33.9 \log(f) - 13.82 \log(h_b) - a(h_m) + [44.9 - 6.55 \log(h_b)] \log(d) \text{-----} 2.42$$

Where;

$$a[h_m] = [1.1 \log(f) - 0.7] h_m - [1.56 \log(f) - 0.8],$$

2.8.8 ECC 33 Model

The ECC 33 path loss model, which is developed by Electronic Communication Committee (ECC), is extrapolated from original measurements by Okumura and modified its assumptions so that it more closely represents a fixed wireless access (FWA) system. The path loss model is defined as [27]

$$P_L \text{ (dB)} = A_{fs} + A_{bm} - G_t - G_r \text{-----} 2.43$$

where;

A_{fs} is free space attenuation, A_{bm} is basic median path loss,

G_t is BS height gain factor and G_r is received antenna height gain factor.

They are individually defined as,

$$A_{fs} = 92.4 + 20 \log(d) + \log(f)$$

$$A_{bm} = 20.41 + 9.83 \log d + 7.894 \log f + 9.56 [\log(f)]^2$$

$$G_t = \log(h_b/200) [13.958 + 5.8 \log d]^2 \text{ for medium city environments,}$$

$$G_r = [42.57 + 13.7 \log(f)] [\log(h_m) - 0.585]$$

where, f is the operating frequency in GHz,

In [28] conducted a study of the three GSM networks in Mubi Adamawa State University, Mubi namely MTN, GLO and Zain and the overall average path loss detected were 144.93, 143.76 and 147.76dB for MTN, ZAIN and GLO and the mean square error obtained were 2, 1.5 and 3dB respectively. In line with the results the modified Equations were developed using Hata model that can help in planning and optimization of the investigated environment.

The measurements were taken at an interval of 500m, 10 times for each of the GSM BSs and thier result showed that the overall average of the path loss measured for all the GSM operators lies between $1 \leq 18.22\text{dB}$. They calculated the mean square error using a formula [29].

$$E = \frac{\sigma}{\sqrt{N}} \dots \dots \dots 2.44$$

Where E is the MSE, σ is the standard deviation and N is the number of terms measured. With the result they modified the Okumura-Hata model for the three GSM companies taking into account their BTS antennas heights and frequencies. The modified formula was then used to compare with the Hata model for Mubi town in Adamawa State.

At the University of Benin, Nigeria The authors, Characterized the propagation path loss at 1.8GHz band for Benin and was published in the

research Journal of applied sciences in 2006 [29] . Investigating GSM signals at 15 different environments, they deduced that the propagation path loss exponent for Benin City was between 2.8 to 3.7 with 3.3 as the average.

The test were carried out on consecutive times between November 2003 - February 2004, April - June 2004, August to October 2004 and January to March 2005, using the net-monitor software of the mobile phone and a tachometer to determine the distance from Base Station.

Applying the power law

$$L = d^{\gamma} \text{-----} (2.45)$$

Using MATLAB they found the exponential path loss by potting the log-log graph as shown, as the slope of the graph [30]

$$\gamma = \frac{10 \log L}{10 \log d} \text{-----} (2.46)$$

They also calculated the standard deviation of the received signal power and used it to understand the environment variability of Benin City.

A path loss model, based on the field measurements performed by [31] for the suburban city of Mehuwala, Dehra Dun, was compared with the HATA model, which is widely used in path loss prediction in CDMA based system. A comparison of the developed model with the HATA model gave significance difference; they therefore recommended that for accurate path

loss prediction, field measurement must be performed, The measured data was then used to correct the existing model for the fringe environment of Dehra, Uttarakhand-India. All the measurements were taken for mobile terminal using 3GHz MICRONIX Spectrum Analyzer MSA338. Noise Figure <4db and 16.5dB antenna gain. Transmitted power is 5 KW. Measurements were taken in all three zones/sectors. For macro cellular system, the reference distance is taken as $d_0 = 1$ km. Starting from 1km, measurements were taken in intervals of 0.5 km in three zones. Measurements were performed up to a distance of 5km from the transmitter. In all, 84 cellular base stations were involved in the field measurements.

The linear regression formula [31]:

$$E(n) = \sum_{i=1}^k \{L_p(d_i) - L_p(d_0)\}^2 \text{-----} (2.45)$$

was used to calculate the path loss exponent by equating the derivative of the equation to zero and solving for n ...

$$\frac{\delta E(n)}{\delta n} = 0 \text{-----} (2.46)$$

The path loss exponent n was found to be 2.67 and as such define a path loss model for the fringe area of Mehuwala in India. The pathloss increases at the rate of 26.7 dB per decade with distance. A comparison of the measured value with Hata of 34.26dB per decade increase showed a considerable difference.

CHAPTER THREE

REASERACH METHODOLOGY AND IMPLEMENTATION

3.1 MEASUREMENTS ENVIRNOMENT DESCRIPTION

This chapter presents all steps needed for the actual model design from field measurement. Twelve MTN Base Stations were visited and measurement were take. Since both Urban and Sub-Urban prediction models are required, the selection of the 12 (twelve) representative sites was done in such a way as to accommodate both environment scenarios in and around Imo State.

There are 226 MTN Base stations in Imo State, Classified as follows

A. 2G ONLY	91 BASE STATIONS
B. 2G AND 3G ONLY	67 BASE STATIONS
C. 3G ONLY	10 BASE STATIONS, NEW COVERAGE
D. 2G AND 3G ONLY	34 BASE STATIONS

INFIL SITE as shown in figure 3.1 shows all the MTN Base station at Imo State. Figure 3.2 shows the map of the sites visited.

The drive test on received signal strength on four (4) base stations in each category was spread to accommodate the classification above when any of the modulation techniques QAM, QPSK and GMSK are changed at respective base station.

RSS measurements up to a distance of 1500 meters were gathered in ten (10) sites where both GSM and W-CDMA systems co-exist, and two (2) other measurements were taken for CDMA and GSM Systems when deployed alone. The site name, angle of antenna alignment for the deployed Systems in Co-Location arrangement, antenna height, transmitting power, operating center frequency and locations (Latitude and Longitude) were noted. The Measuring Instrument was the Transverse Electromagnetic Wave (TEMS). Investigation Application software programmed in a Laptop, sourced from Huawei Technologies (Installers of GSM and CDMA Equipment for both MTN and Visafone).

3.2 DIRECT SEQUENCE SPREAD SPECTRUM (DSSS) BIT ERROR RATE PROBABILITY CALCULATIONS

A DSSS system spreads the baseband data by directly multiplying the baseband data pulses with a pseudo-noise sequence that is produced by a pseudo-noise (PN) code generator [29]. A PN sequence is a binary sequence with an autocorrelation that resembles, over a period, the autocorrelation of a binary sequence. The PN sequence is usually generated using sequential logic circuits (i.e. feedback shift register). A single pulse or symbol of the PN waveform is called *chip*. Spread spectrum signals are demodulated at receiver through cross-correlation with locally generated version of the pseudo random carrier. Cross-correlation with the correct PN sequence de-spreads the spread spectrum signal and restores the modulated message in the same narrow band as the original data,

whereas cross-correlating the signal from an undesired user results in a very small amount of wideband noise at the receiver output.

Unlike modulation and demodulation techniques that have primary objective to achieve power and bandwidth efficiency in AWGN channel, the transmission bandwidth of DSSS has several orders of magnitude greater than the minimum required signal bandwidth. In other words, DSSS modulation transforms an information signal into a transmission signal with a larger bandwidth. It is achieved by encoding the information signal with a code signal that is independent of the data and has a much larger spectral width than that of information signal.

In DSSS, many users can simultaneously use the same bandwidth without significantly interfering one another. DSSS is normally used in Code Division Multiple Access (CDMA) scheme. The received DSSS signal for a single user can be represented as [29]

$$s_m(t) = \sqrt{\frac{2E_s}{T_s}} m(t)p(t) \cos(2\pi f_c t + \theta) \quad \text{-----} \quad (3.1a)$$

Where $m(t)$ is the data sequence, $p(t)$ is the PN spreading sequence, f_c is the carrier frequency and θ is the carrier phase angle at $t = 0$. There are two approaches to calculate BER for DSSS-CDMA operating under AWGN channel [32, 33]. The first approach uses accurate BER approximations because it is presumed that BER evaluation is numerically cumbersome. There are many researches on this approach and most widely used approximation is the so called Standard Gaussian Approximation (SGA) [32]. In the SGA, a central limit theorem (CLT) is employed to approximate the sum of the multiple-access interference (MAI) signals as an AWGN process additional to the background Gaussian noise process. To detect desired user signal, the receiver design consists of a conventional single-user matched filter (correlation receiver). The average variance of the MAI over all possible operating conditions is used to compute the SNR at the

filter (correlator) output. SGA is widely used because it is easy to apply. However, it is known based on performance analysis that SGA often overestimate system performance especially for small number of users. Thus, Improved Gaussian Approximation (IGA) is created to overcome the limitations in SGA. IGA is more accurate than SGA especially for small number of users but with exploiting numerical integration and multiple numerical convolutions.

Simplified IGA (SIGA) is created where neither the knowledge of the conditional variance distribution, nor numerical integration nor convolution is necessary to achieve acceptable BER estimation. This approach is chosen in this thesis to calculate BER in the channel of WCDMA system. The second approach is to perform the evaluation of the DS-SS-CDMA system BER without knowledge of or assumptions about the MAI distribution. This approach is based on previous study on ISI. There are a number of ways to achieve this method. They include moment space technique, characteristic function method, method of moments, and an approximate Fourier series method [32, 33]. Generally, these techniques can achieve more accurate BER estimate than CLT-based approximations at the expense of much higher computational complexity. For BER of DSSS-CDMA systems operating in Rayleigh fading channels, an accurate method has been proposed by [33]. It gives in depth treatment on a generic DSSS-CDMA system with Rayleigh-distributed users under both synchronous and asynchronous operations for random sequences where the IGA and SIGA methods are extended to a Rayleigh fading channel system.

3.3 PATH LOSS EXPONENT CALCULATION

In free space, the wave is not reflected or absorbed. Ideal propagation mean there are equal radiations in all directions from the radiating source and propagation to an infinite distance with no degradation. Spreading the power over greater areas causes the attenuation. Equation (3.1b) illustrates how the power flux is calculated.

$$P_d = P_t / 4\pi d^2 \quad \dots\dots\dots (3.1b)$$

Where P_t is known as transmitted power (W/m²) and P_d is the power at a distance d from antenna.

The actual power received by the antenna depends on the following: (a) The aperture of receiving antenna A_e , (b) the wavelength of received signal λ , (c) and the power flux density at receiving antenna P_d [56].

Effective area A_e of an isotropic antenna is:

$$A_e = \lambda^2 / 4\pi \dots\dots\dots (3.2)$$

The receive power is given as:

$$P_r = P_d \times A_e = P_t \times \pi^2 / (4\pi d)^2 \dots\dots\dots (3.3)$$

It has been found that the received power P_r (d) [dB] at any distance (d) from the transmitter with transmit power P_t [dB] is given by[34]:

$$P_r(d) = P_t - P_L(d) \dots\dots\dots (3.4)$$

In plane terms $P_L(d) = \text{Power transmitted } (P_t \text{ (dB)}) - \text{Power received } (P_r \text{ (dB)})$, this formula will be used extensively in the determination of the measured PL.

Furthermore, substituting equations 3.3 in 3.4, we deduce that

$$PL \text{ (dB)} = 20 \log_{10} (4\pi) + 20 \log_{10}(d) - 20 \log_{10}(\lambda) \dots\dots\dots (3.5)$$

But then substituting (λ (in km) = 0.3/ f (in MHz)) and rationalizing the equation produces the generic free space path loss formula, which is stated as in equation (3.6) [35]:

$$P_L(dB) = 32.5 + 20\log_{10}(d) + 20\log_{10}(f) \dots \dots \dots (3.6)$$

For any distance (d), the $P_L(d)$ is given by [36 and 37]:

$$P_L(d_i) = P_L(d_o) + 10n\log_{10}(d_i/d_o) \dots \dots \dots (3.7)$$

Where (n) the path loss exponent can be manually calculated using eqn (3.8) or derived through the application of linear regression analysis technique.

$$n = \frac{\{P_L(d_i) - P_L(d_o)\}}{10\log_{10}(d_i/d_o)} \dots \dots \dots (3.8)$$

With linear regression, the value of the path loss exponent can be determined from the measured data, by minimizing in a mean square error sense, the difference

Let's **recall** from equation (2.45) [37]. The sum of the path loss exponents can be given by

$$E(n) = \sum \{L_p(d_i) - L_p(d_i)\}^2 \dots \dots \dots (3.9)$$

Where: $L_p(d_i)$ is the measured Path loss at distance d in dB, and $L_P(d_i)$ is predicted using equation (3.7) in dB [38].

Substituting equation (3.7) in (3.9) for $L_P(d_i)$

$$E(n) = \sum [L_p - L_p(d_o) - 10 \log_{10} (d/d_o)]^2 \dots \dots \dots (3.10)$$

Differentiating equation (4.10a) w.r.t. n ,

$$\frac{\delta E(n)}{\delta n} = -20\log_{10} \sum [L_p - L_p(d_o) 10\log_{10}(d/d_o)] \dots \dots \dots (3.11)$$

Equating $\frac{\delta E(n)}{\delta n}$ to zero,

$$0 = -20\log_{10}(d) \sum (L_p - L_p(d_o) - 10n\log_{10}(d/d_o))$$

$$\sum [L_p - L_p(d_o)] - 10n\log_{10} d/d_o = 0$$

$$\sum [L_p - L_p(d_o)] - \sum [10n\log_{10}(d/d_o)] = 0$$

$$\sum [L_p - L_p(d_o)] - \sum [10n\log_{10}(d/d_o)] = 0$$

$$\sum [L_p - L_p(d_o)] - \sum [10n\log_{10}(d/d_o)] = 0$$

$$n = \frac{\sum [L_p - L_p(d_o)]}{\sum [10\log_{10}(d/d_o)]} \dots \dots \dots (3.11)$$

MATLAB code of appendix A shows the execution of Equation (3.11) for the calculation of the pathloss exponents (n). ***The table 3.1 shows the parameters used at a glance***

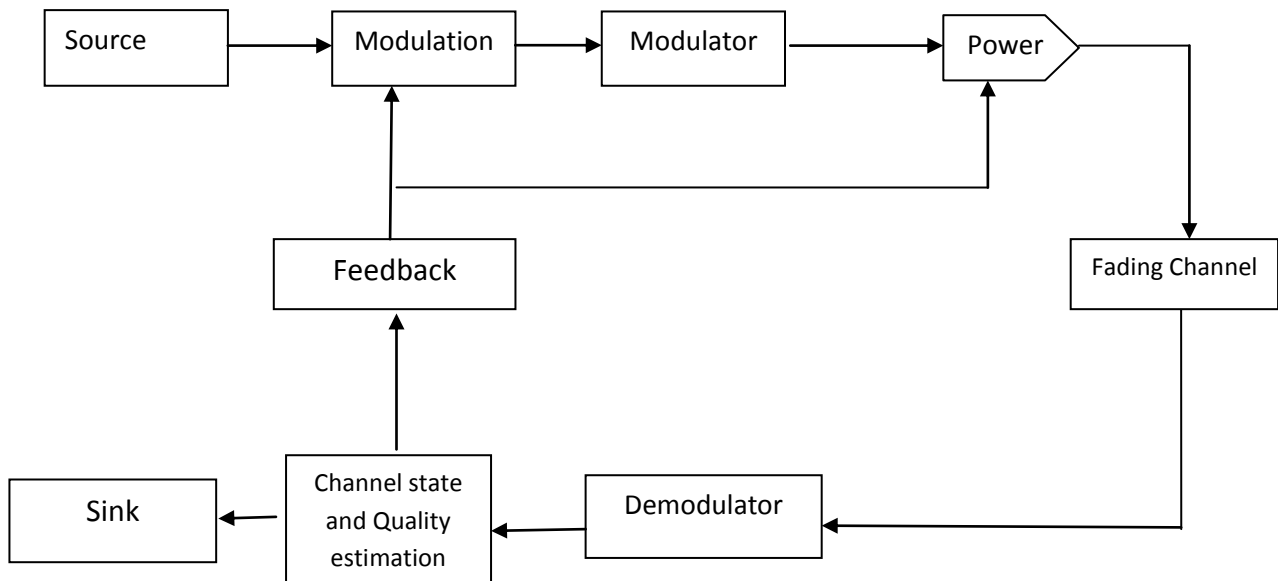
TABLE 3.1 Configuration Parameters at Glance

Parameters	Values
Operating frequency	2116.4 and 910 MHz
Base station transmitter power	43 dBm and 44.1dBm
Mobile transmitter power	30 dBm
Base station antenna height	30m
Mobile station antenna height	1.5 m
Distance between transmitter and receiver	1-500m
Transmitter antenna gain	17.5 dB
Connector losses	2 dB
Cable losses	1.5 dB
BS threshold level	-110 dBm
Building to building distance	15 m
Average building height	15m (urban), 7m (suburban)
Downlink E_b/N_o	2.5 dB
Uplink E_b/N_o	1 dB

3.4 CHANNEL ADAPTIVE MODULATION ALGORITHM

The block diagram, shown in Figure 3.3 reveals the functioning of the link adaptation mechanism (including both adaptive modulation and power control). The transmitter chooses a suitable link characteristic based on the command it receives through the feedback channel. The flowchart shown in Fig. 3.4 depicts the operation of the adaptive modulation module. The function of the transmitter is always to enhance the spectral efficiency subject to the BER constraints. While working with adaptive modulations, one of the critical issues is to find out a suitable means to decide upon the best-suited modulation scheme for the prevailing channel conditions. The received SINR and path loss exponent is used as the channel metric to decide on the modulation type (QAM and QPSK modulation) .If the path loss exponent is small choose QPSK and when it is large choose QAM. There also exists a SINR target for satisfying the target BER of which depends on traffic classes. The next problem is to decide on the range of SINR values that can be used for modulation scheme

Fig. 3.3 Block diagram link adaptation mechanism



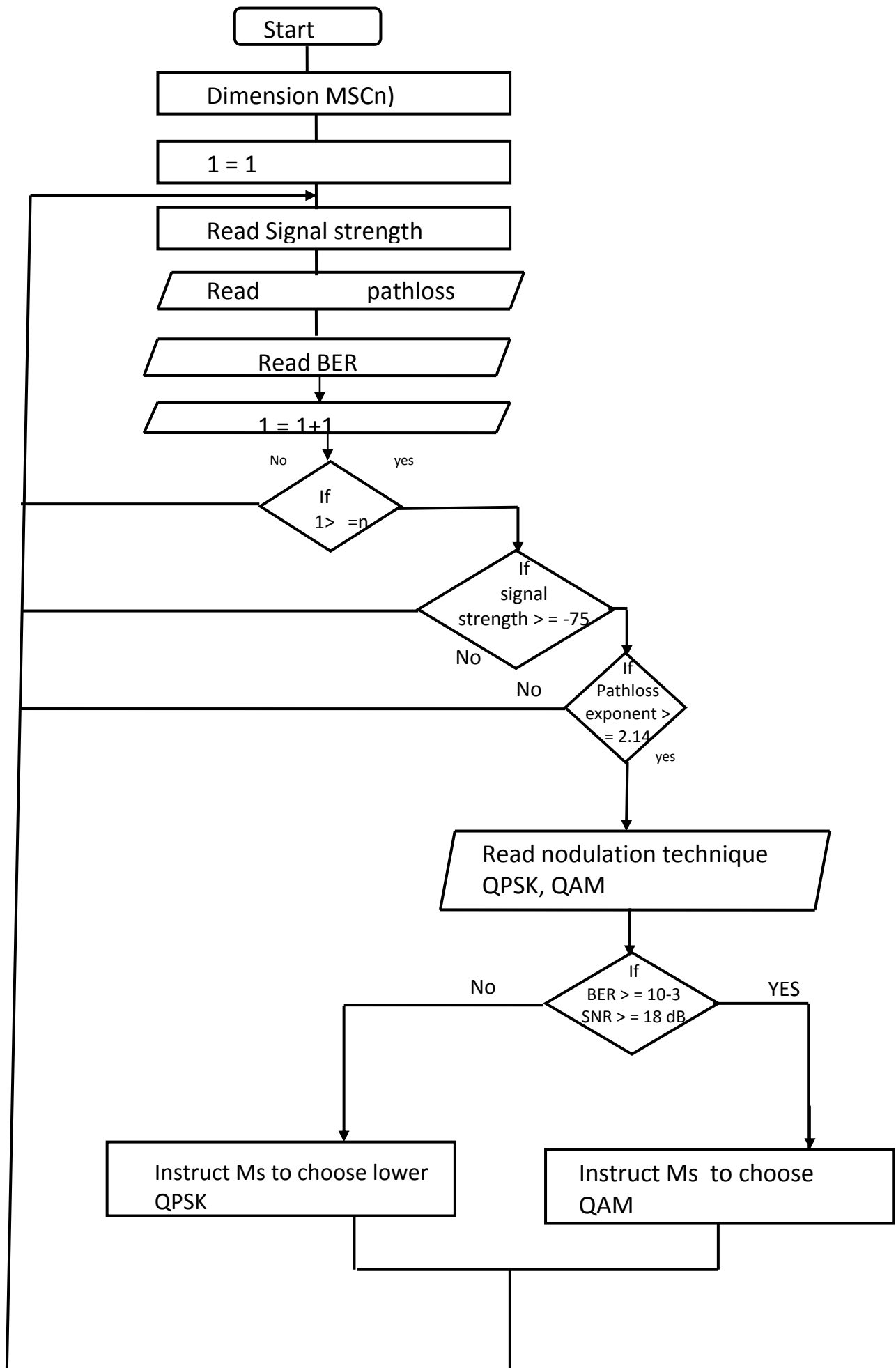


Fig. 3.4: Flow Chart for Adaptive Modulation Mechanism

```

Start
Dimension MS(n)
1=1
Read MS(n)
Read signal strength
Read pathloss
Read BER
1 = 1 +1
If 1> = n
If signal strength > = -75
If Pathloss exponent> = 2.06
Read modulation technique
QPSK, QAM
If BER >= 10-3
IF SNR > = 14 dB
Instruct the MS to change modulation technique
Choose QAM
Else
Choose QPSK
Allow MS to transmit
Return to origin

```

CHAPTER FOUR

DATA COLLECTION AND ANALYSIS

4.1 PRELIMINARY MEASUREMENT

RSS measurements up to a distance of 1500 meters were gathered in twelve (12) sites/ Base Stations where GSM, both GSM and W-CDMA Systems Co-exist, and two (2) other measurements were taken for W-CDMA and GSM Systems when deployed alone. The site name, angle of antenna alignment for the deployed Systems in Co-Location arrangement, antenna height, transmitting power, operating center frequency and Locations (Latitude and Longitude) are noted. The Measuring Instrument was the Transverse Electromagnetic Wave (TEMS) Investigation Application software programmed in a Laptop, sourced from Huawei Technologies (Installers of GSM and CDMA Equipment for both MTN and Visafone).

4.1.1 THE APPARATUS USED IN THE MEASUREMENT INCLUDES

1. GPS (Global Positioning System) GERMIN
2. Test mobile Sony K790 Ericcson Operated at 100% active mode
3. Tilt Adjuster
4. Binacular and digital compass
5. Classical node software
6. Laptop
7. Map Info professional software
8. Car

On start up, the software initializes the system by loading a configuration file which specifies the mode and the frequency of operation. This allows operator independent operation.

The equipment used for the azimuths of the antenna was a digital compass and a set of Binoculars. All readings were taken using true north. The binoculars were used in order to get a reasonable distance away from metal structure and still get an accurate Azimuth.

The tilts were taken using an electronic tilt meter while the height of antenna was measured using tape. Each Sector of the base station has PN code and carrier ID that distinguishes it from the other base station; with the PN code we were able to know which base station/Sector we received from at each test point to be sure that the reference BTS was correct. The following parameters are used in this report- Received Signal Strength, The Distance, frequency; BTS transmit power, Modulation Techniques and BTS antenna Height.

reading was taken at interval of 100m from the BTS and stopped at 1500m so that we do not enter into another BTS. The centres frequency of the transmitter are 2116.4MHz and 910MHz and the transmitter antenna gain of 16dB.

4.1.2 Measurement Site and Drive Route Selection

Twelve MTN BTS were visited and measurement were taken, since both Urban and Sub-Urban Model are required. Towns classified as Terrian Category A for Urban include the following towns- Owerre Towns, St Benedict Nwamadi Road Owerri, Oparaochie Village Mbaitli LGA and Umuejike Amaruru Iho which consists of tall Buildings, Factories, vehicular Traffic and densely Populated with human while towns classified as Terrain Category B for Suburban include the following towns- Ngo Okapla, New Market Area off Douglas Road and Obazu Mbiri which consists of sparsely located storey building, bungalows, Trees and Scattered Settlement.

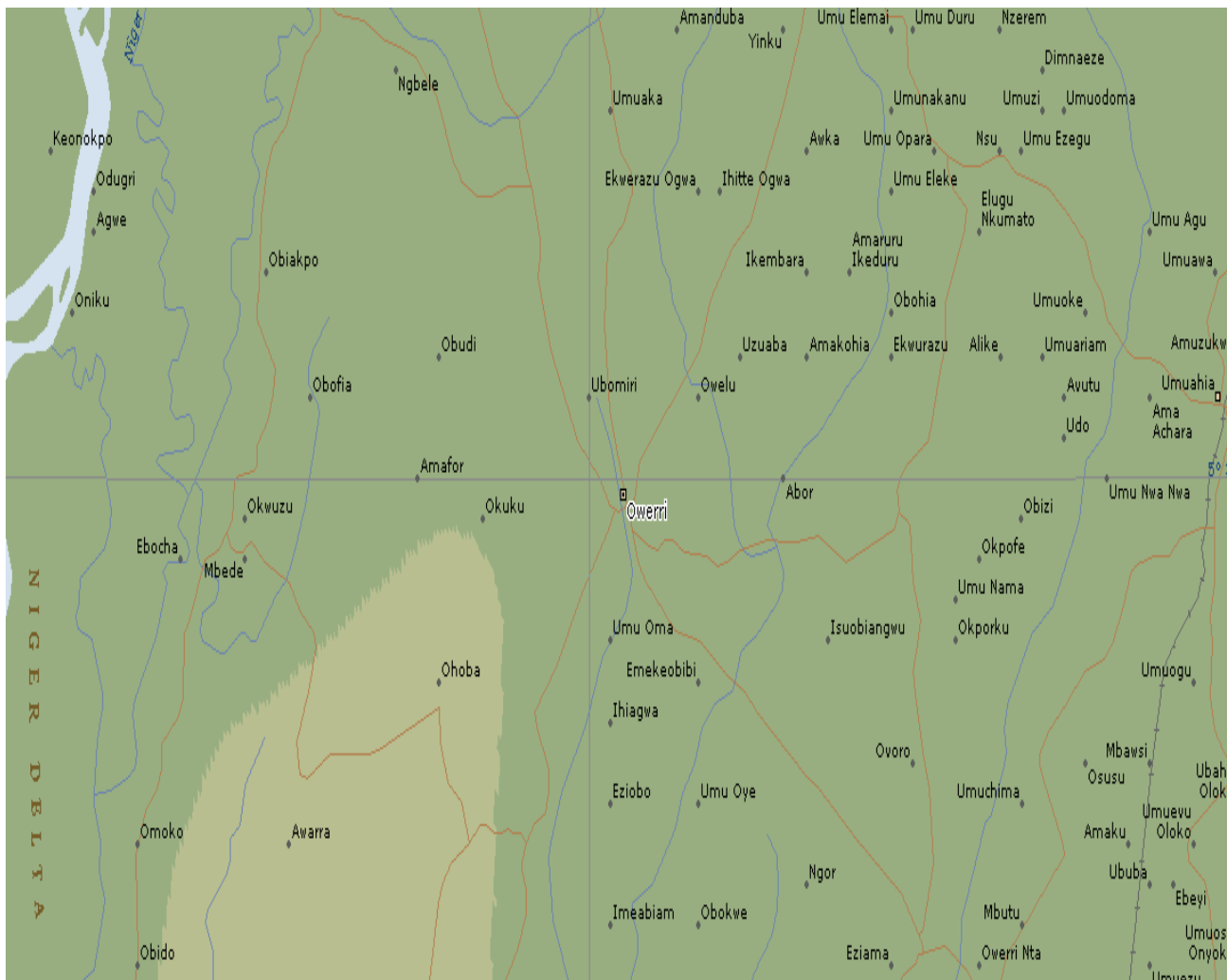
The selection of the 12 representative sites was done in such a way as to accommodate both environment scenarios in and around Imo State, table 4.1 shows the site selection showing the site name, modulation, class and category

Table 4.1 Site Selection and Classification

SITE ID	SITE NAME	CLASS	MODULATION TECHNIQUE	CATEGORY
IMO 322	Oparaochie Village	2G & 3G	QAM & QPSK	URBAN
IMO 323	Umuejike Amaruru Iho	2G & 3G	QAM & QPSK	URBAN
IMO 326	IDEM Rd, Mbaitolu LGA	2G & 3G	QAM & QPSK	SUB-URBAN
IMO 317	No 7, Umuodu Umueze-Uzoagba, Ikeduru LGA	2G & 3G	QAM & QPSK	SEMI-RURAL
IMO 048	OWERRI ROAD	3G ONLY	QAM	SUB-URBAN
IMO 339	Ngor Okpala LGA	2G & 3G	QAM	SUB-URBAN
IMO 344	Owerri North LGA,	2G & 3G	QAM	SUB-URBAN
IMO 473	NEW MKT AREA OFF DOUGLAS RD	2G & 3G	QAM	SUB-URBAN
IMO 047	MBAISE ROAD Owerri	2G ONLY	GMSK	URBAN
IMO 127	St Benedict, Nwamadi road Owerri	2G ONLY	GMSK	URBAN
IMO 054	OWERRI CENTRAL	2G	GMSK	URBAN
1MO 021	OBAZU MBIRI	2G	GMSK	Sub-RURAL

4.1.3 DATA CAPTURING TECHNIQUES

During the measurement drive test, the spacing between the sites is not the same because of the terrain and other factors. The figure 4.1 shows the map of selected base stations at Imo state, figure 4.2 shows the twelve selected sites. While table 4.2 to 4.14 shows the measured data from the twelve base stations and appendix A₂-A₁₄. shows the configuration of the two modulation technique, antenna configuration, antenna coupling, interface of frequency used, cable coupling, 3G and 2G interface, and testing the radio respectively.



The figure 4.1 shows the Map of selected base stations at Imo state for the test.

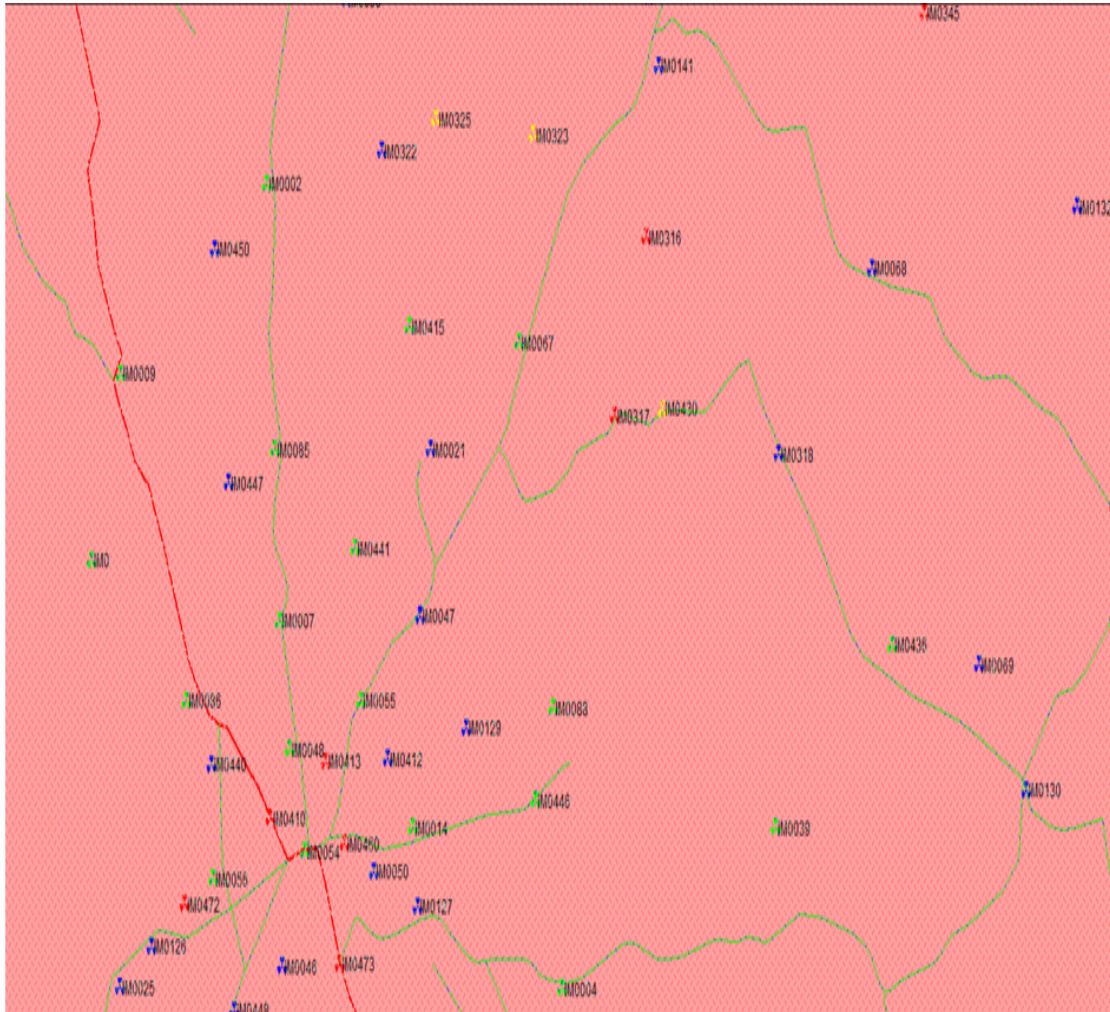


Figure 4.2 shows the selected BTS sites Imo state and its environments

Table 4.2 to 4.14 shows the average of the recorded received signal power (RAX) against respective distances measured.

TABLE 4.2 MEASURED DATA FROM BTS 1

						QAM MODULATION		QPSK MODULATION			
DISTANCE(M)	CLASS	Site ID	Site Name	FREQ (MHz)	TX POWER dBm	Antenna_Tilt	Rxav	Rxav	LATITUDE	LONGITUDE	Antenna Height
100	2G & 3G	IMO 322	Oparaochie Village	2116.4	44.1	4	-62	-50	7.04823	5.59538	30
200	2G & 3G	IMO 322	Oparaochie Village	2116.4	44.1	4	-65	-48	7.09344	5.59775	30
300	2G & 3G	IMO 322	Oparaochie Village	2116.4	44.1	4	-72	-51	7.09883	5.61931	30
400	2G & 3G	IMO 322	Oparaochie Village	2116.4	44.1	4	-85	-55	7.06436	5.60014	30
500	2G & 3G	IMO 322	Oparaochie Village	2116.4	44.1	4	-84	-53	7.07995	5.64786	30
600	2G & 3G	IMO 322	Oparaochie Village	2116.4	44.1	4	-88	-56	6.99528	5.80967	30
700	2G & 3G	IMO 322	Oparaochie Village	2116.4	44.1	4	-90	-55	7.02492	5.79853	30
800	2G & 3G	IMO 322	Oparaochie Village	2116.4	44.1	4	-91	-60	7.01232	5.79456	30
900	2G & 3G	IMO 322	Oparaochie Village	2116.4	44.1	4	-89	-70	7.02755	5.77738	30
1000	2G & 3G	IMO 322	Oparaochie Village	2116.4	44.1	4	-95	-72	7.03346	5.81062	30
1100	2G & 3G	IMO 322	Oparaochie Village	2116.4	44.1	4	-97	-75	7.02736	5.76075	30
1200	2G & 3G	IMO 322	Oparaochie Village	2116.4	44.1	4	-98	-78	7.19647	5.69008	30
1300	2G & 3G	IMO 322	Oparaochie Village	2116.4	44.1	4	-96	-88	6.96209	5.44623	30
1400	2G & 3G	IMO 322	Oparaochie Village	2116.4	44.1	4	-97	-89	7.13248	5.37597	30
1500	2G & 3G	IMO 322	Oparaochie Village	2116.4	44.1	4	-98	-93	7.09578	5.39178	30

TABLE 4.3 MEASURED DATA FROM BTS 2

						QAM MODULATION				
DISTANCE(M)	CLASS	Site ID	Site Name	FREQ (MHz)	TX POWER dBm	Antenna_Tilt	Rxav	LATITUDE	LONGITUDE	Antenna Height
100	2G	IMO 344	Owerri North LGA,	2116.4	17	4	-52	7.02083025	5.50538802	30
200	2G	IMO 344	Owerri North LGA,	2116.4	17	4	-50	7.03044452	5.42936525	30
300	2G	IMO 344	Owerri North LGA,	2116.4	17	4	-53	7.04589247	5.48702654	30
400	2G	IMO 344	Owerri North LGA,	2116.4	17	4	-57	6.99610813	5.38278138	30
500	2G	IMO 344	Owerri North LGA,	2116.4	17	4	-55	7.19702877	5.4248618	30
600	2G	IMO 344	Owerri North LGA,	2116.4	17	4	-58	7.15152713	5.39435815	30
700	2G	IMO 344	Owerri North LGA,	2116.4	17	4	-57	7.02544652	5.48999718	30
800	2G	IMO 344	Owerri North LGA,	2116.4	17	4	-62	7.04208203	5.51274549	30
900	2G	IMO 344	Owerri North LGA,	2116.4	17	4	-65	6.9980316	5.48594597	30
1000	2G	IMO 344	Owerri North LGA,	2116.4	17	4	-67	7.11161477	5.91224577	30
1100	2G	IMO 344	Owerri North LGA,	2116.4	17	4	-70	7.14836158	5.65260958	30
1200	2G	IMO 344	Owerri North LGA,	2116.4	17	4	-75	7.27480299	5.6326357	30
1300	2G	IMO 344	Owerri North LGA,	2116.4	17	4	-78	7.04044422	5.3053065	30
1400	2G	IMO 344	Owerri North LGA,	2116.4	17	4	-83	7.33155667	5.4865555	30
1500	2G	IMO 344	Owerri North LGA,	2116.4	17	4	-92	7.25213979	5.7687578	30

TABLE 4.4 MEASURED DATA FROM BTS 3

DISTANCE(M)	CLASS	Site ID	Site Name	FREQ (MHz)	TX POWER dBm	GMSK MODULATION		LATITUDE	LONGITUDE	Antenna Height
						Antenna_Tilt	Rxav			
100	2G	IMO 047	MBAISE ROAD Owerri,	910	43	4	-52	7.02083025	5.50538802	30
200	2G	IMO 047	MBAISE ROAD Owerri	910	43	4	-50	7.03044452	5.42936525	30
300	2G	IMO 047	MBAISE ROAD Owerri	910	43	4	-53	7.04589247	5.48702654	30
400	2G	IMO 047	MBAISE ROAD Owerri	910	43	4	-57	6.99610813	5.38278138	30
500	2G	IMO 047	MBAISE ROAD Owerri	910	43	4	-55	7.19702877	5.4248618	30
600	2G	IMO 047	MBAISE ROAD Owerri	910	43	4	-58	7.15152713	5.39435815	30
700	2G	IMO 047	MBAISE ROAD Owerri	910	43	4	-57	7.02544652	5.48999718	30
800	2G	IMO 047	MBAISE ROAD Owerri	910	43	4	-62	7.04208203	5.51274549	30
900	2G	IMO 047	MBAISE ROAD Owerri	910	43	4	-72	6.9980316	5.48594597	30
1000	2G	IMO 047	MBAISE ROAD Owerri	910	43	4	-74	7.11161477	5.91224577	30
1100	2G	IMO 047	MBAISE ROAD Owerri	910	43	4	-79	7.14836158	5.65260958	30
1200	2G	IMO 047	MBAISE ROAD Owerri	910	43	4	-82	7.27480299	5.6326357	30
1300	2G	IMO 047	MBAISE ROAD Owerri	910	43	4	-87	7.04044422	5.3053065	30
1400	2G	IMO 047	MBAISE ROAD Owerri	910	43	4	-91	7.33155667	5.4865555	30
1500	2G	IMO 047	MBAISE ROAD Owerri	910	43	4	-95	7.25213979	5.7687578	30

TABLE 4.5 MEASURED DATA FROM BTS 4

						QAM MODULATION		QPSK MODULATION			
DISTANCE(M)	CLASS	Site ID	Site Name	FREQ (MHz)	TX POWER dBm	Antenna_Tilt	Rxav	Rxav	LATITUDE	LONGITUDE	Antenna Height
100	2G & 3G	IMO 317	No 7, Umuodu Umue	2116.4	44.1	2	-62	-68	6.76991	5.37975	30
200	2G & 3G	1MO317	No 7, Umuodu Umue	2116.4	44.1	2	-64	-69	6.74675	5.77912	30
300	2G & 3G	IMO317	No 7, Umuodu Umue	2116.4	44.1	2	-65	-72	7.14811	5.32409	30
400	2G & 3G	IMO 317	No 7, Umuodu Umue	2116.4	44.1	2	-66	-74	7.11987	5.30666	30
500	2G & 3G	1MO317	No 7, Umuodu Umue	2116.4	44.1	2	-67	-75	6.95398	5.40849	30
600	2G & 3G	IMO317	No 7, Umuodu Umue	2116.4	44.1	2	-67	-75	7.2661	5.54182	30
700	2G & 3G	IMO 317	No 7, Umuodu Umue	2116.4	44.1	2	-68	-75	7.32006	5.45109	30
800	2G & 3G	1MO317	No 7, Umuodu Umue	2116.4	44.1	2	-69	-76	7.32672	5.46606	30
900	2G & 3G	IMO317	No 7, Umuodu Umue	2116.4	44.1	2	-71	-77	7.25217	5.45244	30
1000	2G & 3G	IMO 317	No 7, Umuodu Umue	2116.4	44.1	2	-72	-78	7.27684	5.43247	30
1100	2G & 3G	1MO317	No 7, Umuodu Umue	2116.4	44.1	2	-77	-79	7.24378	5.4275	30
1200	2G & 3G	IMO317	No 7, Umuodu Umue	2116.4	44.1	2	-78	-80	7.11419	5.32464	30
1300	2G & 3G	IMO 317	No 7, Umuodu Umue	2116.4	44.1	2	-79	-84	7.17894	5.33116	30
1400	2G & 3G	1MO317	No 7, Umuodu Umue	2116.4	44.1	2	-77	-87	7.12684	5.58244	30
1500	2G & 3G	IMO317	No 7, Umuodu Umue	2116.4	44.1	2	-79	-88	7.11753	5.55553	30

TABLE 4.6 MEASURED DATA FROM BTS 5

DISTANCE(M)	CLASS	Site ID	Site Name	FREQ (MHz)	TX POWER dBm	GMSK MODULATION		LATITUDE	LONGITUDE	Antenna Height
						Antenna_Tilt	Rxav			
100	2G	IMO 127	St Benedict, Nwamadi road Owerri	910	43	4	-50	7.252139	5.768751	24
200	2G	IMO 127	St Benedict, Nwamadi road Owerri	910	43	4	-48	7.178556	5.747722	24
300	2G	IMO 127	St Benedict, Nwamadi road Owerri	910	43	4	-51	7.146528	5.847167	24
400	2G	IMO 127	St Benedict, Nwamadi road Owerri	910	43	4	-55	7.126466	5.796544	24
500	2G	IMO 127	St Benedict, Nwamadi road Owerri	910	43	4	-53	7.089083	5.566583	24
600	2G	IMO 127	St Benedict, Nwamadi road Owerri	910	43	4	-56	7.193944	5.577694	24
700	2G	IMO 127	St Benedict, Nwamadi road Owerri	910	43	4	-55	7.225877	5.518133	24
800	2G	IMO 127	St Benedict, Nwamadi road Owerri	910	43	4	-60	7.019139	5.743583	24
900	2G	IMO 127	St Benedict, Nwamadi road Owerri	910	43	4	-70	6.960305	5.727861	24
1000	2G	IMO 127	St Benedict, Nwamadi road Owerri	910	43	4	-72	7.148366	5.346733	24
1100	2G	IMO 127	St Benedict, Nwamadi road Owerri	910	43	4	-77	7.303677	5.418344	24
1200	2G	IMO 127	St Benedict, Nwamadi road Owerri	910	43	4	-80	6.973056	5.620417	24
1300	2G	IMO 127	St Benedict, Nwamadi road Owerri	910	43	4	-90	6.881806	5.416583	24
1400	2G	IMO 127	St Benedict, Nwamadi road Owerri	910	43	4	-95	7.106056	5.666222	24
1500	2G	IMO 127	St Benedict, Nwamadi road Owerri	910	43	4	-93	7.12344	5.413444	24

TABLE 4.7 MEASURED DATA FROM BTS 6

						GMSK MODULATION				
DISTANCE(M)	CLASS	Site ID	Site Name	FREQ (MHz)	TX POWER dBm	Antenna_Tilt	Rxav	LATITUDE	LONGITUDE	Antenna Height
100	2G	IMO 054	OWERRI CENTRAL	910	43	4	-47	7.02083025	5.50538802	30
200	2G	IMO 054	OWERRI CENTRAL	910	43	4	-47	7.03044452	5.42936525	30
300	2G	IMO 054	OWERRI CENTRAL	910	43	4	-50	7.04589247	5.48702654	30
400	2G	IMO 054	OWERRI CENTRAL	910	43	4	-49	6.99610813	5.38278138	30
500	2G	IMO 054	OWERRI CENTRAL	910	43	4	-49	7.19702877	5.4248618	30
600	2G	IMO 054	OWERRI CENTRAL	910	43	4	-53	7.15152713	5.39435815	30
700	2G	IMO 054	OWERRI CENTRAL	910	43	4	-60	7.02544652	5.48999718	30
800	2G	IMO 054	OWERRI CENTRAL	910	43	4	-61	7.04208203	5.51274549	30
900	2G	IMO 054	OWERRI CENTRAL	910	43	4	-66	6.9980316	5.48594597	30
1000	2G	IMO 054	OWERRI CENTRAL	910	43	4	-72	7.11161477	5.91224577	30
1100	2G	IMO 054	OWERRI CENTRAL	910	43	4	-77	7.14836158	5.65260958	30
1200	2G	IMO 054	OWERRI CENTRAL	910	43	4	-80	7.27480299	5.63263577	30
1300	2G	IMO 054	OWERRI CENTRAL	910	43	4	-90	7.04044422	5.30530658	30
1400	2G	IMO 054	OWERRI CENTRAL	910	43	4	-90	7.33155667	5.48655556	30
1500	2G	IMO 054	OWERRI CENTRAL	910	43	4	-95	7.25213979	5.76875788	30

TABLE 4.8 MEASURED DATA FROM BTS 7

						QPSK MODULATION				
DISTANCE(M)	CLASS	Site ID	Site Name	FREQ (MHz)	TX POWER dBm	Antenna_Tilt	Rxav	Antenna Height	LATITUDE	LONGITUDE
100	2G & 3G	IMO 473	NEW MKT AREA OFF DOUGLAS RD	2116.4	19	2	-62	30	7.32006	5.45109
200	2G & 3G	IMO 473	NEW MKT AREA OFF DOUGLAS RD	2116.4	19	2	-64	30	7.32672	5.46606
300	2G & 3G	IMO 473	NEW MKT AREA OFF DOUGLAS RD	2116.4	19	2	-65	30	7.25217	5.45244
400	2G & 3G	IMO 473	NEW MKT AREA OFF DOUGLAS RD	2116.4	19	2	-66	30	7.27684	5.43247
500	2G & 3G	IMO 473	NEW MKT AREA OFF DOUGLAS RD	2116.4	19	2	-67	30	7.24378	5.43256
600	2G & 3G	IMO 473	NEW MKT AREA OFF DOUGLAS RD	2116.4	19	2	-67	30	7.11419	5.32464
700	2G & 3G	IMO 473	NEW MKT AREA OFF DOUGLAS RD	2116.4	19	2	-68	30	7.17894	5.33116
800	2G & 3G	IMO 473	NEW MKT AREA OFF DOUGLAS RD	2116.4	19	2	-69	30	7.12684	5.58244
900	2G & 3G	IMO 473	NEW MKT AREA OFF DOUGLAS RD	2116.4	19	2	-71	30	7.11753	5.55553
1000	2G & 3G	IMO 473	NEW MKT AREA OFF DOUGLAS RD	2116.4	19	2	-72	30	7.16613	5.54977
1100	2G & 3G	IMO 473	NEW MKT AREA OFF DOUGLAS RD	2116.4	19	2	-77	30	7.04823	5.59538
1200	2G & 3G	IMO 473	NEW MKT AREA OFF DOUGLAS RD	2116.4	19	2	-78	30	7.09344	5.59775
1300	2G & 3G	IMO 473	NEW MKT AREA OFF DOUGLAS RD	2116.4	19	2	-79	30	7.09883	5.61931
1400	2G & 3G	IMO 473	NEW MKT AREA OFF DOUGLAS RD	2116.4	19	2	-77	30	7.06436	5.60014
1500	2G & 3G	IMO 473	NEW MKT AREA OFF DOUGLAS RD	2116.4	19	2	-79	30	7.07995	5.64786

TABLE 4.9 MEASURED DATA FROM BTS 8

						QAM MODULATION				
DISTANCE(M)	CLASS	Site ID	Site Name	FREQ (MHz)	TX POWER dBm	Antenna_Tilt	Rxav	LATITUDE	LONGITUDE	Antenna Height
100	2G & 3G	1MO 048	OWERRI ROAD	2116.4	44.1	4	-51	7.02083025	5.50538802	30
200	2G & 3G	1MO 048	OWERRI ROAD	2116.4	44.1	4	-53	7.03044452	5.42936525	30
300	2G & 3G	1MO 048	OWERRI ROAD	2116.4	44.1	4	-57	7.04589247	5.48702654	30
400	2G & 3G	1MO 048	OWERRI ROAD	2116.4	44.1	4	-58	6.99610813	5.38278138	30
500	2G & 3G	1MO 048	OWERRI ROAD	2116.4	44.1	4	-65	7.19702877	5.4248618	30
600	2G & 3G	1MO 048	OWERRI ROAD	2116.4	44.1	4	-67	7.15152713	5.39435815	30
700	2G & 3G	1MO 048	OWERRI ROAD	2116.4	44.1	4	-69	7.02544652	5.48999718	30
800	2G & 3G	1MO 048	OWERRI ROAD	2116.4	44.1	4	-70	7.04208203	5.51274549	30
900	2G & 3G	1MO 048	OWERRI ROAD	2116.4	44.1	4	-72	6.9980316	5.48594597	30
1000	2G & 3G	1MO 048	OWERRI ROAD	2116.4	44.1	4	-74	7.11161477	5.91224577	30
1100	2G & 3G	1MO 048	OWERRI ROAD	2116.4	44.1	4	-79	7.14836158	5.65260958	30
1200	2G & 3G	1MO 048	OWERRI ROAD	2116.4	44.1	4	-82	7.27480299	5.6326357	30
1300	2G & 3G	1MO 048	OWERRI ROAD	2116.4	44.1	4	-86	7.04044422	5.3053065	30
1400	2G & 3G	1MO 048	OWERRI ROAD	2116.4	44.1	4	-88	7.33155667	5.4865555	30
1500	2G & 3G	1MO 048	OWERRI ROAD	2116.4	44.1	4	-94	7.25213979	5.7687578	30

TABLE 4.10 MEASURED DATA FROM BTS 9

DISTANCE(M)	CLASS	Site ID	Site Name	FREQ (MHz)	TX POWER dBm	QAM MODULATION		LATITUDE	LONGITUDE	Antenna Height
						Antenna_Tilt	Rxav			
100	2G & 3G	IMO 339	Ngor Okpala LGA	2116.4	44.1	4	-41	7.13248	5.37597	30
200	2G & 3G	IMO 339	Ngor Okpala LGA	2116.4	44.1	4	-46	7.09578	5.39178	30
300	2G & 3G	IMO 339	Ngor Okpala LGA	2116.4	44.1	4	-52	7.08044	5.34838	30
400	2G & 3G	IMO 339	Ngor Okpala LGA	2116.4	44.1	4	-55	7.0962	5.43181	30
500	2G & 3G	IMO 339	Ngor Okpala LGA	2116.4	44.1	4	-57	7.11198	5.44681	30
600	2G & 3G	IMO 339	Ngor Okpala LGA	2116.4	44.1	4	-58	7.06105	5.40975	30
700	2G & 3G	IMO 339	Ngor Okpala LGA	2116.4	44.1	4	-60	7.20953	5.61616	30
800	2G & 3G	IMO 339	Ngor Okpala LGA	2116.4	44.1	4	-62	7.24019	5.62272	30
900	2G & 3G	IMO 339	Ngor Okpala LGA	2116.4	44.1	4	-72	7.19778	5.6315	30
1000	2G & 3G	IMO 339	Ngor Okpala LGA	2116.4	44.1	4	-74	7.0615	5.76759	30
1100	2G & 3G	IMO 339	Ngor Okpala LGA	2116.4	44.1	4	-79	7.06183	5.78347	30
1200	2G & 3G	IMO 339	Ngor Okpala LGA	2116.4	44.1	4	-82	7.28658	5.53703	30
1300	2G & 3G	IMO 339	Ngor Okpala LGA	2116.4	44.1	4	-88	7.01522	5.49511	30
1400	2G & 3G	IMO 339	Ngor Okpala LGA	2116.4	44.1	4	-89	7.03006	5.44083	30
1500	2G & 3G	IMO 339	Ngor Okpala LGA	2116.4	44.1	4	-93	7.04985	5.50388	30

TABLE 4.11 MEASURED DATA FROM BTS 10

						QAM MODULATION		QPSK MODULATION				
DISTANCE(M)	CLASS	Site ID	Site Name	FREQ (MHz)	TX POWER dBm	Antenna_Tilt	Rxav	Antenna_Tilt	Rxav	LATITUDE	LONGITUDE	Antenna Height
100	2G & 3G	1MO 323	Umuejike Amaruru Iho	2116.4	44.1	4	-52	4	-50	7.03346	5.81062	30
200	2G & 3G	1MO 323	Umuejike Amaruru Iho	2116.4	44.1	4	-50	4	-48	7.02736	5.76075	30
300	2G & 3G	1MO 323	Umuejike Amaruru Iho	2116.4	44.1	4	-53	4	-51	7.19647	5.69008	30
400	2G & 3G	1MO 323	Umuejike Amaruru Iho	2116.4	44.1	4	-57	4	-55	6.96209	5.44623	30
500	2G & 3G	1MO 323	Umuejike Amaruru Iho	2116.4	44.1	4	-55	4	-53	7.13248	5.37597	30
600	2G & 3G	1MO 323	Umuejike Amaruru Iho	2116.4	44.1	4	-58	4	-56	7.09578	5.39178	30
700	2G & 3G	1MO 323	Umuejike Amaruru Iho	2116.4	44.1	4	-57	4	-55	7.08044	5.34838	30
800	2G & 3G	1MO 323	Umuejike Amaruru Iho	2116.4	44.1	4	-62	4	-60	7.0962	5.43181	30
900	2G & 3G	1MO 323	Umuejike Amaruru Iho	2116.4	44.1	4	-72	4	-70	7.11198	5.44681	30
1000	2G & 3G	1MO 323	Umuejike Amaruru Iho	2116.4	44.1	4	-74	4	-72	7.06105	5.40975	30
1100	2G & 3G	1MO 323	Umuejike Amaruru Iho	2116.4	44.1	4	-79	4	-77	7.20953	5.61616	30
1200	2G & 3G	1MO 323	Umuejike Amaruru Iho	2116.4	44.1	4	-82	4	-80	7.24019	5.62272	30
1300	2G & 3G	1MO 323	Umuejike Amaruru Iho	2116.4	44.1	4	-99	4	-85	7.19778	5.6315	30
1400	2G & 3G	1MO 323	Umuejike Amaruru Iho	2116.4	44.1	4	-97	4	-87	7.0615	5.76759	30
1500	2G & 3G	1MO 323	Umuejike Amaruru Iho	2116.4	44.1	4	-95	4	-89	7.06183	5.78347	30

TABLE 4.12 MEASURED DATA FROM BTS 11

							QAM MODULATION	QPSK MODULATION			
DISTANCE(M)	CLASS	Site ID	Site Name	FREQ (MHz)	TX POWER dBm	Antenna_Tilt	Rxav	Rxav	LATITUDE	LONGITUDE	Antenna Height
100	2G & 3G	IMO 326	IDEM Rd, Mbaitolu LGA	2116.4	44.1	2	-63	-60	7.07995	5.64786	30
200	2G & 3G	IMO 326	IDEM Rd, Mbaitolu LGA	2116.4	44.1	2	-65	-62	6.99528	5.80967	30
300	2G & 3G	IMO 326	IDEM Rd, Mbaitolu LGA	2116.4	44.1	2	-67	-65	7.02492	5.7985	30
400	2G & 3G	IMO 326	IDEM Rd, Mbaitolu LGA	2116.4	44.1	2	-70	-68	7.0123	5.79456	30
500	2G & 3G	IMO 326	IDEM Rd, Mbaitolu LGA	2116.4	44.1	2	-72	-70	7.02755	5.77738	30
600	2G & 3G	IMO 326	IDEM Rd, Mbaitolu LGA	2116.4	44.1	2	-74	-68	7.03346	5.81062	30
700	2G & 3G	IMO 326	IDEM Rd, Mbaitolu LGA	2116.4	44.1	2	-75	-72	7.02736	5.76075	30
800	2G & 3G	IMO 326	IDEM Rd, Mbaitolu LGA	2116.4	44.1	2	-77	-73	7.19647	5.69008	30
900	2G & 3G	IMO 326	IDEM Rd, Mbaitolu LGA	2116.4	44.1	2	-78	-74	6.96209	5.44623	30
1000	2G & 3G	IMO 326	IDEM Rd, Mbaitolu LGA	2116.4	44.1	2	-80	-75	7.13248	5.37597	30
1100	2G & 3G	IMO 326	IDEM Rd, Mbaitolu LGA	2116.4	44.1	2	-82	-75	7.09578	5.39178	30
1200	2G & 3G	IMO 326	IDEM Rd, Mbaitolu LGA	2116.4	44.1	2	-83	-78	7.08044	5.34838	30
1300	2G & 3G	IMO 326	IDEM Rd, Mbaitolu LGA	2116.4	44.1	2	-84	-79	7.0962	5.43181	30
1400	2G & 3G	IMO 326	IDEM Rd, Mbaitolu LGA	2116.4	44.1	2	-87	-80	7.11198	5.44681	30
1500	2G & 3G	IMO 326	IDEM Rd, Mbaitolu LGA	2116.4	44.1	2	-93	-82	7.06105	5.40975	30

TABLE 4.13 MEASURED DATA FROM BTS 12

						GMSK MODULATION				
DISTANCE(M)	CLASS	Site ID	Site Name	FREQ (MHz)	TX POWER dBm	Antenna Tilt	Rxav	LATITUDE	LONGITUDE	Antenna Height
100	2G	IMO 021	OBAZU MBIRI	910	43	2	-62	7.32006	5.45109	30
200	2G	IMO 021	OBAZU MBIRI	910	43	2	-64	7.32672	5.46606	30
300	2G	IMO 021	OBAZU MBIRI	910	43	2	-65	7.25217	5.45244	30
400	2G	IMO 021	OBAZU MBIRI	910	43	2	-66	7.27684	5.43247	30
500	2G	IMO 021	OBAZU MBIRI	910	43	2	-67	7.24378	5.43256	30
600	2G	IMO 021	OBAZU MBIRI	910	43	2	-67	7.11419	5.32464	30
700	2G	IMO 021	OBAZU MBIRI	910	43	2	-68	7.17894	5.33116	30
800	2G	IMO 021	OBAZU MBIRI	910	43	2	-69	7.12684	5.58244	30
900	2G	IMO 021	OBAZU MBIRI	910	43	2	-71	7.11753	5.55553	30
1000	2G	IMO 021	OBAZU MBIRI	910	43	2	-72	7.16613	5.54977	30
1100	2G	IMO 021	OBAZU MBIRI	910	43	2	-77	7.04823	5.59538	30
1200	2G	IMO 021	OBAZU MBIRI	910	43	2	-78	7.09344	5.59775	30
1300	2G	IMO 021	OBAZU MBIRI	910	43	2	-79	7.09883	5.61931	30
1400	2G	IMO 021	OBAZU MBIRI	910	43	2	-77	7.06436	5.60014	30
1500	2G	IMO 021	OBAZU MBIRI	910	43	2	-79	7.07995	5.64786	30

Equation (3.11) was used in the MATLAB code for the calculation of the pathloss exponents (n).

4.2. DETERMINATION OF PATH LOSS CHARACTERIZATION FOR CATEGORY A

Applying equation (3.4), the Path loss for each BTS was measured and the average path loss of Terrain category-'A' sites was determined. Tables 4.15, 4.16 and 4.17 show the determined average path loss for the sites in categories –A for QAM, QPSK and GMSK Modulation techniques respectively and Figure 4.4 show the path loss against distance for the three modulation techniques aforementioned

TABLE 4.15: Average Pathloss For Category A QAM Modulation Technique

D (KM)	ANTENNA TILT	QAM MODULATION MEDIAN Rx dBm	Pt (dBm)	MEDIAN PL (dbm)
0.1	2	-63	44.1	107
0.2	2	-65	44.1	109
0.3	2	-67	44.1	111
0.4	2	-70	44.1	114
0.5	2	-72	44.1	116
0.6	2	-74	44.1	118
0.7	2	-75	44.1	119
0.8	2	-77	44.1	121
0.9	2	-78	44.1	122
1.0	2	-80	44.1	124
1.1	2	-82	44.1	126
1.2	2	-83	44.1	127
1.3	2	-84	44.1	128
1.4	2	-87	44.1	131
1.5	2	-93	44.1	137

TABLE 4.16: Average Pathloss for Category A QPSK Modulation Technique

D (KM)	ANTENNA TILT	QPSK MODULATION MEDIAN Rx dBm	Pt (dBm)	MEDIAN PL (dbm)
0.1	2	-60	44.1	104
0.2	2	-62	44.1	106
0.3	2	-65	44.1	109
0.4	2	-68	44.1	112
0.5	2	-70	44.1	114
0.6	2	-68	44.1	112
0.7	2	-72	44.1	116
0.8	2	-73	44.1	117
0.9	2	-74	44.1	118
1.0	2	-75	44.1	119
1.1	2	-75	44.1	119
1.2	2	-78	44.1	122
1.3	2	-79	44.1	123
1.4	2	-80	44.1	124
1.5	2	-82	44.1	126

TABLE 4.17: Average Pathloss for Category A GMSK Modulation Technique

D (KM)	ANTENNA TILT	GMSK MODULATION MEDIAN Rx dBm	Pt (dBm)	MEDIAN PL (dbm)
0.1	4	-50	43	93
0.2	4	-48	43	91
0.3	4	-51	43	94
0.4	4	-55	43	98
0.5	4	-53	43	96
0.6	4	-56	43	99
0.7	4	-55	43	98
0.8	4	-60	43	103
0.9	4	-70	43	113
1.0	4	-72	43	115
1.1	4	-77	43	120
1.2	4	-80	43	123
1.3	4	-90	43	133
1.4	4	-95	43	138
1.5	4	-93	43	136

Figure 4.3 shows the path loss against distance for three modulation techniques QAM,QPSK and GMSK.

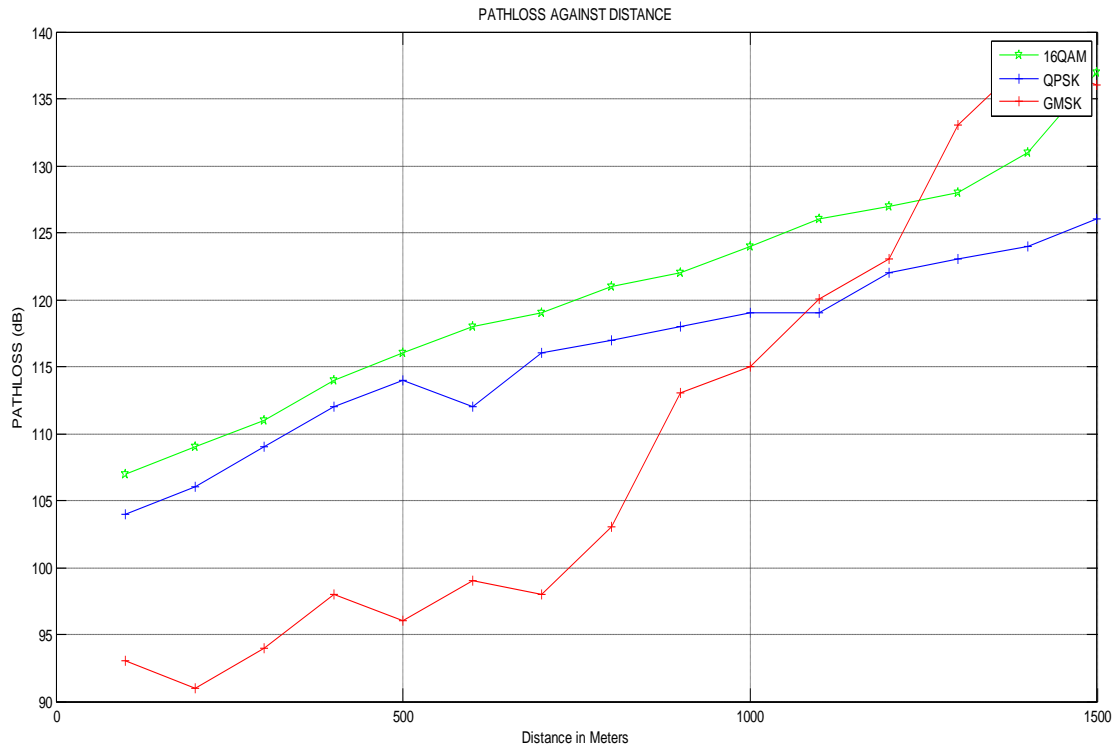


Figure 4.3 shows the path loss against distance for three modulation techniques QAM, QPSK and GMSK. generated using Matlab code (Appendix A) based on measured data. The path loss is greater in QAM followed by QPSK then GMSK as indicated in the figure 4.3

The mean values for the three modulation techniques shown in figure 4.3 are given as - see (appendix A),

- 1 The path loss exponent of the terrain category A using QAM MODULATION was derived as 2.06.
2. The path loss exponent of the terrain category A using QPSK MODULATION was derived as 1.49
3. The path loss exponent of the terrain category A using GMSK MODULATION was derived as 2.11

The resultant equation for path loss of this category is given from equation (3.7) as

$$L_p(d_i) = L_p(d_o) + n \log_{10}(d_i/d_o) + s \dots \dots \dots (4.1)$$

Where s is the shadow fading variation about the linear relationship and has a *rms* value that best minimizes the error that can be determined by equation (4.2) [64]

$$\text{Where: } S = \sqrt{\sum_{i=1}^k \frac{(P_m - P_r)^2}{N}} \dots \dots \dots 4.2$$

P_m : Measured path loss (dB), P_r : Predicted path loss (dB) and N : Number of Measured Data Points, here it is 15.

The value of s was calculated using MATLAB (see appendix B for code.

- The value of s was calculated for QAM MODULATION was derived as 4.16
- The value of s was calculated for QPSK MODULATION was derived as 2.033
- The value of s was calculated for GMSK MODULATION was derived as 10.95

❖ DETERMINATION OF PATHLOSS MODEL FOR QAM MODULATION in Urban

Substituting $s = 4.16$ and the $L_p(d_o) = 107$ of table 4.15 in equation (4.1), the resultant Path loss Model for urban cities using QAM modulation technique is given as:

$$L_p\{d\} = 107 + 20.633 \log(d/d_o) + 4.16 \dots \dots \dots (4.2)$$

Hence,

$$L_p\{d\} = 111 + 20.63 \log_{10}(d/d_o) \dots \dots \dots (4.2)$$

Equation 4.2 represents the measured Model for urban cities using QAM Modulation.

➤ DETERMINATION OF PATHLOSS MODEL FOR QPSK

MODULATION in Urban Category A

Substituting $s = 2.033$ and the $L_p(d) = 104$ of table 4.16 in equation (4.1), the resultant Path loss Model for urban cities using QPSK modulation technique is given as:

$$L_p\{d\} = 104 + 14.938\log(d/d_0) + 2.0331 \dots\dots\dots (4.3)$$

Hence,

$$L_p\{d\} = 106 + 14.94\log_{10}(d/d_0) \dots\dots\dots (4.3)$$

Equation 4.3 represents the measured Model for urban cities using QPSK Modulation.

➤ DETERMINATION OF PATHLOSS MODEL FOR GMSK

MODULATION IN URBAN

Substituting $s = 10.95$ and the $L_p(d) = 93$ of table 4.19 in equation (4.1), the resultant Path loss Model for urban cities using GMSK modulation technique is given as:

$$L_p\{d\} = 93 + 21.104\log(d/d_0) + 10.95 \dots\dots\dots (4.4)$$

Hence,

$$L_p\{d\} = 103 + 21.104\log_{10}(d/d_0) \dots\dots\dots (4.4)$$

Equation 4.4 represents the measured Model for urban cities USING GMSK Modulation.

4.3 HATA'S MODEL FOR CATEGORY A

Recall that from equation (2.39), the Hata's model for an urban environment was stated as:

$$L_p(\text{Urban}) = 69.55 - 26.161\log_{10}(f) - 13.82 \log_{10}(hb) - a(hm) + (44.9 - 6.55 \log_{10}(hb)\log_{10}(d), \text{ where:}$$

$$a(hm) = (1.1\log_{10}(f) - 0.7)hm - (1.56 \log_{10}(d).$$

Where hm is the mobile antenna height, hb is the Base station antenna height and f is the frequency in MHz.

At Frequency of 2116.4Mhz

Substituting the values: $f=2116.4\text{MHz}$, $hm=1.5\text{m}$ and $hb=30\text{m}$ into the equation above yields:

$$L_p(\text{Urban}) = 176.6 + 8.12 \log d \dots\dots\dots (4.5)$$

At Frequency of 910Mhz

Substituting the values: $f=910.\text{MHz}$, $hm=1.5\text{m}$ and $hb=30\text{m}$ into the equation above yields:

$$L_p(\text{Urban}) = 77.82 + 8.12 \log d \dots\dots\dots (4.6)$$

4.4 COST-231 EXTENDED HATA MODEL FOR CATEGORY A

A model that is widely used for predicting path loss in mobile wireless system is the COST-231 Hata model.

The COST-231 Hata model is designed to be used in the frequency band from 500MHz to 2000MHz. It also contains corrections for urban, suburban and rural environments. Thus its frequency range is within that of the measurements, its simplicity and the availability of correction factors have made it widely used for path loss prediction. The basic equation for path loss in dB is:

$$PL = 46.3 + 33.9 \log(f) - 13.82 \log(hb) - ahm + (44.9 - 6.55 \log(hb)) \log_d + Cm \dots\dots\dots (4.7)$$

Where, f is the frequency in MHz, d is the distance between AP and CPE antennas in km , and hb is the AP antenna height above ground level in meters. The parameter Cm is defined as 0dB for suburban or open environments and 3dB for urban environments. The parameter ahm is defined for urban environments as:

$$ahm = 3.20(\log(11.75hr))^2 - 4.97, f > 400\text{MHz} \dots\dots\dots (4.8)$$

For suburban or rural (flat) environments,

$$ahm = (1.1 \log f - 0.7) - (1.56 \log f - 0.8) \dots\dots\dots (4.9)$$

Where, hr is the CPE antenna height above ground level. The path loss exponent of the predictions made by COST-231 Hata mode is given by:

$$n_{\text{cost}} = (44.9 - 6.55 \log(hb)) / 10 \dots\dots\dots (4.10)$$

To evaluate the applicability of the cost-231 model for the 3.5GHz band, the model predictions are compared against measurements for three different environments, namely, rural (flat), suburban and urban.

substituting the values: $F=2116.4\text{MHz}$ $hr=1.5\text{m}$ and $hb=30\text{m}$, into equations 4.7 and 4.8 yields the COST-231 Hata model as:

$$Lp_{\text{cost}} = 183.5 + 9.68 \log d \dots\dots\dots (4.11)$$

4.5 FREE-SPACE MODEL FOR CATEGORY A

Recall that from equation (4.6), the free-space model was given as:

At Frequency of 2116.4Mhz

$$Lp_{fr} = 32.5 + 20 \log_{10}(d) + 20 \log_{10} f$$

This gives:

$$Lp_{fs} = 91.36 + 20 \log d, \text{ where: } f = 2116.4\text{MHz} \dots\dots\dots (4.12)$$

At Frequency of 910Mhz

$$Lp_{fs} = 91.68 + 20 \log d, \text{ where: } f = 910\text{MHz} \dots\dots\dots (4.13)$$

Table 4.18, shows the comparison between the measured data at Frequency 2116.4Mhz for QAM and QPSK ,Hata ,COST-231, and Free Space Models using equation 4.2,4.3, 4.11and 4.12

Table 4.18 The comparison between the measured data at Frequency 2116.4Mhz

D (KM)	QAM Measured (dB)	QPSK Measured (dB)	HATA (dB)	COST- 231 (dB)	Free space (dB)
0.1	90	91	168	173	79
0.2	96	95	170	176	85
0.3	100	98	172	178	88
0.4	102	100	173	179	91
0.5	104	101	174	180	93
0.6	106	102	175	181	95
0.7	107	103	175	182	96
0.8	109	104	176	183	97
0.9	110	105	176	183	98
1.0	111	106	176	184	99
1.1	112	107	177	184	100
1.2	113	107	177	184	101
1.3	113	108	178	185	101
1.4	114	109	178	185	102
1.5	115	109	178	185	103

Table 4.19, shows the comparison between the measured data at Frequency 910 MHz for GMSK , Hata ,COST-231, and Free Space Models using equation 4.4, 4.11, 4.12 and 4.13 while plotting this Comparison using the MATLAB code of Appendix C gives the figure 4.4

TABLE 4.19 the comparison between the measured data at Frequency 910 MHz

D (KM)	GMSK Measured (dB)	HATA (dB)	COST- 231 (dB)	Free space (dB)
0.1	81	69	161	71
0.2	88	72	164	77
0.3	92	73	166	81
0.4	94	74	167	85
0.5	96	75	168	87
0.6	98	76	169	88
0.7	99	77	170	89
0.8	100	77	170	90
0.9	102	77	171	91
1.0	103	78	171	93
1.1	104	78	172	94
1.2	105	79	172	94
1.3	105	79	172	95
1.4	106	79	173	95
1.5	107	79	173	103

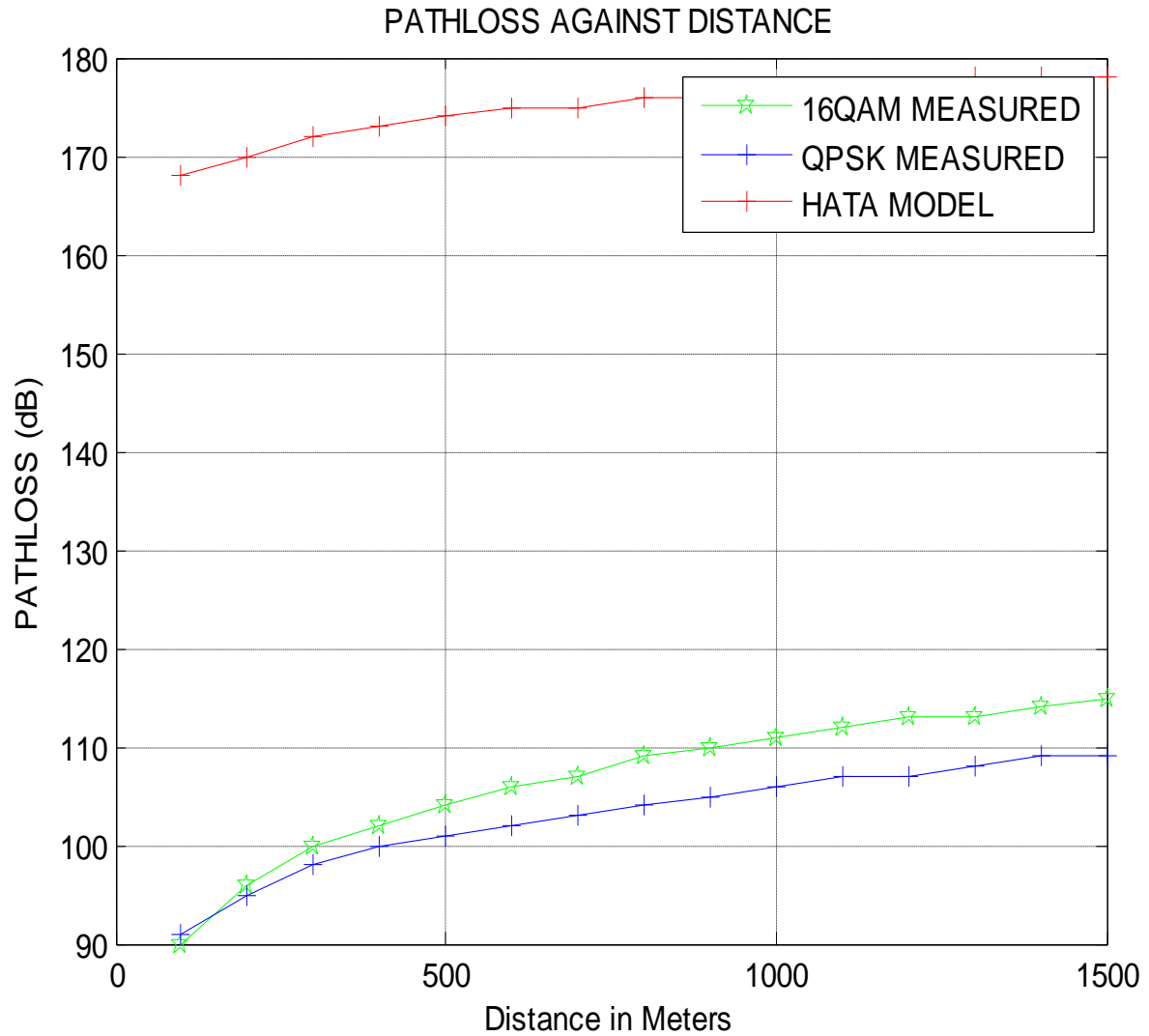


Figure 4.4 A Comparison of path loss models (Hata Model) with Measured Models For Urban, The path loss is greater in Hata Model compared to measured data using QAM and QPSK Technique.

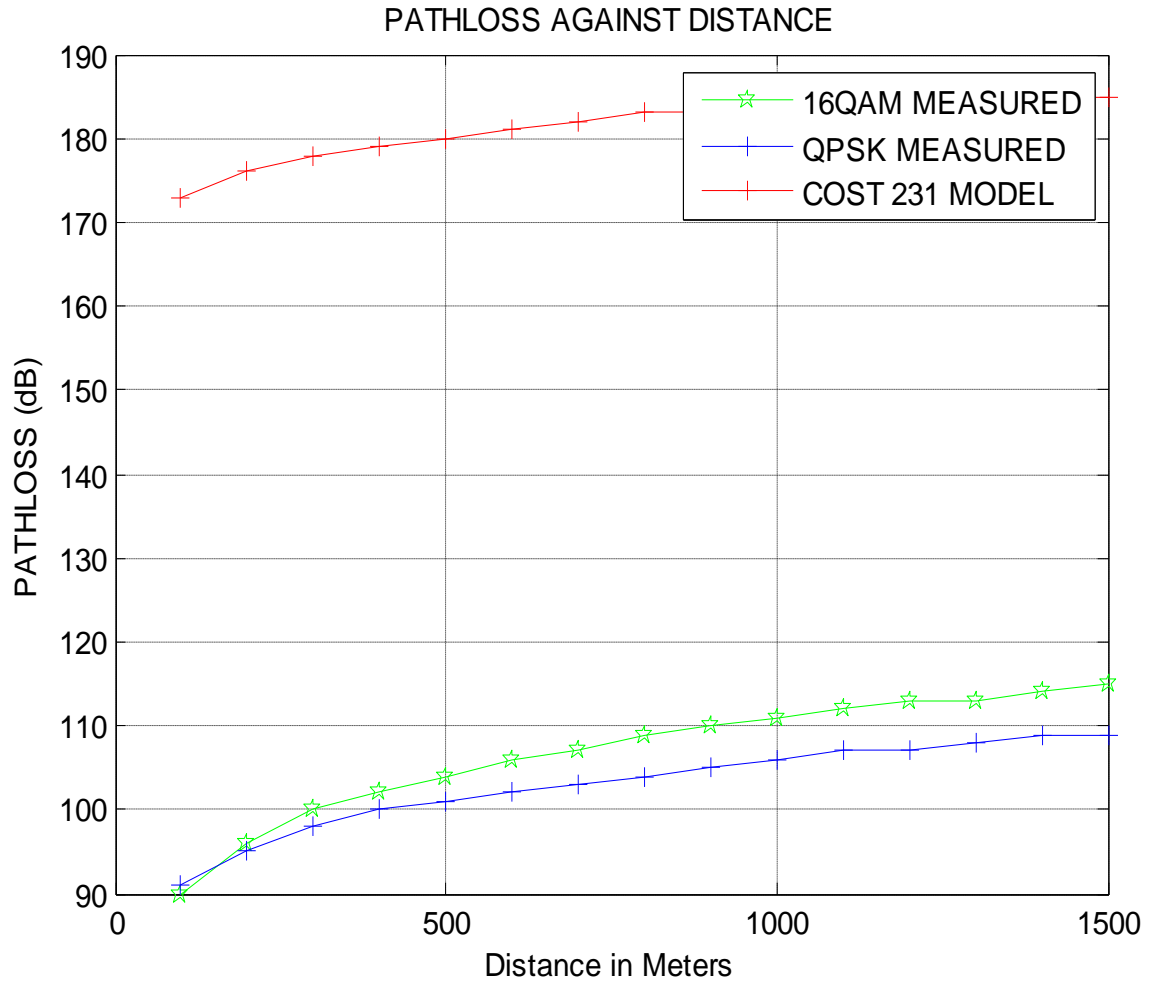


Figure 4.5 Comparison of path loss models (COST 231 Model) with Measured Models for Urban Category A. The path loss is greater in COST 231 Model compared to measured data using QAM and QPSK Technique.

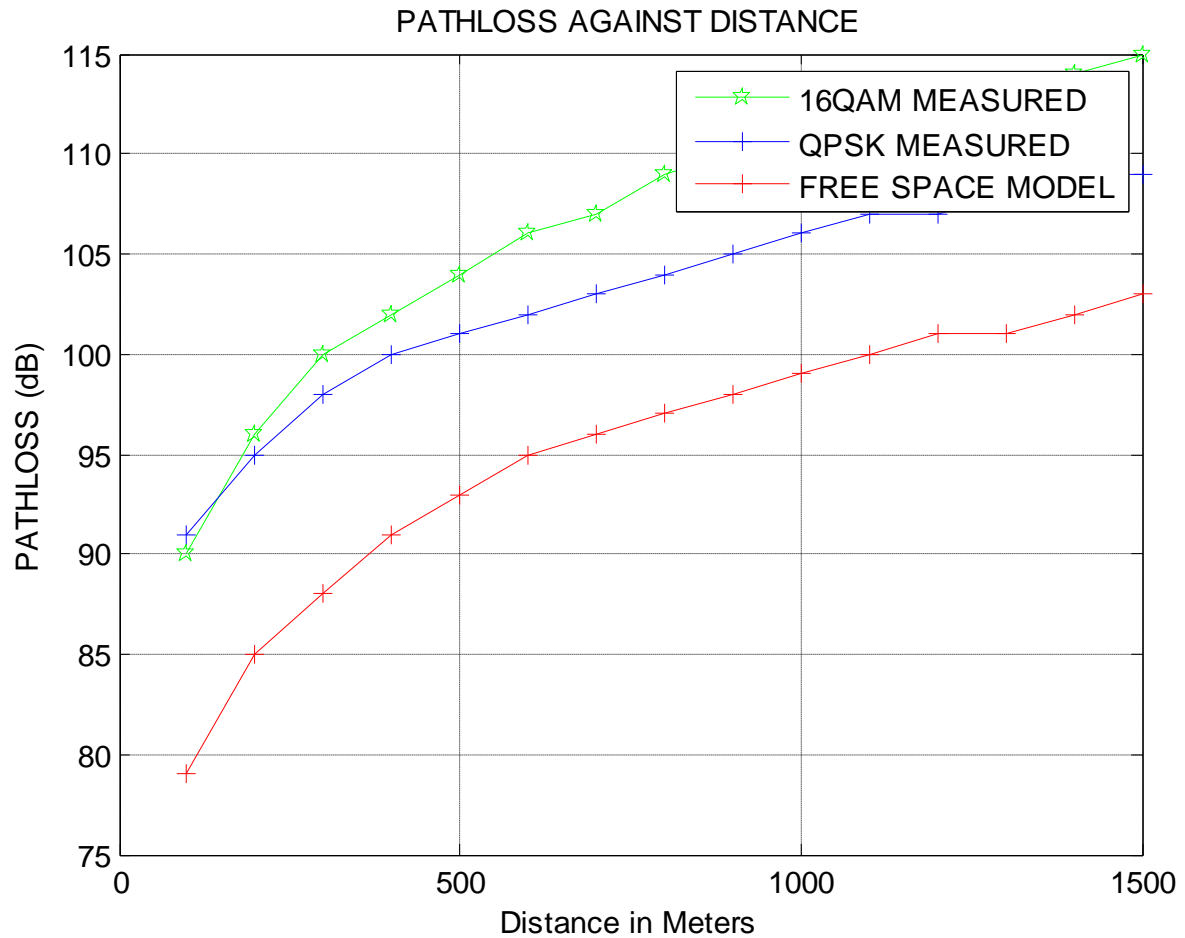


FIGURE 4.6 Comparison of path loss models (Free Space Model) with Measured Models for Urban Category A. The path loss is greater in measured data using QAM and QPSK modulation Model compared to free space loss because in free space model it assumed that there is no obstruction between the transmitter and receiver.

4.6: MODIFICATION OF HATA MODEL FOR CATEGORY A

The modification of the Hata model was done by calculating the mean square error (MSE) between the measured and the Hata models using equation (4.2)

Where P_r is the Hata predicated values and

$$S = \sqrt{\sum_{i=1}^k \frac{(P_m - P_r)^2}{N}}$$

P_m is the measured values for each instance of distance d (see Appendix D).

This MSE was found to be.

The value of s was calculated using MATLAB (see appendix B for code) .

- The value of s was calculated for QAM MODULATION was derived as 6.82
- The value of s was calculated for QPSK MODULATION was derived as 7.96
- The value of s was calculated for GMSK MODULATION was derived as 2.94

Subtracting this MSE from the original Hata model gives its modified version. Obviously, as can be seen by the comparison plot of figure 4.7 and 4.8, the modified version of the Hata model can suitably be used for network planning in the urban cities of Imo State, as it correlates with the measured model. This figure was simulated using the MATLAB code of Appendix E.

Table 4.20, shows the comparison between the measured data at Frequency 2116.4 MHz for QAM and QPSK, Hata, COST-231, Free Space Models and Modified Hata Models for Urban Cities of Imo State

Table 4.20 Comparison between Measured Models and Modified Hata Model

D (KM)	QAM Measur ed (dB)	QPSK Measured (dB)	HATA (dB)	COST-231 (dB)	Free space (dB)	MODIFIED HATA FOR QAM (dB)	MODIFIED HATA FOR QPSK (dB)
0.1	90	91	168	173	79	99.81	96.04
0.2	96	95	170	176	85	101.81	98.04
0.3	100	98	172	178	88	103.81	100.04
0.4	102	100	173	179	91	104.81	101.04
0.5	104	101	174	180	93	105.81	102.04
0.6	106	102	175	181	95	106.81	103.04
0.7	107	103	175	182	96	106.81	103.04
0.8	109	104	176	183	97	107.81	104.04
0.9	110	105	176	183	98	107.81	104.04
1.0	111	106	176	184	99	107.81	104.04
1.1	112	107	177	184	100	108.81	105.04
1.2	113	107	177	184	101	108.81	105.04
1.3	113	108	178	185	101	109.81	106.04
1.4	114	109	178	185	102	109.81	106.04
1.5	115	109	178	185	103	109.81	106.04

Figure 4.7 and 4.8 show comparison between the measured Models (QAM and QPSK modulation) and Modified Hata Models For Urban Category A

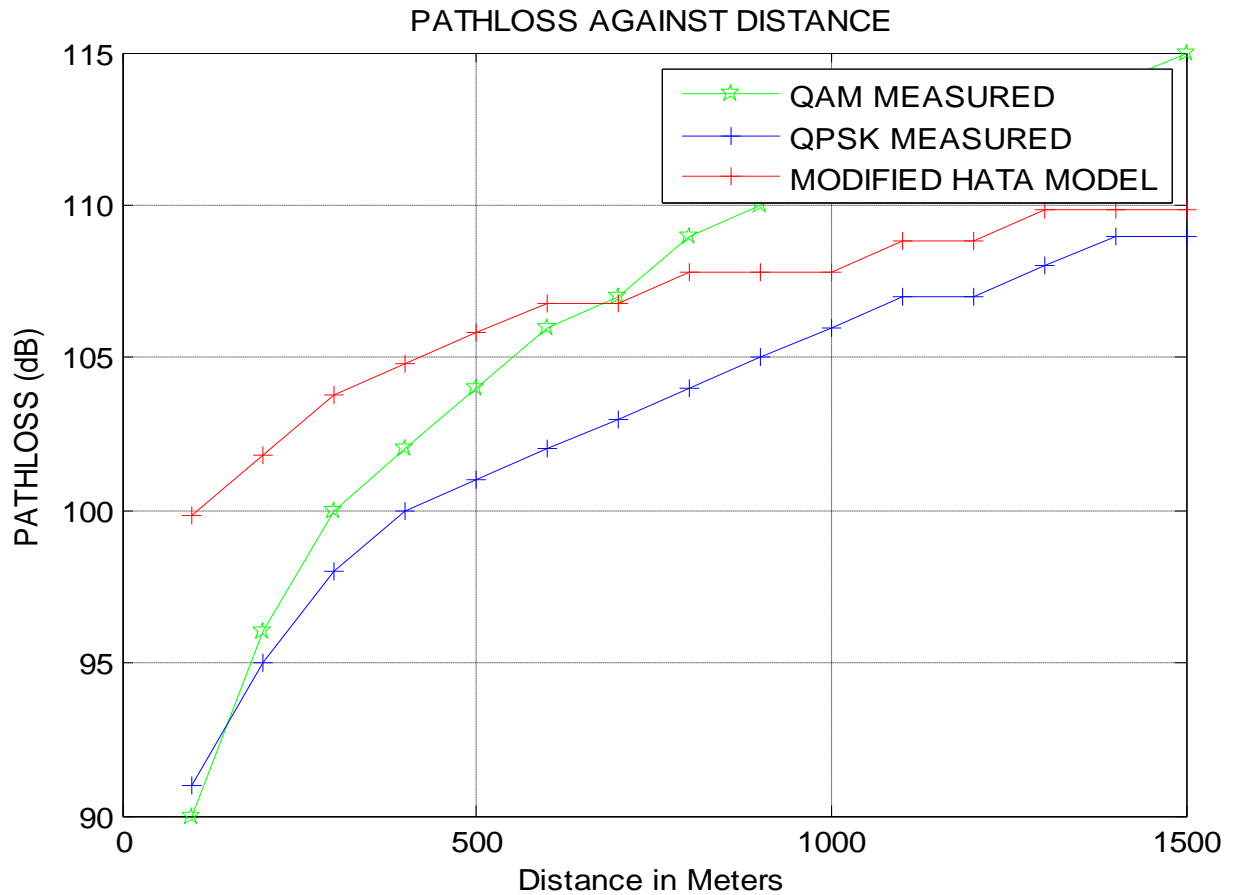


Figure 4.7 Comparison between the measured Models and Modified Hata Model for QAM for Urban Category A. The path loss is greater in QAM Model followed by modified Hata model then QPSK model, thus the three model can be adaptively deployed in category A as in indicated in figure 4.7

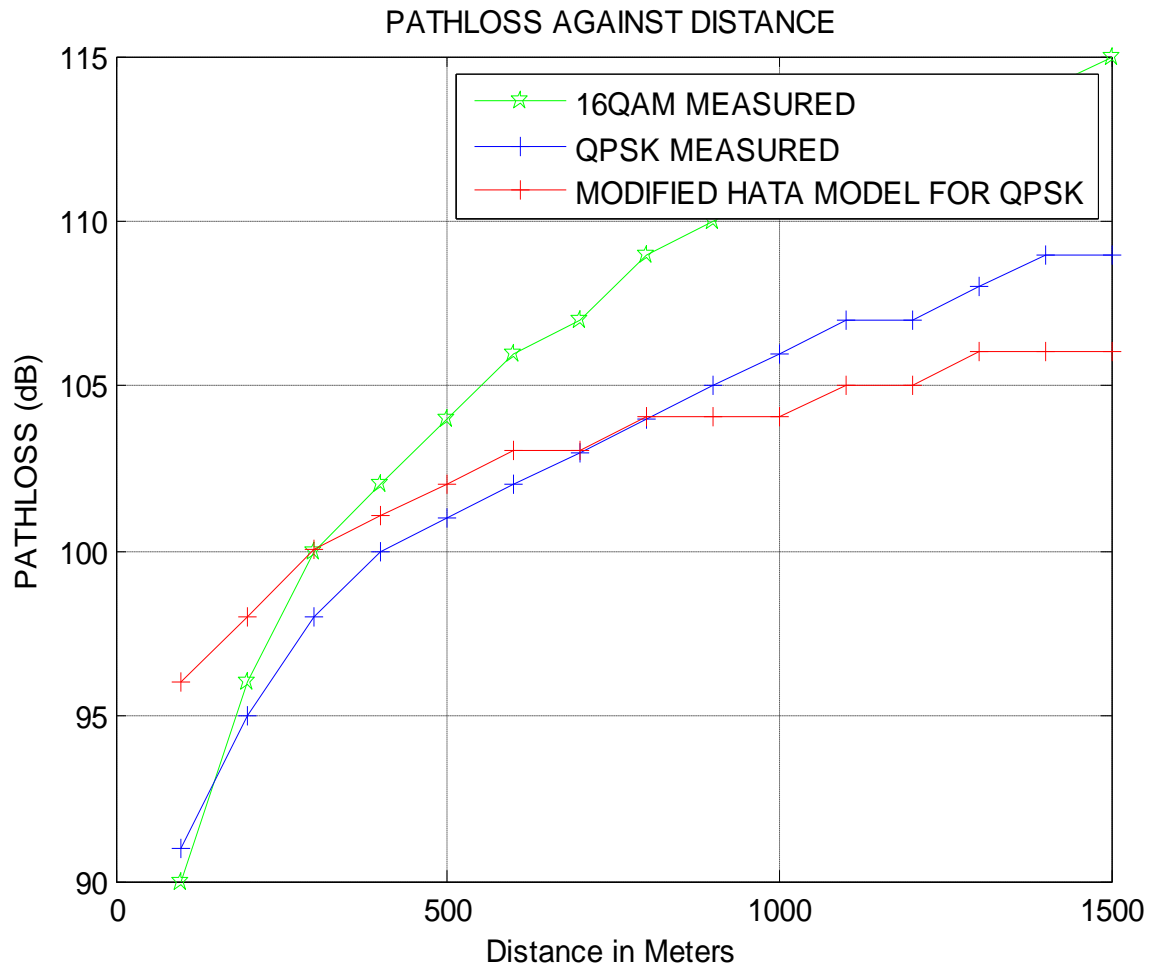


Figure 4.8 shows comparison between the measured Models and Modified Hata Models for QPSK For Urban Category A. The path loss is greater in QAM Model followed by QPSK model then modified Hata model, thus the three model can be adaptively deployed in category A as in indicated in figure 4.8

4.7 DETERMINATION OF PATH LOSS CHARACTERIZATION FOR CATEGORY B

TABLE 4.21: Average Pathloss For Category B , QAM Modulation Technique

D (KM)	ANTENNA TILT	QAM MODULATION MEDIAN Rx dBm	Pt (dBm)	MEDIAN PL (dbm)
0.1	4	-51	44.1	95
0.2	4	-53	44.1	97
0.3	4	-57	44.1	102
0.4	4	-58	44.1	102
0.5	4	-65	44.1	109
0.6	4	-67	44.1	113
0.7	4	-69	44.1	113
0.8	4	-70	44.1	114
0.9	4	-72	44.1	116
1.0	4	-74	44.1	118
1.1	4	-79	44.1	123
1.2	4	-82	44.1	126
1.3	4	-86	44.1	130
1.4	4	-88	44.1	132
1.5	4	-94	44.1	138

TABLE 4.22: Average Pathloss For Category B , QPSK Modulation Technique

D (KM)	ANTENNA TILT	QPSK MODULATION MEDIAN Rx dBm	Pt (dBm)	MEDIAN PL (dbm)
0.1	2	-62	19	81
0.2	2	-64	19	83
0.3	2	-65	19	84
0.4	2	-66	19	85
0.5	2	-67	19	86
0.6	2	-67	19	86
0.7	2	-68	19	87
0.8	2	-69	19	88
0.9	2	-71	19	90
1.0	2	-72	19	91
1.1	2	-77	19	96
1.2	2	-78	19	97
1.3	2	-79	19	98
1.4	2	-77	19	96
1.5	2	-79	19	98

A plot of the path loss against distance is shown in figure 4.9

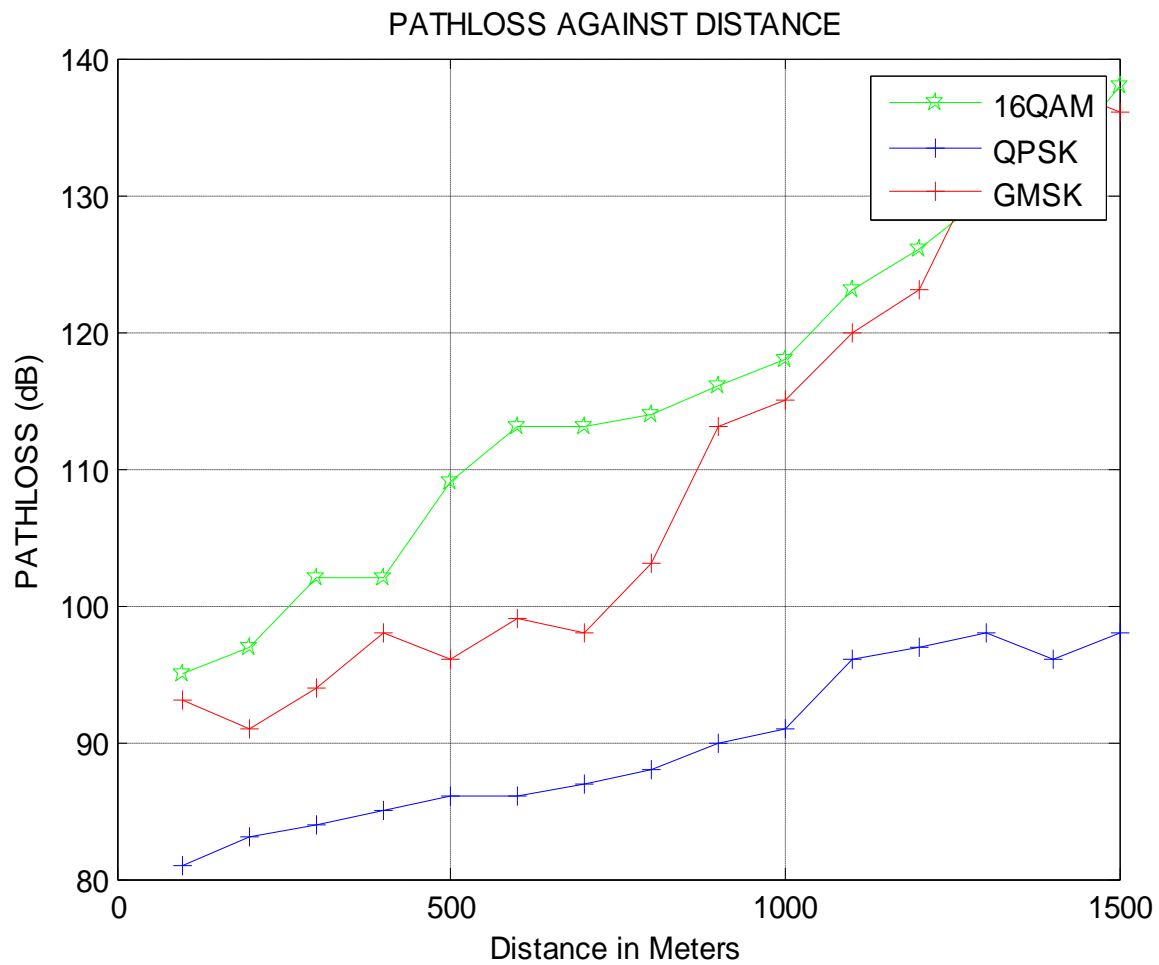


Figure 4.9, A plot of the path loss against distance for category B.

The path loss is greater in QAM Model followed by GMSK model then QAM model, thus the three model can be adaptively deployed in category B

Again, simulating equation (3.11) using MATLAB (Appendix F),

The path loss exponent of the terrain category B using

QAM MODULATION was derived as 2.5

The path loss exponent of the terrain category B using QPSK MODULATION was derived as 1.08

And the corresponding Shadow factor for QAM and QPSK for Category B, was derived as 5.24 and 2.83 respectively.

(Appendix G). Following the equation (4.12), the model for this category is:

❖ **DETERMINATION OF PATHLOSS MODEL FOR QAM MODULATION**

In Sub-Urban and the $L_p(d_0) = 95$ of table 4.21 in equation (4.14), the resultant Path loss Model for sub-urban cities using QAM modulation technique is given as:

$$L_p\{d\} = 95 + 25\log(d/d_0) + 5.24 \text{ -----(4.14)}$$

Hence,

$$L_p\{d\} = 100.24 + 25\log_{10}(d/d_0) \text{(4.14)}$$

Equation 4.14 represents the measured Model for sub-urban cities using QAM Modulation.

➤ **DETERMINATION OF PATHLOSS MODEL FOR QPSK MODULATION in Sub-Urban**

Substituting $s = 2.83$ and the $L_p(d) = 81$ of table 4.22 in equation (4.15), the resultant Path loss Model for sub-urban cities using QPSK modulation technique is given as:

$$L_p\{d\} = 81 + 10.8\log(d/d_0) + 2.83 \text{ (4.15)}$$

Hence,

$$L_p\{d\} = 83.83 + 10.8\log_{10}(d/d_0) \text{ (4.15)}$$

Equation 4.15 represents the measured Model for sub-urban cities using QPSK Modulation for Category B.

4.8 : HATA'S MODEL FOR CATEGORY B

Given that,

$$L_p(\text{Urban}) = 69.55 + 26.161 \log_{10}(f) - 13.82 \log_{10}(hb) - a(hm) + (44.9 - 6.55 \log_{10}(hb) \log_{10}(d)),$$

where:

$$a(hm) = (1.1 \log_{10}(f) - 0.7)hm - (1.561 \log_{10}(d)),$$

$$L_p(\text{suburban}) = L_p\{\text{urban}\} - 2[\log(f/28)]^2 - 5.4 \dots \dots \dots (4.16)$$

Substituting the parameters: $hb=30m$, $f=2116.4\text{MHz}$ and $hm=1.5m$ into the equations above gives that, for this category, Hata's model becomes:

$$L_p\{\text{suburban}\} = 164.96 + 8.12 \log d \dots \dots \dots (4.17)$$

4.9: COST-231 EXTENDED HATA MODEL FOR CATEGORY B

Substituting the parameters: $hb=45m$, $f=2116.4\text{MHz}$ and $hm=1.5m$ into equations 4.17 and 4.19 gives the COST-231 model for this category as:

$$L_p\{\text{suburban}\} = 184.96 + 9.6 \log d \dots \dots \dots (4.18)$$

The Comparison between the measured models, Hata, COST 231 and Free Space models is shown in table 4.10. A plot of this Comparison is given by the MATLAB code of (Appendix H) is shown in figure 4.10, 4.11 and 4.12 respectively,

TABLE 4.23 Comparison among the models for suburban category B

D (KM)	QAM Measured (dB)	QPSK Measured (dB)	HATA (dB)	COST-231 (dB)	Free space (dB)
0.1	75	73	156	175	79
0.2	83	76	159	178	85
0.3	87	78	161	180	88
0.4	90	79	162	181	91
0.5	93	80	163	182	93
0.6	95	81	163	183	95
0.7	97	82	164	183	96
0.8	98	82	164	184	97
0.9	99	83	164	185	98
1.0	100	84	165	185	99
1.1	102	84	165	185	100
1.2	102	85	166	186	101
1.3	103	85	166	186	101
1.4	104	85	166	186	102
1.5	105	86	166	187	103

Comparison of path loss models with Measured Models for Sub- Urban

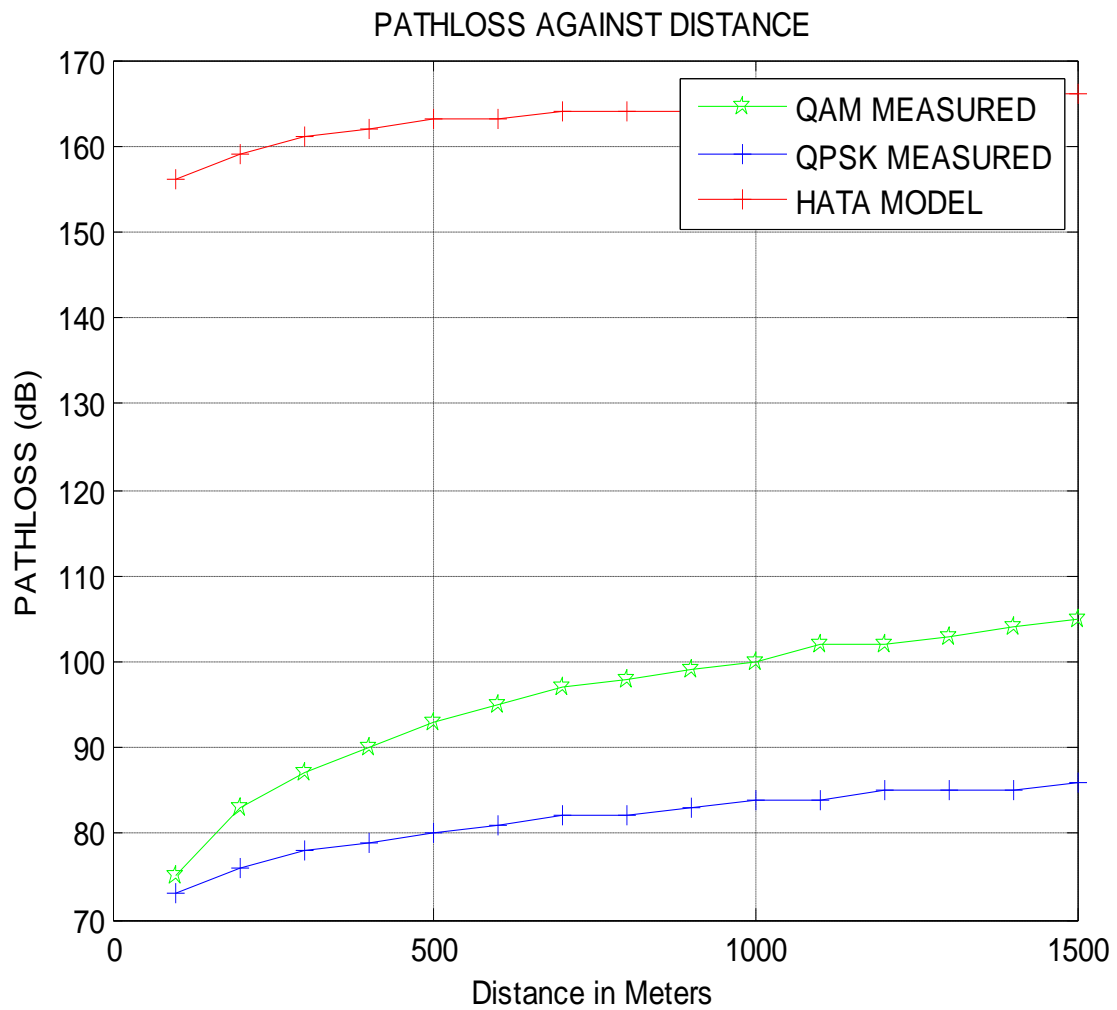


Figure 4.10 Comparison of path loss models (HATA Model) with Measured Models for Sub- Urban Category B. From the figure 4.10 the path loss is greater in Hata Model compared to measured data using QAM and QPSK Technique, in category B , sub –urban.

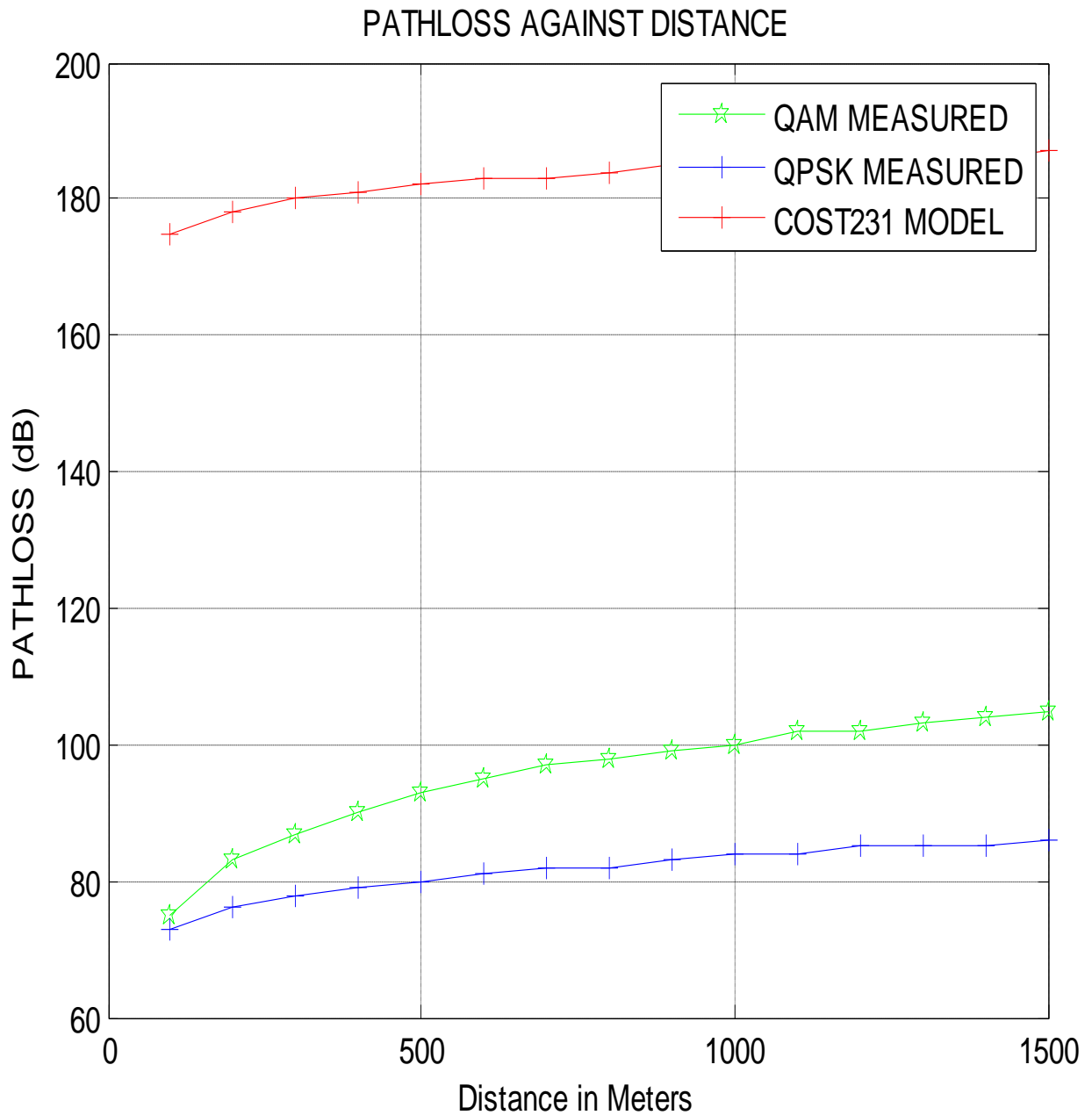


Figure 4.11 Comparison of path loss models (COST 231 Model) with Measured Models for Sub-Urban Category B. From the figure 4.11 the path loss is greater in COST 231 Model compared to measured data using QAM and QPSK Model, in category B , sub -urban

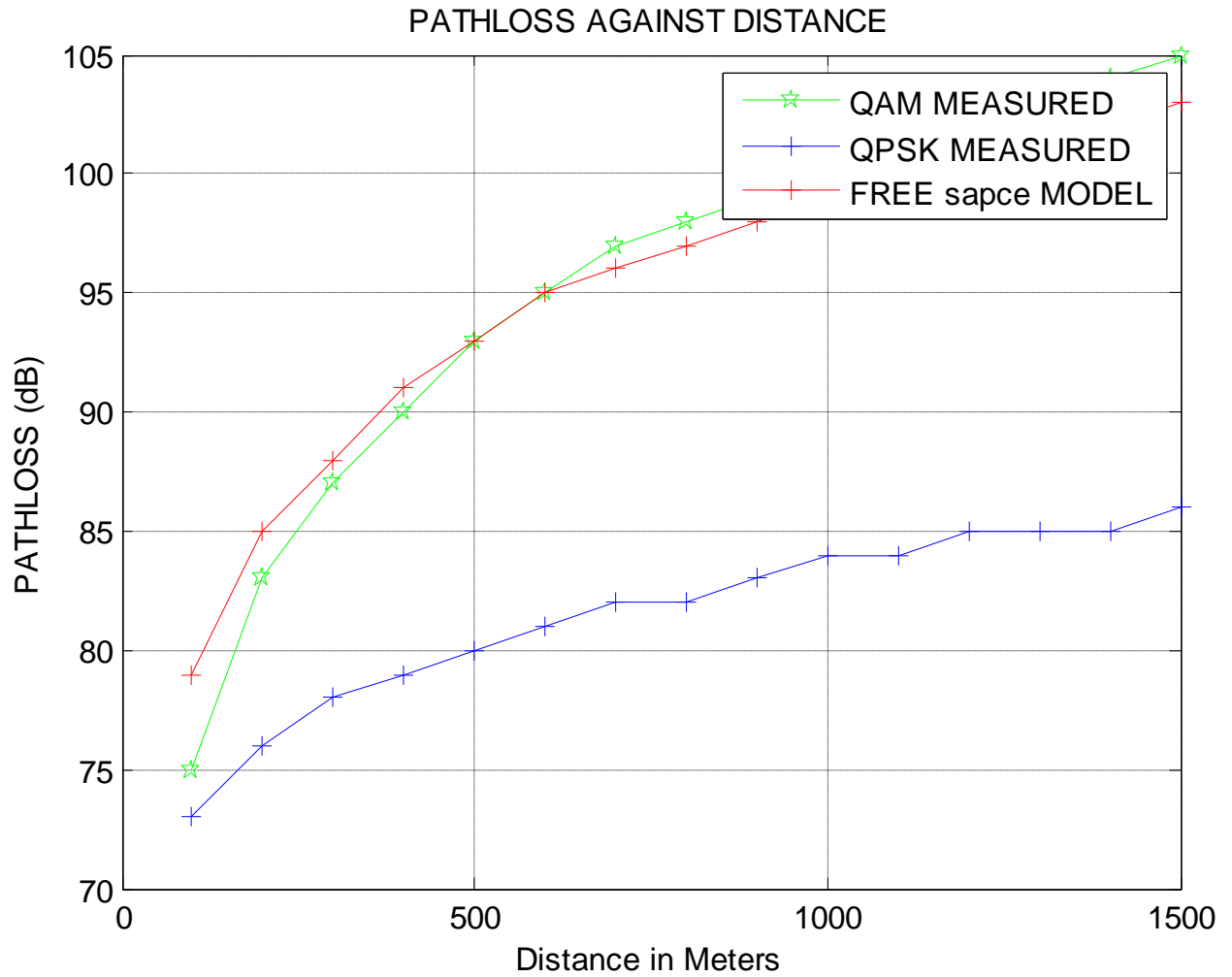


Figure 4.12 Comparison of path loss models (free Space Model) with Measured Models for Sub- Urban Category B

The path loss is greater in measured data using QAM and QPSK modulation Model compared to free space loss

4.10 MODIFICATION OF HATA MODEL FOR CATEGORY B

The modification of the Hata model was done by calculating the mean square error(MSE) between the measured and the Hata models using equation (4.2)

Where P_r is the Hata predicated values and

$$S = \sqrt{\sum_{i=1}^k \frac{(P_m - P_r)^2}{N}}$$

P_m is the measured values for each instance of distance d (see Appendix G).

The value of s was calculated using MATLAB codes (see appendix B for code) .

This MSE was found to be:

- The value of s was calculated for QAM MODULATION was derived as 6.89
- The value of s was calculated for QPSK MODULATION was derived as 7.19

Subtracting this MSE values from the original Hata model gives the modified version of Hata for QAM and QPSK respectively as shown in table 4.23 and the figure was simulated using MATLAB code of Appendix H

Table 4.23 Comparison between Measured Models and Modified Hata Model

D (KM)	QAM Measured (dB)	QPSK Measured (dB)	HATA (dB)	COST- 231 (dB)	Free space (dB)	Modified HATA for QAM (dB)	MODIFIED HATA FOR QPSK (dB)
0.1	75	73	156	175	79	99.81	96.04
0.2	83	76	159	178	85	101.81	98.04
0.3	87	78	161	180	88	103.81	100.04
0.4	90	79	162	181	91	104.81	101.04
0.5	93	80	163	182	93	105.81	102.04
0.6	95	81	163	183	95	106.81	103.04
0.7	97	82	164	183	96	106.81	103.04
0.8	98	82	164	184	97	107.81	104.04
0.9	99	83	164	185	98	107.81	104.04
1.0	100	84	165	185	99	107.81	104.04
1.1	102	84	165	185	100	108.81	105.04
1.2	102	85	166	186	101	108.81	105.04
1.3	103	85	166	186	101	109.81	106.04
1.4	104	85	166	186	102	109.81	106.04
1.5	105	86	166	187	103	109.81	106.04

Figure 4.13 and 4.14 show comparison between the measured Model for QAM, QPSK modulation and Modified Hata Models for Sub-Urban Category B

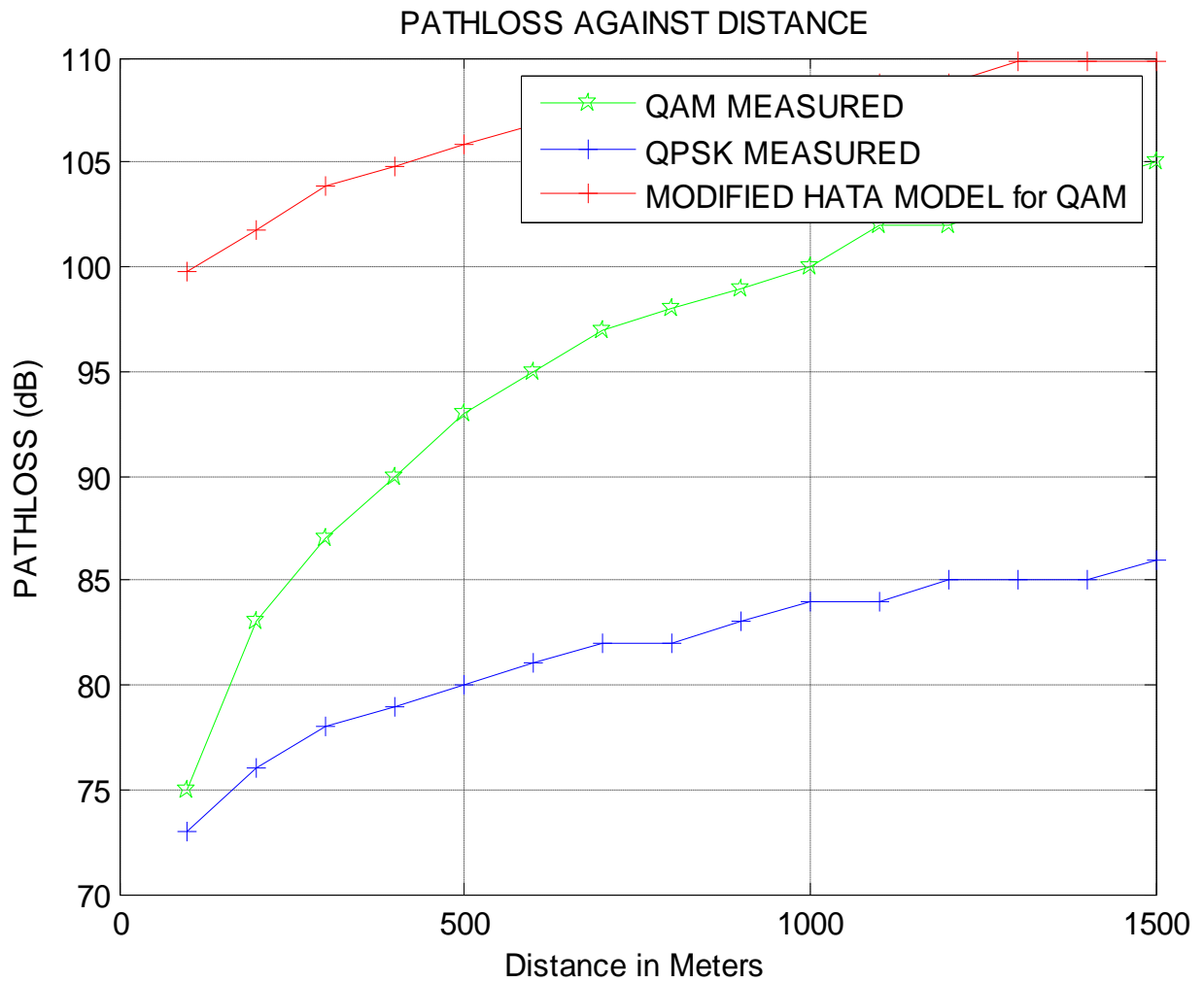


Figure 4.13 shows comparison between the measured Models and Modified Hata Model for QAM for Sub-Urban Category B.

The path loss is greater in modified Hata Model compared to measured data using QAM and QPSK Technique, in category B , sub-urban.

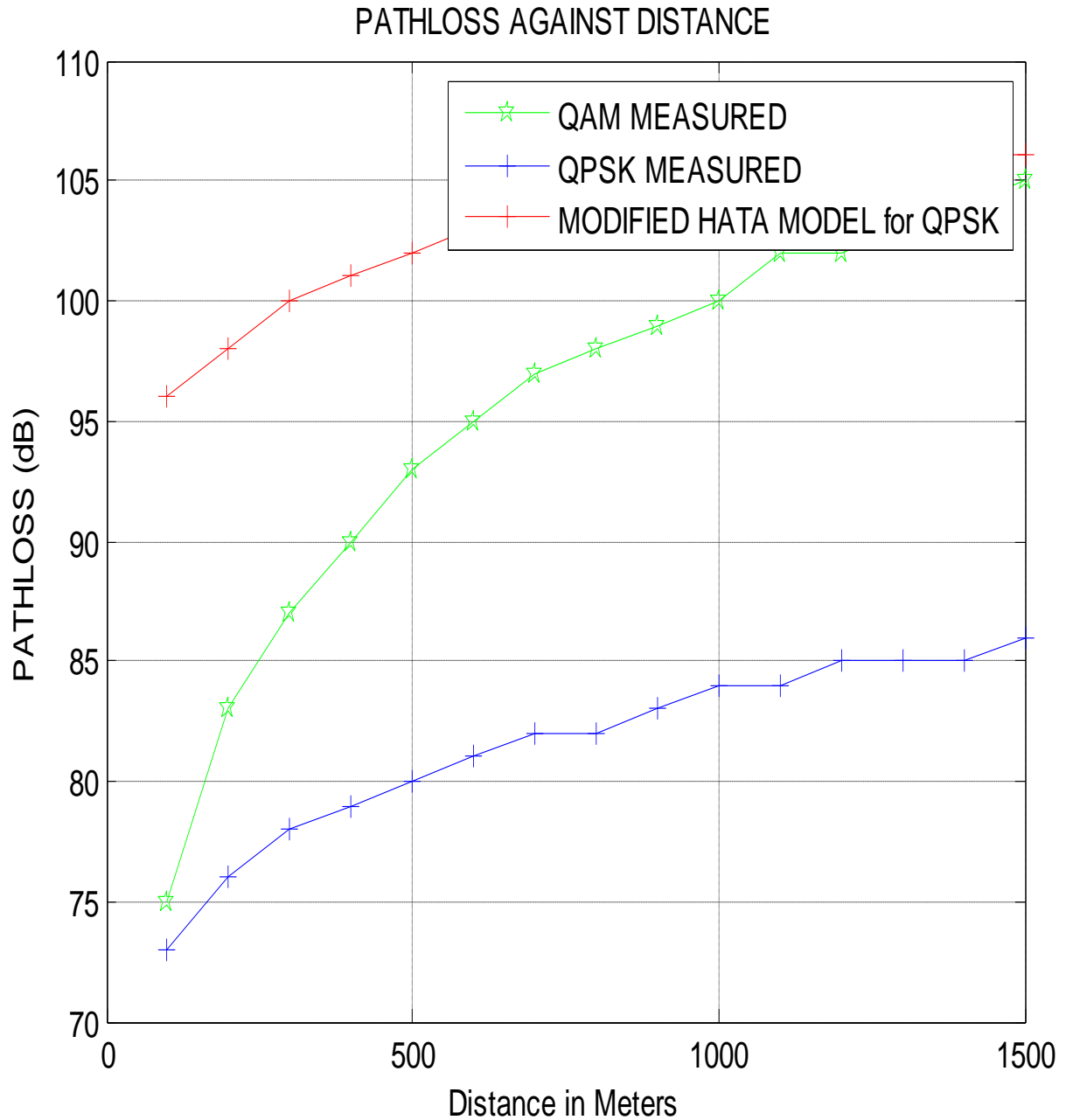


Figure 4.14 show comparison between the measured Models and Modified Hata Model for QPSK for Sub-Urban Category B, the path loss is greater in modified Hata Model compared to measured data using QAM and QPSK Technique, in category B, this might be as result of shadowing , scattering and foliage loss.

4.11 Effects of variation in antenna height, antenna power and antenna tilt on RF coverage area and capacity

In this section the coverage of GSM and W-CDMA network is evaluated on the basis of received signal level and the impact imposed on network coverage and capacity by varying the BS antenna height, antenna power and tilt are investigated.

4.11.1 Impact of BS antenna height on coverage

The base station coverage area is primarily dependent on the antenna height . If the antenna height is increased path loss is lessened and on decreasing the antenna height path loss increases. The relation of path loss with antenna height is given as

$$P_{\text{loss}} = A + B \log(d) \dots\dots\dots 4.19$$

$A = 69.55 + 26.16 \log(f) - 13.82 \log(h_b) - a(h_m)$, $B = 44.9 - 6.55 \log(h_b)$
(measurements by Hata Okumura), $a(h_m)$ is correction factor in dB.

Substituting the value of (frequency of operation (MHz)), h_b (BS antenna height (m)), and d (distance between Tx and Rx (km))

Table 4.24 Effect of varying BS antenna height on path loss

<i>BS Antenna height (m)</i>	<i>Hata L_p (dB)</i>	<i>COST231 L_p (dB)</i>	<i>ECC-33 L_p (dB)</i>
20	165.23	164.86	549.78
22	164.37	164.02	533.62
24	163.60	163.25	518.87
26	162.89	162.54	505.30
28	162.23	161.88	492.74
30	161.63	161.27	481.04
32	161.06	160.70	470.10
34	160.52	160.17	459.82
36	160.02	159.66	450.13
38	159.54	159.18	440.96

Also path loss is related to received power as $R_{xd} \text{ (dBm)} = E_{iRPTx} - L_{\text{MASK}} - L_p$: where $R_{xd} \text{ (dBm)}$ is the received power in dBm.

E_{iRPTx} is the maximum Effective Isotropic Radiated Power of the cell in dBm (that is, at the peak gain point of the antenna).

L_{MASK} is the antenna mask loss value for azimuth and elevation angles respectively in the direction of the path being calculated in dB. When the received signal is directly on the main beam of the antenna, this value will be zero. L_p is the path loss in dB.

$$E_{iRP} = P_{\text{APower}} + \text{antennaG}$$

Where:

AntennaG = antennaGain + 2.14 (if the gain is in dB)

So, if path loss increases then received power will decrease. If path loss decreases then received power will increase so the signal from the BTS will cover more distance. This is illustrated in the table 4.25

Table 4.25 Effect on received signal strength by varying BS antenna height

<i>BS Antenna height (m)</i>	<i>Hata (dBm) R_{xd}</i>	<i>COST231 R_{xd} (dBm)</i>	<i>ECC-33 R_{xd} (dBm)</i>
20	-533.24	-532.89	-917.81
22	-516.24	-515.89	-885.49
24	-500.72	-500.37	-855.99
26	-486.44	-486.09	-828.85
28	-473.22	-472.87	-803.72
30	-460.91	-460.56	-780.33
32	-449.40	-449.05	-758.44
34	-438.59	-438.23	-737.89
36	-428.39	-428.04	-718.51
38	-418.75	-418.39	-700.17

4.11.2 Impact of Transmitted Power on Coverage

As the BTS power increases, received power also increases. The Impact on received signal level (coverage area) by varying the transmitted power from 30 dBm to 110 dBm is shown in the table 4.26.

Table 4.26 Effects on received signal strength by varying transmitted power

Txd power (dBm)	Hata R_{xd} (dBm)	COST231 R_{xd} (dBm)	ECC-33 R_{xd} (dBm)
30	-135.50	-135.14	-150.05
32	-133.50	-133.14	-148.05
34	-131.50	-131.14	-146.05
36	-129.50	-129.14	-144.05
38	-127.50	-127.14	-142.05
40	-125.50	-125.14	-140.05
42	-123.50	-123.14	-138.05
44	-121.50	-121.14	-136.05
46	-119.50	-119.14	-134.05

4.11.3 Impact of Antenna Tilt on Coverage

The efficiency of a cellular network depends on its correct configuration and adjustment of radiant systems, the transmit and the receive antennas. And one of the more important system optimizations task is based on correct adjusting tilts, or the inclination of the antenna in relation to an axis. With the tilt, we direct irradiation further down (or higher), concentrating the energy in the new desired direction. When the antenna is tilted down, it is called downtilt, which is the most common use. If the inclination is up (very rare and extreme cases), we call uptilt. The tilt is used when we want to

reduce interference and/or coverage in some specific areas, having each cell to meet only its designed area.

When selecting the optimum tilt angle, the goal is to have as high signal strength as possible in the area where the cell should be serving traffic. Beyond the serving area of the cell, the signal strength should be as low as possible.

When the cell site uses a high-gain antenna, downward tilting can direct the nulls in the antenna pattern towards the horizon to prevent energy from propagating into other cells. A too aggressive down tilting strategy will however lead to an overall loss of coverage. Down tilting the antenna limits the range by reducing the field strength in the horizon and increases the radiated power in the cell that is actually to be covered.

Down tilting can be done in two ways: Electrical down tilt and Mechanical down tilt . Total tilt effect is the sum of both electrical tilt and mechanical tilt. Electrical tilt is constant at 2° as it is manufacturer specific and mechanical tilt is varied from 0° to 5° . So the total tilt is varied from 0° to 7° . The table 4.27 summarized the impact on received signal level (coverage area) by varying the Antenna Tilt

Table 4.27 Effect on received signal strength by varying the BS antenna tilt

Tilt angle (degree)	0°	1°	2°	3°	4°	5°
Hata Okumura R_{xd} (dBm)	-248.11	-249.02	-225.13	-301.50	-250.01	-228.30
COST-231 R_{xd} (dBm)	-249.00	-249.16	-225.20	-302.03	-250.50	-229.00
ECC-33 R_{xd} (dBm)	-350.72	-340.25	-302.00	-441.15	-350.00	-290.20

4.11.4 The impact on coverage and capacity by varying the BS Antenna height, tilt and power

The target of radio network topology planning is to provide a configuration that offers the required coverage for different services, and simultaneously maximizes the system capacity. This section addresses the impact of antenna height, tilt and power on network coverage and system capacity. Moreover, the impact of the aforementioned elements is addressed in fig. 4.15

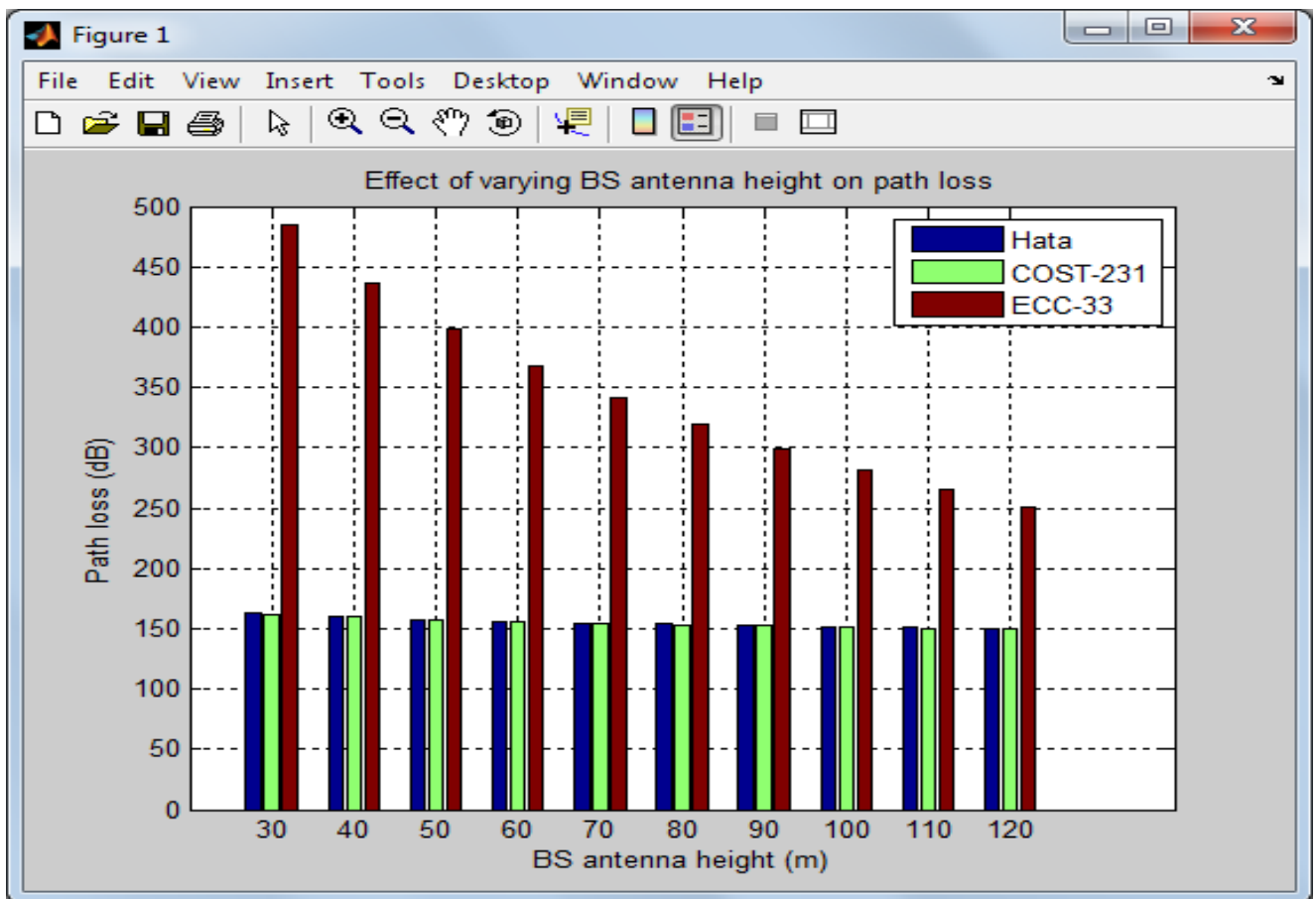


Fig.4.15 Bar chart showing path loss against BS antenna height for the various empirical propagation models

It can be observed that coverage is highly influenced by the antenna height, the path loss is the same for hata model and cost 231 model but increases with ECC-33 model. For better performance of the network it is required that antenna height and power should be high. While antennas tilt should be optimum.

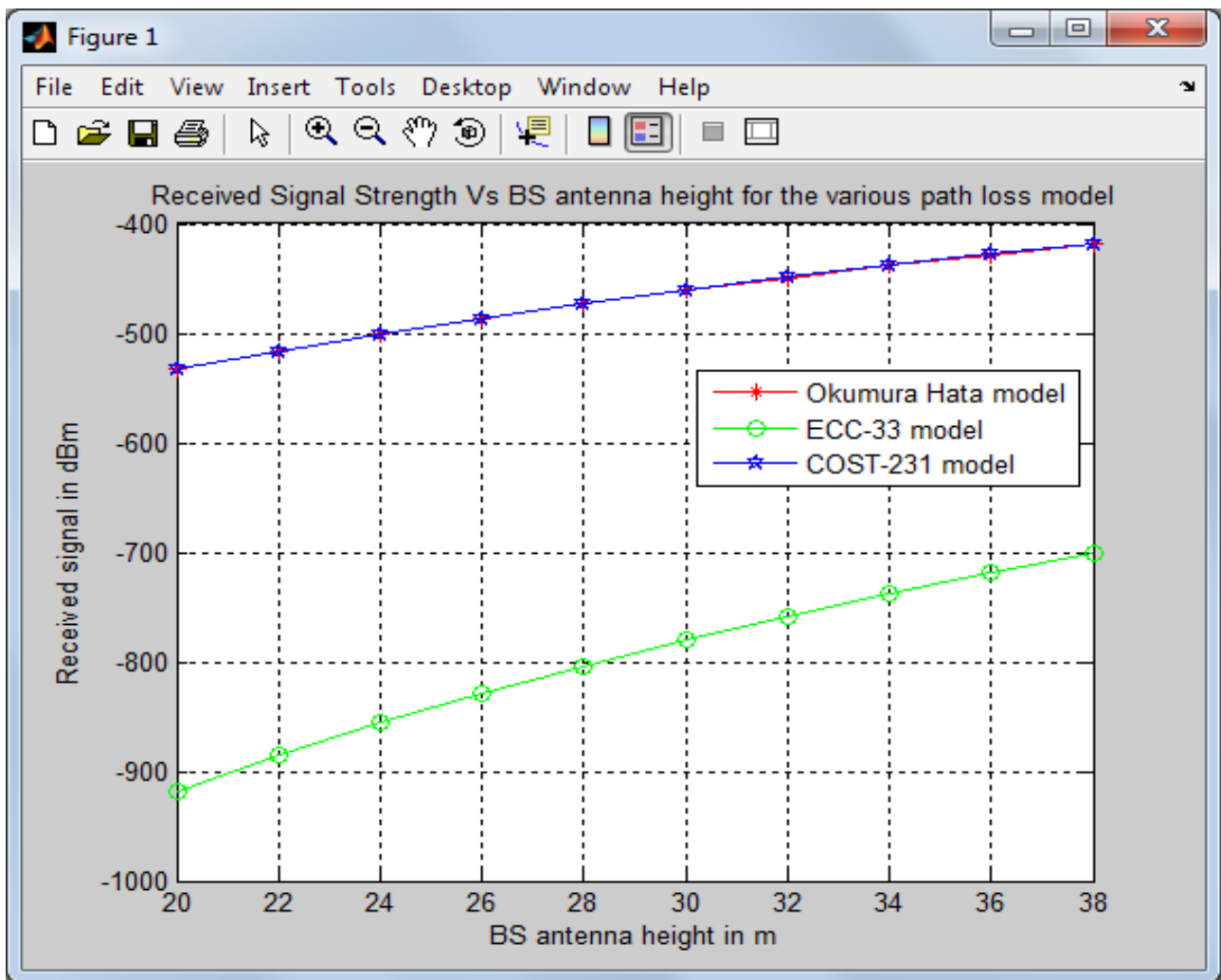


Fig.4.16 Plot showing received signal strength against BS antenna height for the various empirical propagation models

From the figure the antenna height has greater impact on the received signal strength, Hata- Okumura and COST 231 models have the same received signal power compare compared to ECC-33 at different antenna height.

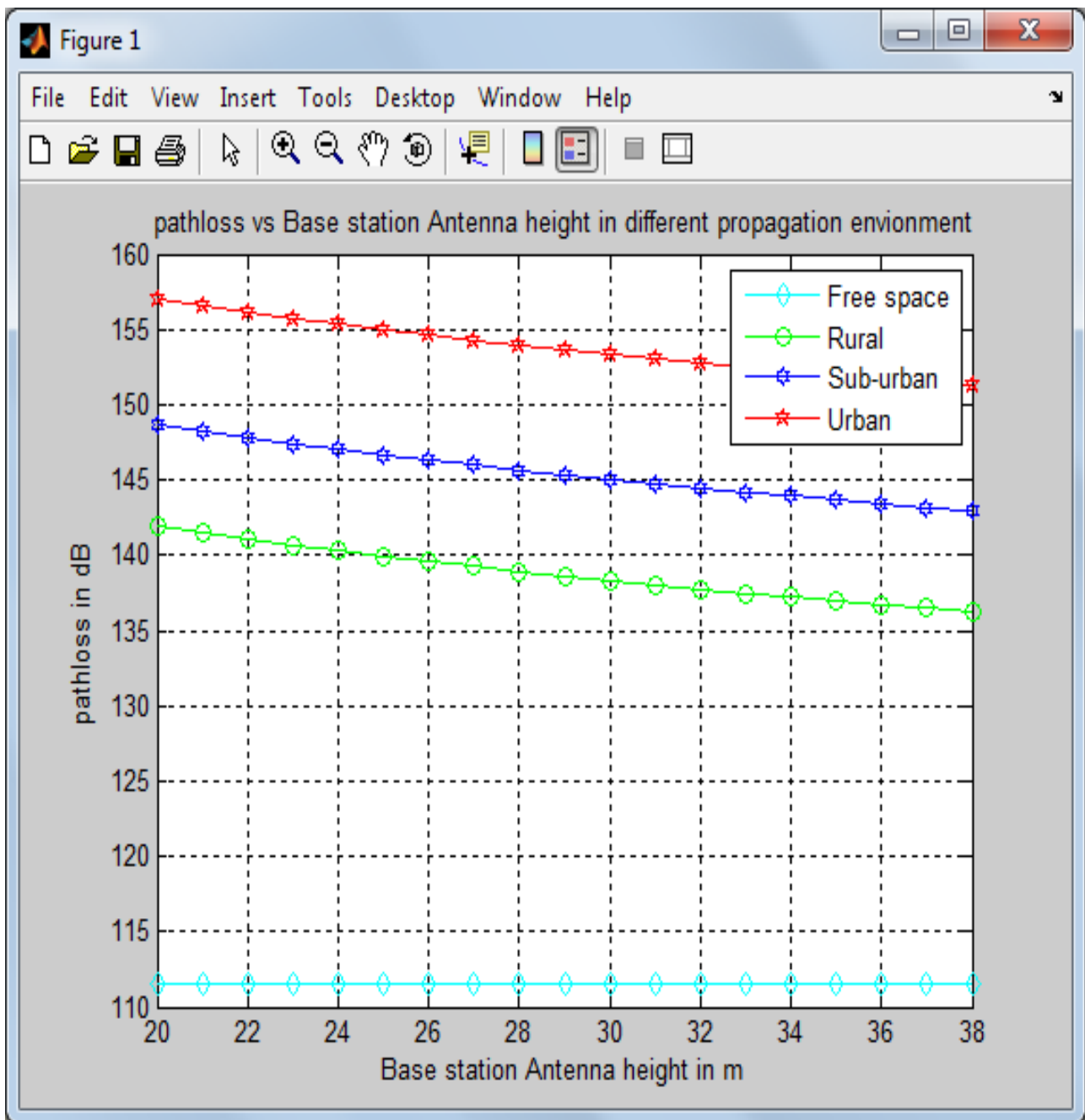


Fig.4.17 Plot showing path loss against BS antenna height in different propagation environment

The path loss for free space and rural area are less compared to urban and sub urban area where the signal experience multipath fading, reflection, diffraction and scattering thereby weakening the received signal strength

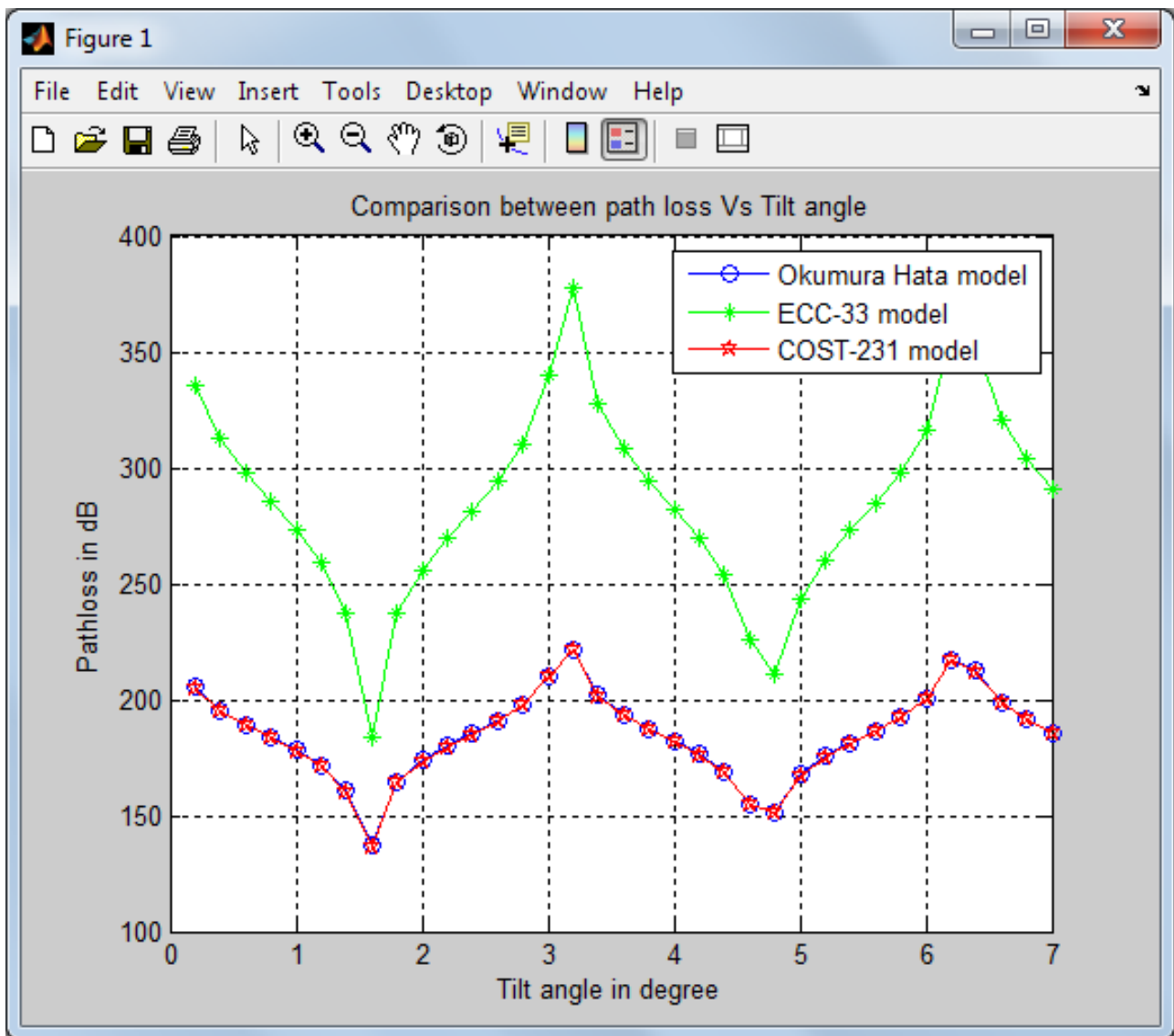


Fig.4.18 Plot showing the effect of tilt on path loss.

The path loss is greater in ECC-33 Model, while hata-okumura model and COST 231 model have the same path loss at same antenna tilt angle.

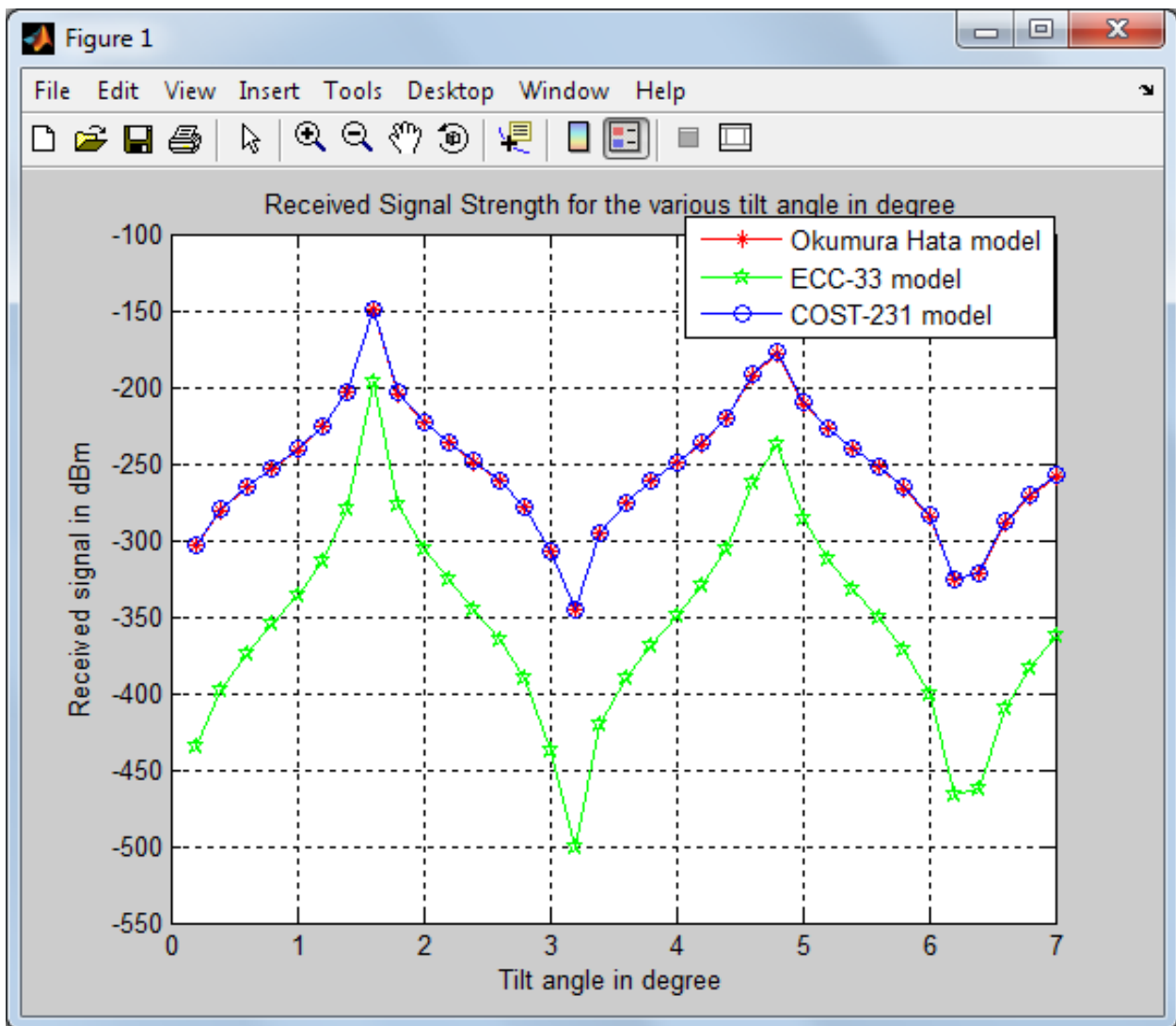


Fig.4.19 Plot showing the effect Received signal Strength on tilt angle. The received signal strength is the same for Hata – okumura model and COST 231 compared to ECC-33 model at the same antenna tilt angle.

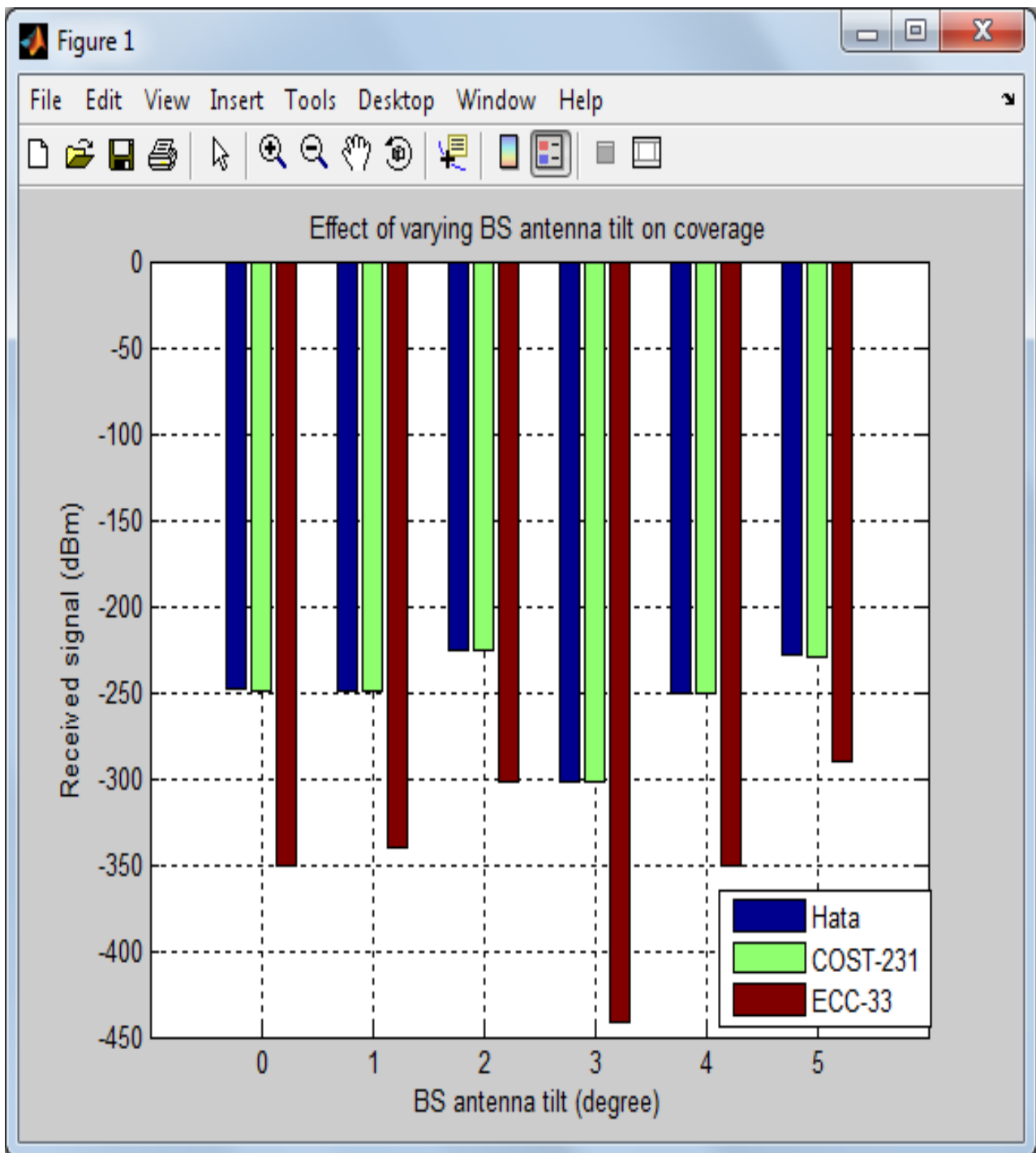


Fig. 4.20 Coverage Prediction Plots showing impact of BS antenna tilt on coverage area (received signal strength)

Hata- Okumura Model and COST 231 model have the same coverage area at specific base station antenna tilt and received signal strength

compared to ECC-33 which varies as the base station antenna tilt angles varies.

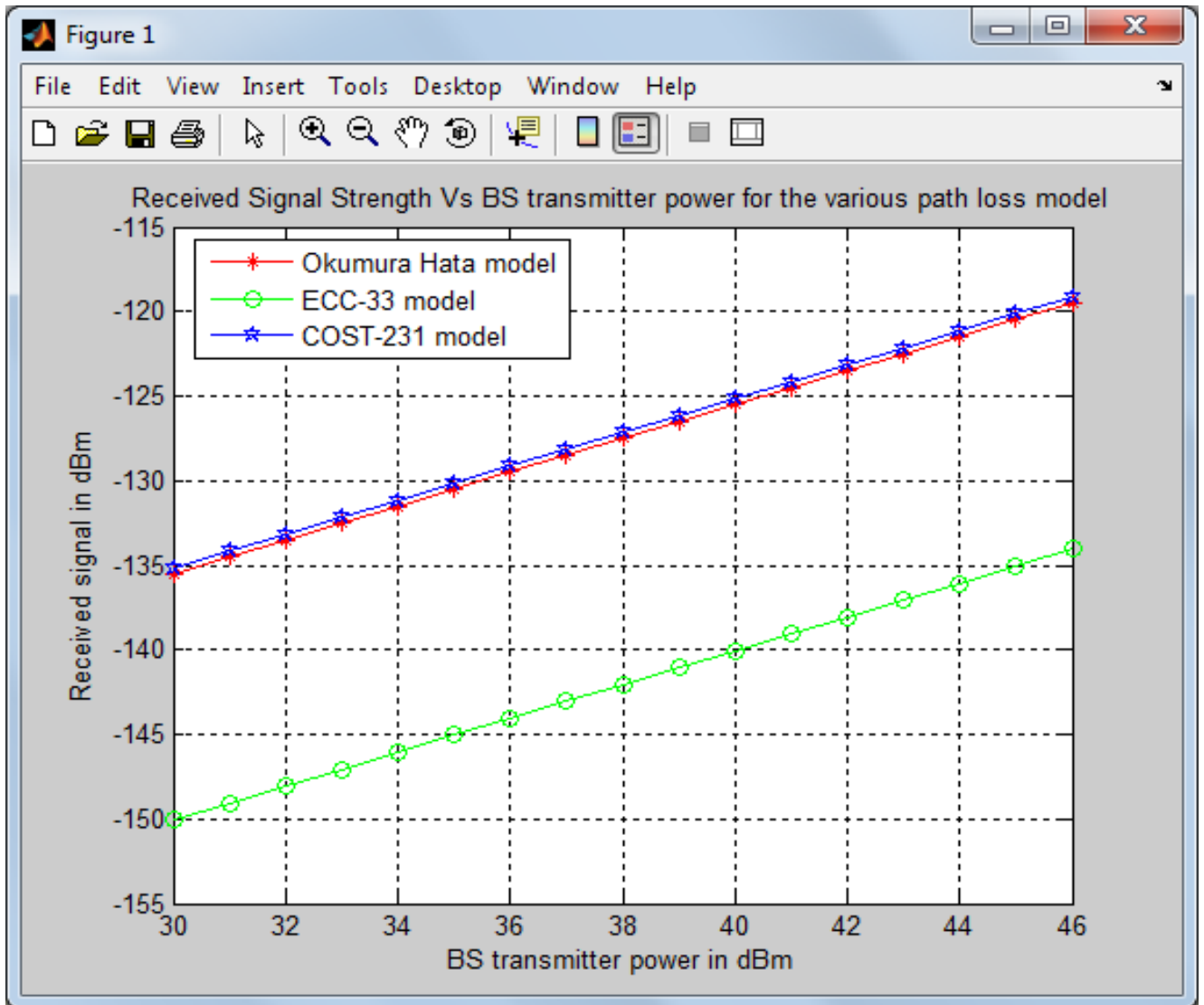


Fig.4.21 Coverage Prediction Plot showing the impact of transmitted power on coverage area (received signal strength),

The received signal strength is the same for Hata – okumura model and COST 231 compared to ECC-33 model at the same base station transmitter power..

4.11.5 Estimation of Signal to noise Ratio (SNR) from the measured Data

SNR is defined as the ratio of average signal to average noise power. SNR can be expressed in dB as [55]

$$SNR_{(dB)} = 10 \log SNR \dots\dots\dots 4.19$$

$$SNR = P_t - P_{L(d)} - S_r \dots\dots\dots 4.20$$

Where P_t is the transmitted power in dBm , 44dBm for W-cdma and 43dBm for Gsm, $P_{L(d)}$ is the path loss model and S_r is the receiver sensitivity in dBm (-110dBm). Equation 4.19 and 4.20 were used to calculate the SNR of the environment under study Urban and Sub-Urban respectively and Matlab program were written to plot the SNR against distance of the testbed. Table 4.28 to 4.32 show the average path loss and average SNR_{dB} appendix E1, E2 and E3 show the matlab codes used.

TABLE 4.28 AVERAGE PATHLOSS AND SNR(dB) FOR CATEGORY A QAM MODULATION TECHNIQUE (Urban)

D (KM)	Average Path loss	SNR (dB)
0.1	107	16.73
0.2	109	16.54
0.3	111	16.34
0.4	114	16.03
0.5	116	15.81
0.6	118	15.57
0.7	119	15.45
0.8	121	15.20
0.9	122	15.06
1.0	124	14.78
1.1	126	14.49
1.2	127	14.32
1.3	128	14.17
1.4	131	13.64
1.5	137	12.33

TABLE 4.29 AVERAGE PATHLOSS AND SNR FOR CATEGORY A QPSK
MODULATION TECHNIQUE (Urban)

D (KM)	Average Path loss	SNR(dB)
0.1	104	16.99
0.2	106	16.87
0.3	109	16.54
0.4	112	16.24
0.5	114	16.03
0.6	112	16.24
0.7	116	15.81
0.8	117	15.69
0.9	118	15.57
1.0	119	15.45
1.1	119	15.45
1.2	122	15.06
1.3	123	14.93
1.4	124	14.78
1.5	126	14.48

**TABLE 4.30 AVERAGE PATHLOSS AND SNR(dB) FOR CATEGORY A GMSK
MODULATION TECHNIQUE (Urban)**

D (KM)	Average Path loss	SNR (dB)
0.1	93	17.78
0.2	91	17.92
0.3	94	17.71
0.4	98	17.40
0.5	96	17.55
0.6	99	17.32
0.7	98	17.40
0.8	103	16.98
0.9	113	16.02
1.0	115	15.80
1.1	120	15.19
1.2	123	14.77
1.3	133	13.01
1.4	138	11.76

1.5	136	12.30
-----	-----	-------

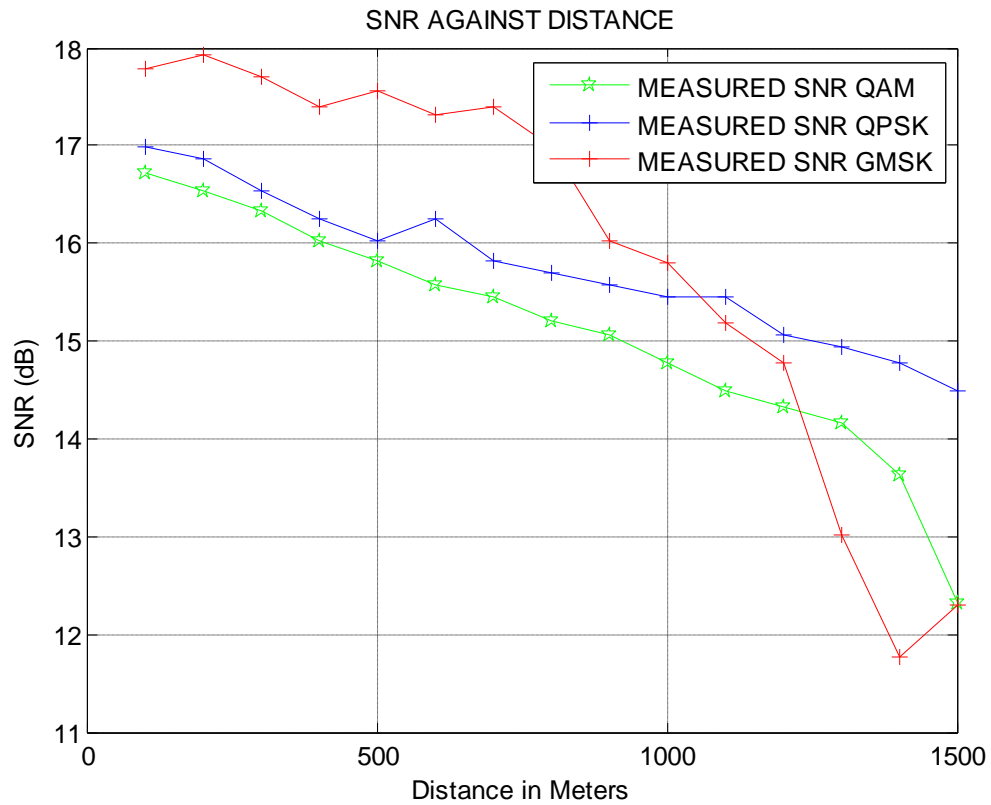


Fig.4.22 Plot showing the average SNR of the three modulation techniques against distance.

The signal to noise ratio is greater in GSMK followed by QPSK then QAM modulation technique as the distance varies.

TABLE 4.31 AVERAGE PATHLOSS AND SNR(dB) FOR CATEGORY B QAM MODULATION TECHNIQUE (Sub-Urban)

D (KM)	Average Path loss	SNR (dB)
0.1	95	17.72
0.2	97	17.57
0.3	102	17.17
0.4	102	17.17
0.5	109	16.54
0.6	113	16.13
0.7	113	16.13
0.8	114	16.03
0.9	116	15.81
1.0	118	15.58
1.1	123	14.93
1.2	126	14.49
1.3	130	13.80
1.4	132	13.44
1.5	138	12.07

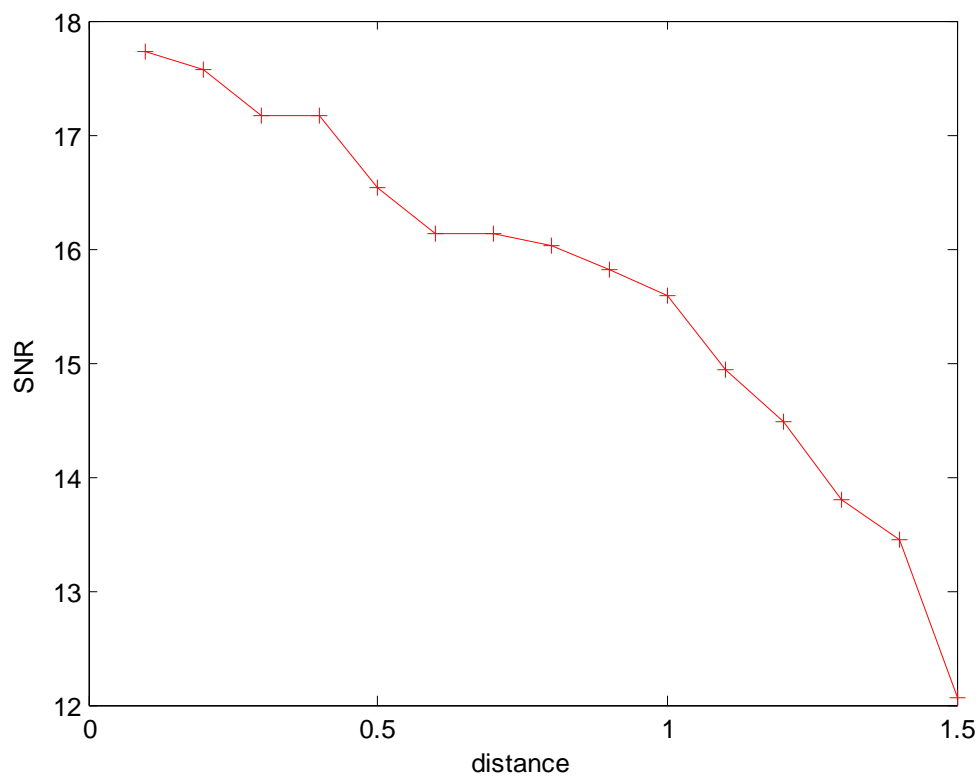


Fig.4.23 Plot showing the average SNR of QAM modulation techniques against distance for Sub-urban.

The signal to noise ratio shows a normal distribution for QAM modulation technique as the distance varies for sub-urban category B.

TABLE 4.32 AVERAGE PATHLOSS AND SNR FOR CATEGORY B QPSK
MODULATION TECHNIQUE (Sub- Urban)

D (KM)	Average Path loss	SNR(dB)
0.1	81	18.64
0.2	83	18.52
0.3	84	18.45
0.4	85	18.39
0.5	86	18.33
0.6	86	18.33
0.7	87	18.23
0.8	88	18.20
0.9	90	18.07
1.0	91	18.00
1.1	96	17.64
1.2	97	17.56
1.3	98	17.49
1.4	96	17.64
1.5	98	17.49

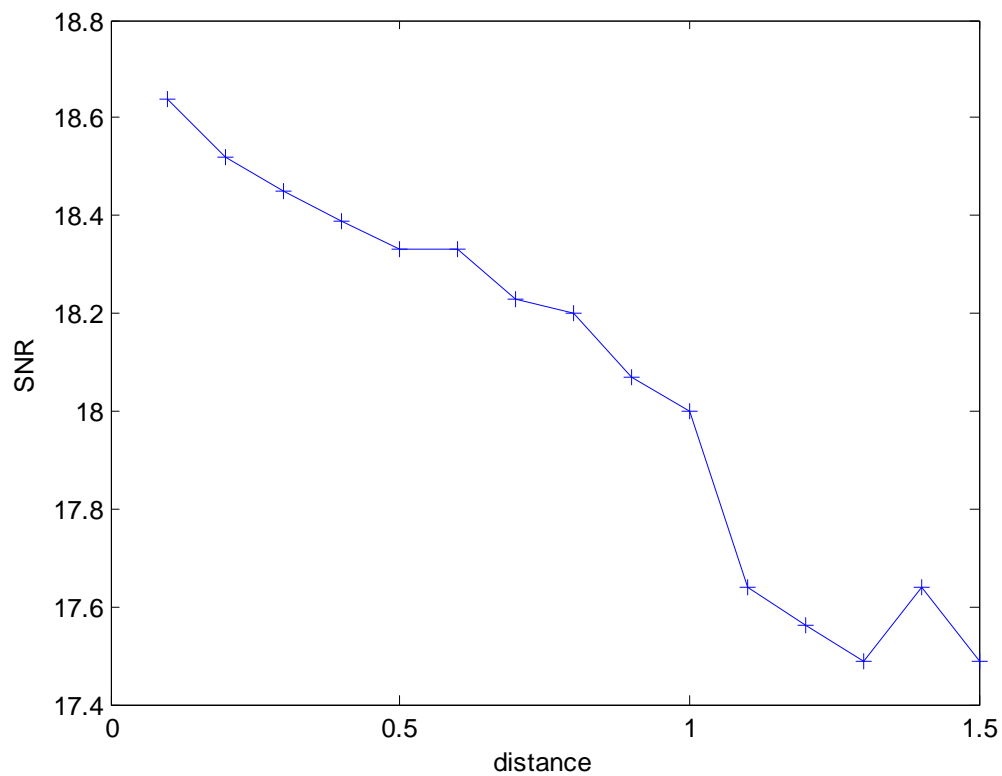


Fig.4.24 Plot showing the average SNR of QPSK modulation techniques against distance for Sub-urban.

The signal to noise ratio shows a normal distribution for QPSK modulation technique as the distance varies for sub-urban category B.

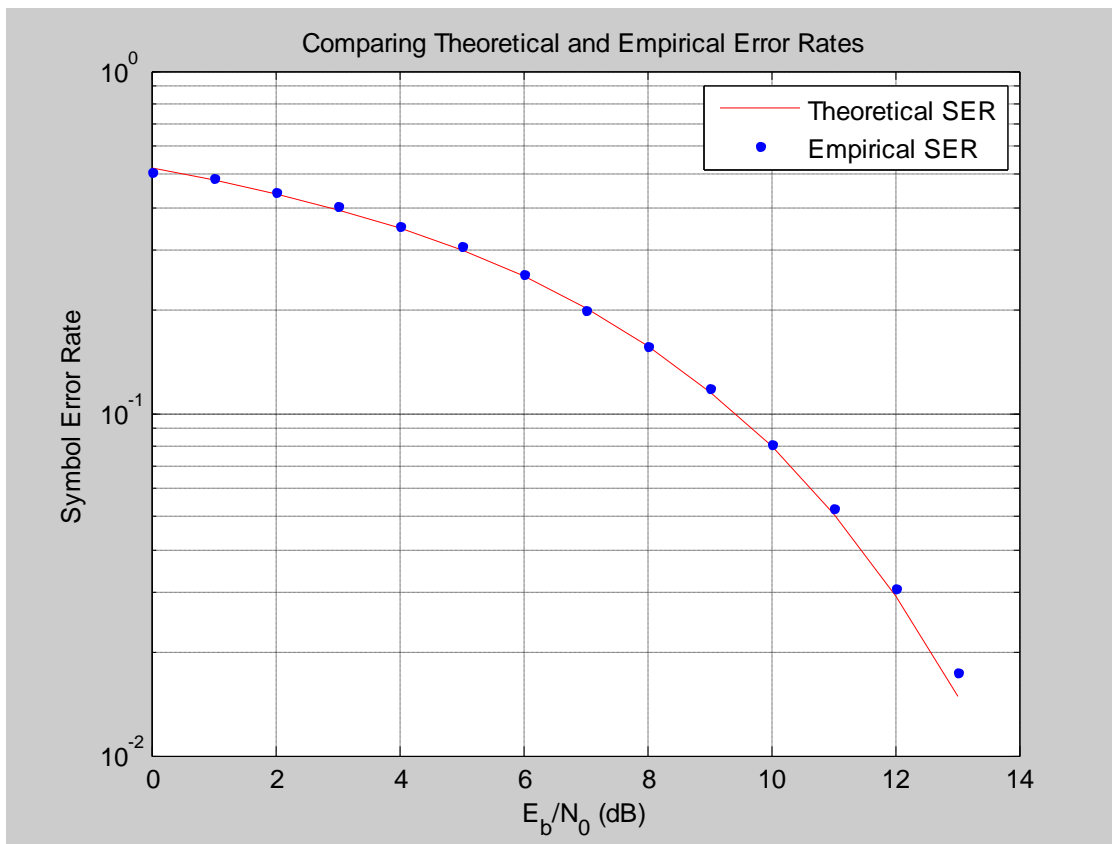


Fig.4.25 Plot showing the average Empirical Symbol error rate and Theoretical symbol error rate against SNR for the Environment under study.

- DEDUCTIONS

The necessity of these graphs is to show the relationship of average SNR with distance, it was observed that the SNR and path loss depends on the distance and measurement environment. In this experiment, the channel or the link is very good, since the theoretical symbol error and empirical symbol error are nearly the same, thus no bit error .

CHAPTER FIVE

SYSTEM IMPLEMENTATION AND PERFORMANCE ANALYSIS

5.1 BIT ERROR RATE AND ADAPTIVE MODULATION IN WCDMA SYSTEM

A generic model of DSSS W-CDMA is shown in figure 5.1 and it is simulated using QPSK then followed by QAM. QPSK and QAM are chosen in this thesis because they are the primary candidates to deliver higher data rate for High Speed Downlink Packet Access (HSDPA), an extension of 3G networks. The simulation is done under noise and multipath fading channel using MATLAB 7.5. R2007b

As it is shown in figure 5.1, the user data is assumed to be Bernoulli distributed and it is represented as $b_n(t)$. Each user data is then multiplied with independent or different PN code produced by a PN generator using XOR logical operator. The multiplied signal of each user is represented as $s_n(t)$ after the signal is modulated by either QPSK or QAM. Each signal is added before it is subjected to the channel. At the receiver, the signal $s_k(t)$ is demodulated before the user data is separated from PN code by XOR logical operator. Finally, when the necessary simulations are done, tables and graphs of BER as a function of SNR for various parameters are plotted. Analysis, comments and conclusion will be drawn based on the simulation results.

AWGN and Rayleigh fading are chosen to represent fading effect in the channel because we want to make a comparison of WCDMA system

models in two extreme channel conditions. There are many fading effects that can be categorized as large-scale and small-scale fading. Rayleigh fading represents the worst case of multipath fading where it represents small-scale fading due to small changes in position. On the other hand, AWGN represents the thermal noise generated electrical instruments

There will be three WCDMA wireless cellular system models that will be used in this thesis. The models are:

1. WCDMA system in AWGN channel
2. WCDMA system in AWGN and Multipath Rayleigh Fading.
3. Multi-user WCDMA system in AWGN and Multipath Rayleigh Fading.

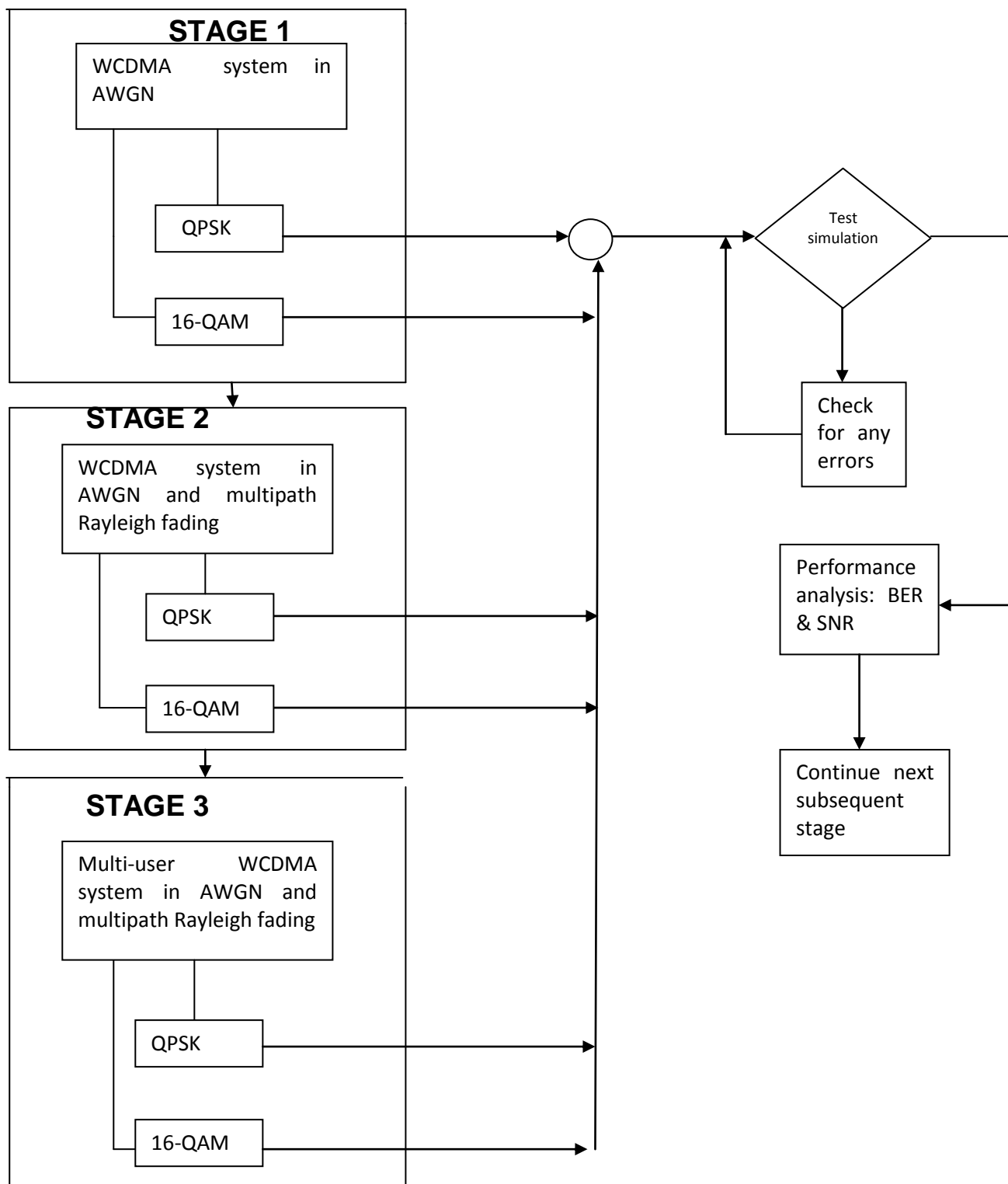


Figure 5.1: Simulation flow chart for W-CDMA system models used in Simulink.

5.2 SIMULATION USING SIMULINK

Two types of simulation have been chosen to study the performance of modulation techniques of WCDMA subjected to multipath fading in the channel. The thesis begins with simulation using simulink. Simulink is a software package that has the capabilities to model, simulate, and analyze dynamic systems whose outputs and states change with time. Simulink can be used to explore the behavior of a wide range of real-world dynamic systems making it suitable computer software to study the performance of modulation techniques under multipath fading. Simulating a dynamic system is a two-step process with simulink. First, a graphical model of the system is simulated, using the simulink model editor. The model depicts the time-dependent mathematical relationships among the system's inputs, states, and outputs. Then, simulink uses information entered into the model to perform the simulation.

TABLE 5.0: REAL DATA OBTAINED USING CLASSIC NODE SOFTWARE FROM MTN (URATTA T0176-20P NELLY MODEL).

Configured Radio Parameter	16 QAM MODULATION	QPSK MODULATION
Near end Radio Terminal ID	0065	0065
Far end Radio Terminal ID	4228	4228
BTX TX POWER dBm	17	19
TOTAL RECEIVED POWER dBm	-36.6	-34.7
Channel spacing	28	28
BER Threshold for Data	0.000	0.000
BER Threshold for Voice	10^{-3}	10^{-3}
TX FREQUENCY GHz	2.1	2.1
Packet Capacity Mbps	94.47	94.47
Capacity Modulation Mbps	154	154
Number of E1s	30	30
Output Power mode	Fixed RTPC	Fixed RTCP

5.2.1: Simulation in Phase 1: WCDMA system in AWGN Channel

In Phase 1, both transmitter and receiver part are built based on the system model as shown in **Figure 5.5**. The channel is subjected to AWGN only. This phase is divided into five parts as follows:

- i. Assumptions
- ii. Transmitter part
- iii. Receiver part
- iv. Channel part
- v. Performance Analysis

5.2.2 Assumptions in Phase 1

The assumptions made for this phase of simulation are stated as follows:

- Evaluation of the performance is made on one user in the multi-user environment. It considers the rest of the users contribute the multi user interference to the reference user in the system.
- Decision statistic of the receiver, Z_0 is modeled as Gaussian Random Variable.
- Decision statistic of the desired user, 1_0 is deterministic.
- Multi-User Interference (MUI), ζ is the system is assumed as zero-mean Gaussian Variables and it is an additive white Gaussian noise (AWGN). This is based on the ARIB proposal which states that all interference from other users is modeled as Additive White Gaussian Noise (AWGN).
- Thermal noise η is very small and negligible. This is based on the data in ARIB proposal.
- In this simulation, only downlink (base station to mobile station) transmission is considered.

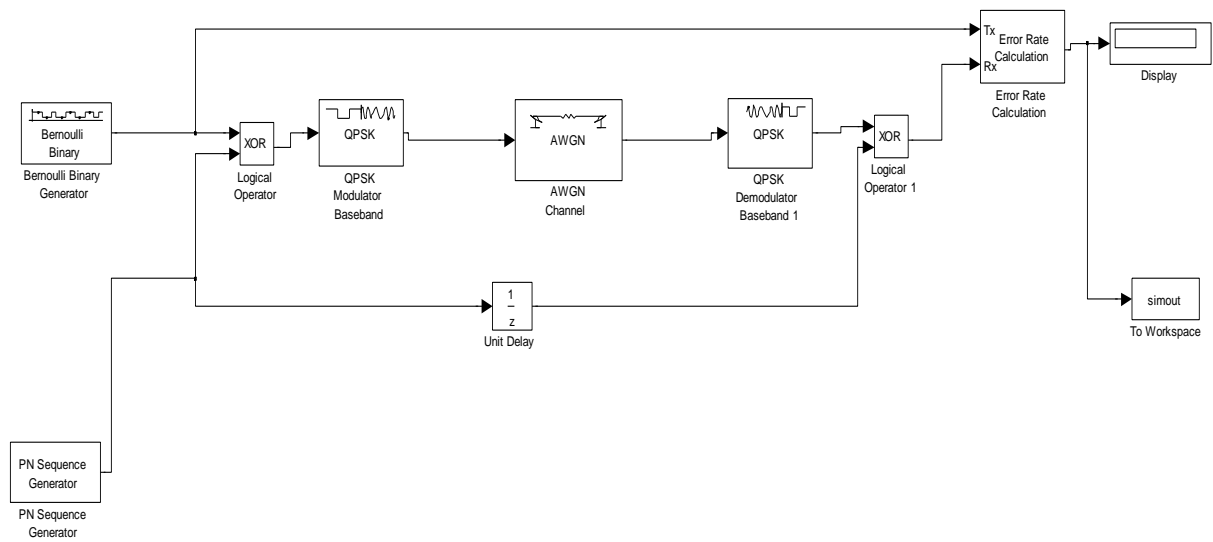


**FIGURE 5.2: W-CDMA MODEL USING QPSK MODULATION
TECHNIQUE IN AWGN CHANNEL**

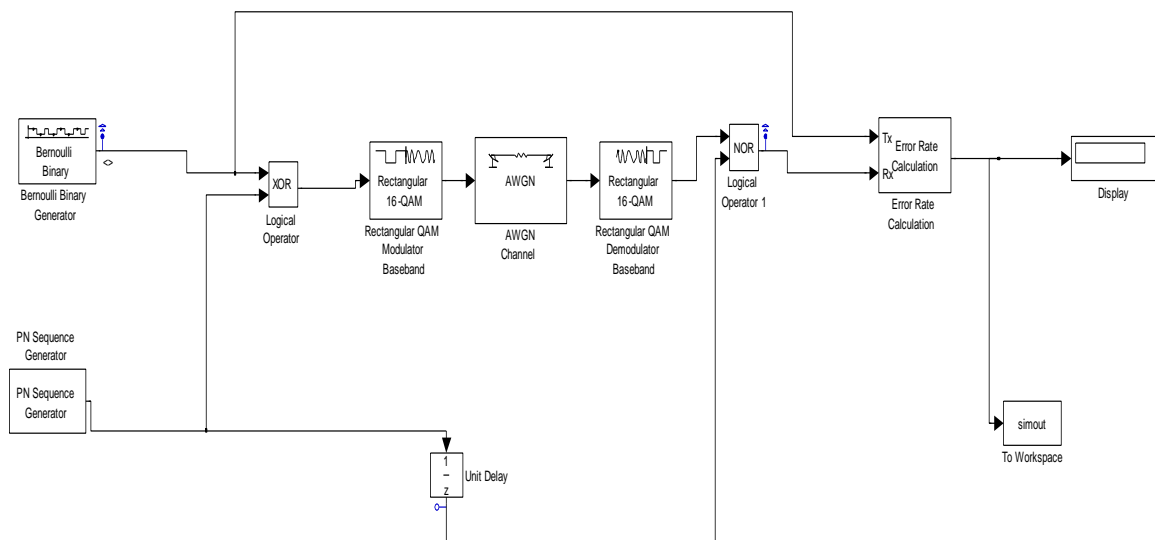


**FIGURE 5.3: W-CDMA MODEL USING 16-QAM MODULATION
TECHNIQUE IN AWGN CHANNEL**

5.3. Characterization of the Simulink block

5.3.1 Transmitter blocks (User Data Sequence Generator)

The signal is produced by Bernoulli Data Generator. The Bernoulli Binary Generator block generates random binary numbers using a Bernoulli distribution. The Bernoulli distribution with parameter p produces zero with probability p and one with probability $1-p$. the Bernoulli distribution has mean value $1-p$ and variance $p(1-p)$. the probability of a zero parameter specifies p , and can be real number between zero and one. Table below shows the parameters used in Bernoulli Binary Generator block.

Table 5.1: Parameters for Bernoulli Binary Generator Block

Parameter	Value
Probability of Zero	0.5
Initial Seeds	12345
Sample Time	Tsample
Frame-based output	Unchecked
Interpret Vector Parameter as i-D	Unchecked

Parameters for Bernoulli Binary Generator Block

- **Probability of Zero:** The probability with which a zero output occurs. The value of 0.5 means the random binary numbers generated having equal amount of '0' and '1'.

- **Initial Seeds:** The initial seed value for the random number generator. 12345 has been chosen.
- **Sample Time:** The period of each sample-based vector or each row of a frame-based matrix. Here, T_{sample} is declared and it has a value of 1/384000 seconds or an inverse of bit rate of 384 kbps.
- **Attribute of Output Signal:** In this block, we declare the signal to be sample-based where the frame-based outputs box is unchecked.

5.3.2 Spreading Sequence Generator blocks

The PN Sequence Generator block generates a sequence of pseudorandom binary numbers. A pseudo-noise sequence can be used in a pseudorandom scrambler and descrambler. It can also be used in a direct-sequence spread-spectrum system. The PN Sequence Generator block uses a shift register to generate sequences. Table 5.2 below shows the parameter that has been used in the simulation.

Parameter	Value
Generator Polynomial	[1000011]
Initial States	[100001]
Shift (or mask)	0
Sample time, T_c	T_{chip}
Attribute of Output Signal	Sample-based output

Parameters Specific to PN Sequence Generator

The Generator Polynomial parameter has been specified using this format:

- A vector that lists the coefficients of the polynomial in descending order of powers. The first and last entries must be 1. Note that the length of this vector is one more than the degree of the generator polynomial. It is known that the degree of the generator polynomial is 6 so the length of the vector is 7. So, in this simulation, the value of Generator Polynomial specifies as [1000011] represent the same polynomial, $p(z) = z^6 + z^1 + 1$ to fulfill the format above.
- a. **The Initial States** parameter is a vector specifying the initial values of the registers. The initial states parameter must satisfy these criteria:
- All elements of the initial states vector must be binary numbers.
 - The length of the initial states vector must equal the degree of the generator polynomial.
 - At least one element of the initial states vector must be nonzero in order for the block to generate a nonzero sequence. That is, the initial state of least one of the registers must be nonzero.

So, in this simulation, the value of initial states specifies as [100001] to satisfy the criteria above.

b. **Sample Time, T_c** in this case is equal to chip period. In this simulation chip period 260.4167 ns inverse of chip rate, 3.84 M chips per second (Mcps) is used.

c. **Attribute of Output Signal:**

In Simulink, each matrix signal has a frame attribute that declares the signal to be either frame-based or sample-based, but not both. (A one-dimensional array signal is always sample-based, by definition). Simulink indicates the frame attribute visually by using a double connector line in the model window instead of a single connector line. In general, simulink interprets frame-based and sample-based signals as follows:

- ❖ A frame-based signal in the shape of an M-by-1 (column) matrix represents M successive samples from a single time series.
- ❖ A frame-based signal in the shape of a 1-by-N (row) matrix represents a sample on N independent channels, taken at a single instant in time.
- ❖ A sample-based matrix signal might represent a set of bits that collectively represent an integer, or a set of symbols that collectively represent a code word, or something else other than a fragment of a single time series.

So, in this block, we declare the signal to be sample-based with unchecked frame-based output box.

5.3.4 Spreader block

XOR block has been used to operate like a spreader. Spreader causes the data symbols to be spread to a higher bandwidth, by multiplying the random binary data symbols, bit rate equal to T_b with a high bit rate code sequence (pseudo noise chip sequence), chip rate equal to T_c .

Parameters Specific to Logical Operator Block

- a. Operator XOR has been selected
- b. Number of inputs ports=2
- c. Show additional parameters' box is checked
- d. Require all inputs and outputs to have same data type' box is checked.
- e. **Output data type mode:** Logical has been selected. To avoid any data or signal incompatibility, the following steps are taken. Go to the menu bar of simulation/simulation parameters/Advanced tab. Select Boolean Logic Signals to off, then the output data type will match the input data type, which may be Boolean or double.

5.4 MODULATION TECHNIQUE BLOCKS

5.4.1 QPSK Modulator block

In this simulation, Quadrature Phase Shift Keying (QPSK) Passband modular has been used. The M-PSK Modular Passband block modulates using the M-ary phase shift keying method. The output is a passband representation of the modulated signal. The M-ary number parameter, M, is the number of points in the signal constellation.

This block uses the baseband equivalent block, M-PSK Modular Baseband, for internal computations and converts the resulting baseband signal to a passband representation. The following parameters in this block are the same as those of the baseband equivalent block:

- i. M-ary number
- ii. Input type
- iii. Constellation ordering

The input must be sample-based. If the input type parameter is Bit, then the input must be a vector of length $\log_2(M)$. If the input type parameter is integer, then the input must be a scalar. This block uses a baseband representation of the modulated signal as an intermediate result during internal computations.

Table 5.3: Below shows the parameter that has been used in simulation.

Parameter	Value
M-ary number	4
Input type	Integer
Symbol period (s)	1/3840000 Hz
Baseband samples per symbol	1
Carrier frequencies (in Hz)	15000000
Carrier initial phase (in rad)	Pi/4
Output sample time (s)	1/38000000 Hz

Parameters Specific to Passband Simulation

- a. **M-ary number** is set up to 4 meaning it uses four points in the signal constellation. This setting also indicates the modular to function as a QPSK modulator.
- b. **Input Type** parameter is set up to integer means the input must be a scalar.
- c. **The symbol period** parameter must equal the sample time of the input signal. The sample time of the input signal is equal to $T_c = 260.4167$ ns. So, the symbol period equal to 260.4167 ns or inverse of 1/3840000 Hz.
- d. **Baseband samples per symbol.** The baseband samples per symbol parameter indicates how many baseband samples correspond to each integer or binary word in the input, before the block converts them to a passband output. In this simulation, baseband samples per symbols specify to one baseband sample per symbol.

- e. Passband simulation uses a carrier signal. **Carrier frequency (f_c)**, 15, 000,000 Hertz (Hz) has been used. The actual carrier frequency that should be used is 2 GHz to fulfill the third generation requirements. Smaller frequency is used because of the computer ability to simulate larger value of the carrier frequency. Simulation runs very slow when value 2 GHz applied. The assumption made for simulation environment, the differences between values of carrier frequency does not affect the system.
- f. **Carrier initial phase** in radians specify the initial phase of the carrier signal. In this simulation, the initial phase = $(\pi/4)$ or $\pi/4$ indicates the initial phase for QPSK modulation scheme.
- g. **Output sample time.** The output sample time parameter determines the sample time of the output signal. The timing-related parameters must satisfy these relationships:
- Symbol period $> (\text{Carrier frequency})^{-1}$
 - Output sample time $< [2 * \text{Carrier Frequency} + 2/(\text{Symbol period})]^{-1}$
- Furthermore, carrier frequency is typically much larger than the highest frequency of the unmodulated signal.

$$\text{First Condition} = \text{symbol period} > (\text{Carrier Frequency})^{-1}$$

$$\text{Symbol period} = 260.4167 \text{ ns}$$

$$\text{Carrier frequency } (f_c) = 15,000,000 \text{ Hz}$$

$$[\text{Carrier frequency}] (f_c) = 66.6667 \text{ ns}$$

So, 260. 4167 ns $>$ 66.667 ns, satisfy first condition

When first condition satisfied, the value of output sample time should satisfy the second condition.

$$\text{Output sample time} < [2 \cdot (15,000,000 \text{ Hz}) + 2 / (260.4167 \text{ ns})]^{-1}$$

$$\text{Output sample time} < [30 \text{ MHz} + 7.68 \text{ MHz}]^{-1}$$

$$\text{Output sample time} < 26.54 \text{ ns}$$

So, in this simulation, the Output sample time has been determined to 26.32 ns or inverse of 1/38,000,000 Hz.

5.5 16-QM MODULATOR BLOCK

Same design procedures are implemented for 16-QAM modulator. Table below shows the parameters used in rectangular 16-QAM modulator passband block.

Table 5.4: Parameters used in M-QAM modulation block.

Parameter	Value
M-ary number	16
Input type	Integer
Normalized method	Min. Distance between symbols
Minimum distance	2
Symbol period	1/100
Baseband samples per symbol	1
Carrier frequency (Hz)	15e6
Carrier initial phase (rad)	0
Output sample time	1/38e6

❖ **Normalization method** determines how the block scales the signal constellation.

- ❖ **Minimum distance** is the distance between two nearest constellation points.
- ❖ **Symbol period (s)** is the symbol period, which must equal the chip sample time of the PN sequence generator.
- ❖ **Baseband sample per symbol** is the number of baseband samples that correspond to each integer or binary word in the input, before the block converts them to a passband output.

5.5.1 Channel Specification

The following table 5.5 shows the parameters used in AWGN block.

Table 5.5: Parameters used in AWGN block

Parameter	Value
Initial seeds	1237
Mode	Signal to noise ratio (Es/No)
Es/No	EbNo
Input signal power (Watt)	1
Symbols-period (s)	Tchip

In the generic m file, the EbNo will produce a sequence of 2 EbNo intervals for 12 EbNo. The Symbol period of AWGN block is Tchip that is equivalent to 1/38e6.

5.6. RECEIVER BLOCKS

5.6.1 QPSK Demodulator block

The M-PSK Demodular Passband block demodulates a signal that was modulated using the M-ary phase shift keying method. The input is a passband representation of the modulated signal. The M-ary number parameter, M , is the number of points in the signal constellation. This block converts the input to an equivalent baseband representation and then uses the baseband equivalent block, M-PSK Demodulator Baseband, for internal computations. The following parameters in this block are the same as those of the baseband equivalent block:

- i. M-ary number
- ii. Output type
- iii. Constellation ordering

The input must be a sample-based scalar signal. Similar parameters for QPSK Demodulator will be used as QPSK Modulator except for parameter input sample time. In this simulation, input sample time is equal to output sample time of QPSK Modulator.

Table 5.6 shows the parameter that has been used in the simulation.

Table 5.6: Parameters used in QPSK Demodulator Passband Block

Parameter	Value
M-ary number	4
Input type	Integer
Symbol period (s)	1/3840000 Hz
Baseband samples per symbol	1
Carrier frequency (in Hz)	15000000
Carrier initial phase (in rad)	Pi/4
Input sample time (s)	1/38000000 Hz

Delays from QPSK Demodulation block

Digital modulation and demodulation blocks sometimes incur delays between their inputs and outputs, depending on their configuration and on properties of their signals. Refer to the Release Notes 'Communication Blockset for Use with Simulink', all passband demodulators except OQPSK will experience delays in amount of one output period. So, QPSK passband demodulator causes delays of one output period occur in this simulation block.

To calculate the bit error rate correctly, additional delay of 1 second to the transmitted signal to synchronize it with the received signal. This is done directly in the mask for the Error Rate Calculation block by setting the receive delay to 1.

For the same reason, the PN chip sequence and received signals need to be synchronized before they enter the despreader block. In this case, integer delay block has been used, which delays a signal by the number of sample periods specified by the Delay parameter. Set the Delay to 1. This is indicated by the exponent-1 on the block. The delay synchronizes the PN chip sequence signal with the received signal so that the Despreader block can recover block the original data symbols correctly.

5.6.2 16-QAM Demodulator block

As in QPSK demodulator, similar design procedure will be employed for 16-QAM. Table 5.7 shows the parameters used in rectangular 16-QAM Demodulator block. The parameters are the same parameters used in initializing the parameters in 16-QAM modulator block.

Table 5.7: Parameters used in 16QAM Demodulator Passband Block

Parameter	Value
M-ary number	16
Input type	Integer
Normalized method	Min. Distance between symbols
Minimized distance	2
Symbol period	1/100
Baseband samples per symbol	1

Carrier frequency (Hz)	15e6
Carrier initial phase (rad)	0
Output sample time	1/38e6

5.7.1. Despreader block

In order to recover the data symbols from the spreading signal, the process of despreading is applied. This is done by 'XOR' the high bit rate noise-like signal with a local spreading chip code that has the same sequence with the transmitting code. When this right code is chosen with right synchronization, in this case delay is one output period; the output from the 'XOR' block will be exactly the same as the source signal. Parameters for Despreader block are same like the spreader block.

5.7.2 Error Rate estimator block

The error rate calculation block compares input data from a transmitter with input data from a receiver. It calculates the error rate as a running statistic, by dividing the total number of unequal pairs of data elements by the total number of input data elements from one source.

Table 5.8: shows the parameter that has been used in the simulation

Table 5.8: Parameters used in Error Rate calculation Block

Parameter	Value
Received delay	1
Computation delay	0
Computation mode	Entire frame
Output data	Port
Reset port box	Unchecked
Stop simulation box	Checked
Maximum number of symbols	5000

- a. Receive delay set up to 1 due to delay caused by QPSK Demodulator.
Referring to the release notes 'Communication Blockset for use with simulink', the delay should be put as 1 to ensure the transmitted signal synchronize with the received signal.
- b. Computation mode is set to entire frame. Then the block compares the entire transmitted frame with the entire received frame.
- c. Output Data. This block produces a vector of length three, whose entires correspond to:
 - The error rate
 - The total number of errors, that is, comparisons between unequal elements.
 - The total number of comparison that the block made.

Output data parameter is set to port, and then an output port appears.

This output port contains the running error statistics. Output port from this block connected to the display.

- d. The simulation stops when the maximum number of symbols is reached at 5000 data symbols even the target number of errors not reached 5000 errors.

5.7.3 Display block

The display block shows the value of its input, the amount of data displayed and the time steps at which the data is displayed are determined by block parameters:

- ❖ The display format can be control by selecting a format choice: short, which displays a 5-digit scaled value with fixed decimal point.
- ❖ The decimation parameter enables you to display data at every nth sample, where n is the decimation factor. The default decimation, 1, displays data at every time step.
- ❖ The sample time parameter enables you to specify a sampling interval at which to display points. This parameter is useful when you are using a variable-step solver where the interval between time steps might not be the same. The default value of -1 causes the block to ignore the sampling interval when determining the points to display.

Table 5.9 shows the parameter that has been used in the simulation.

Table 5.9: parameters used in Display Block

Parameter	Value
Format	Short
Decimation parameter	1
Floating display cox	Unchecked
Sample time	-1

The display, block shows the bit error rate, number of errors and the total number of bits that are transmitted.

5.8. PERFORMANCE ANALYSIS FOR PHASE 1

In this simulation, a generic m files is used together with simulink to simulate BER vs Eb/No graphs (refer to Appendix F, F1 to F13). This m file declares the parameters defined in the simulink's block diagram check box. For example, variable tsample declared in the m file is the sampling time of Bernoulli binary Generator. Tchip, on the other hand, is the sampling time of spreading sequence generator. EbNoVec is signal to noise ration and it is taken at 6 evenly points starting from 0. Then, for loop is used to calculate the BER for every EbNoVec assigned to it, the value of EbNo will be stored in the work space. Command simout is used to simulate simulink mdl file. Finally, command semilog is used to create the graph for BER vs Eb vs Eb/No.

First, the simulation is done by running the concerned mdl file. Once the output values are stored in the workspace, the associated m file is typed under the command window and it is run. Finally, BER graph vs EbNo graphs are obtained once the simulation is completed.

In this phase, the system is simulated based on the following conditions

1. Bit Error Rate (BER) versus Signal-to-Noise ratio (SNR) in AWGN channel for QPSK modulation technique.
2. BER Versus SNR in AWGN channel for 16-QAM modulation scheme.

5.2.2 Simulation phase 2: WCDMA system in AWGN and multipath Rayleigh fading

In phase 2, both transmitter and receiver part are built based on the system model as shown in figure 5.2 and figure 5.3. In this model, multipath fading channel block is added in the system. The rest of system blocks and parameters are unchanged.

In this phase of simulation, the model is simulated in the baseband simulation environment. The input of multipath Rayleigh fading block requires complex signal which can be obtained through baseband simulation only.

Moreover, in passband simulation, the simulation models the carrier frequency.

Since the carrier frequency is usually a high frequency signal, modeling passband communication systems involves high computation loads. To alleviate this problem, baseband simulation techniques are used.

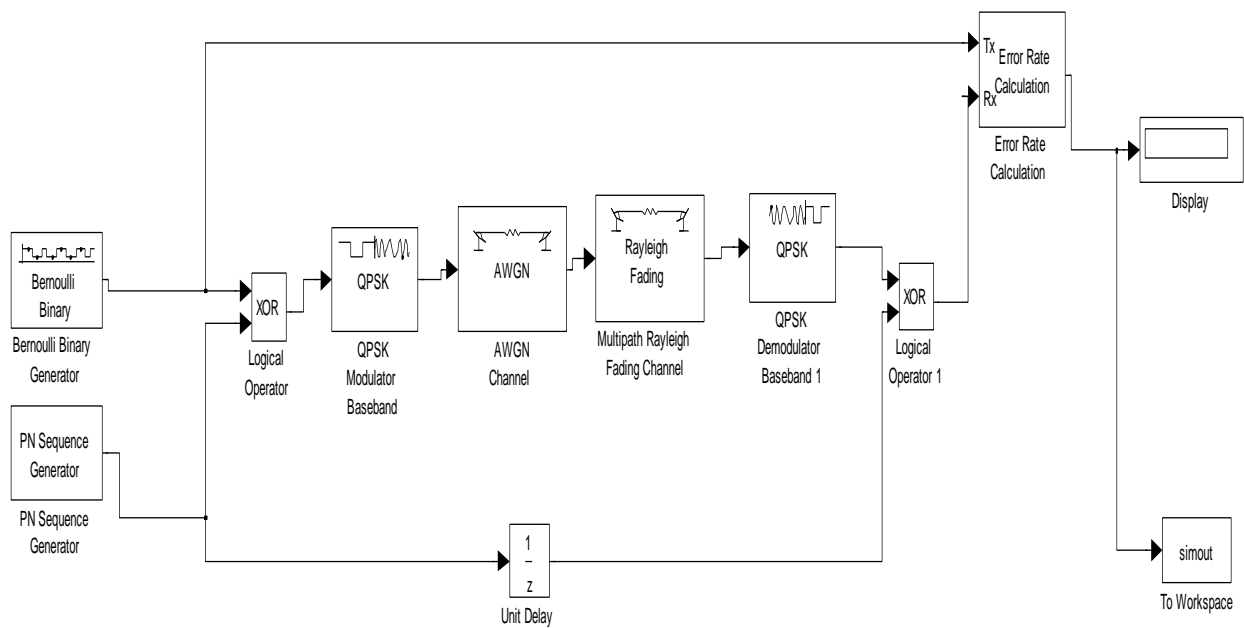


Figure 5.4: W-CDMA Model with Multipath Raleigh Fading Channel And AWGN Channel Using QPSK Modulation

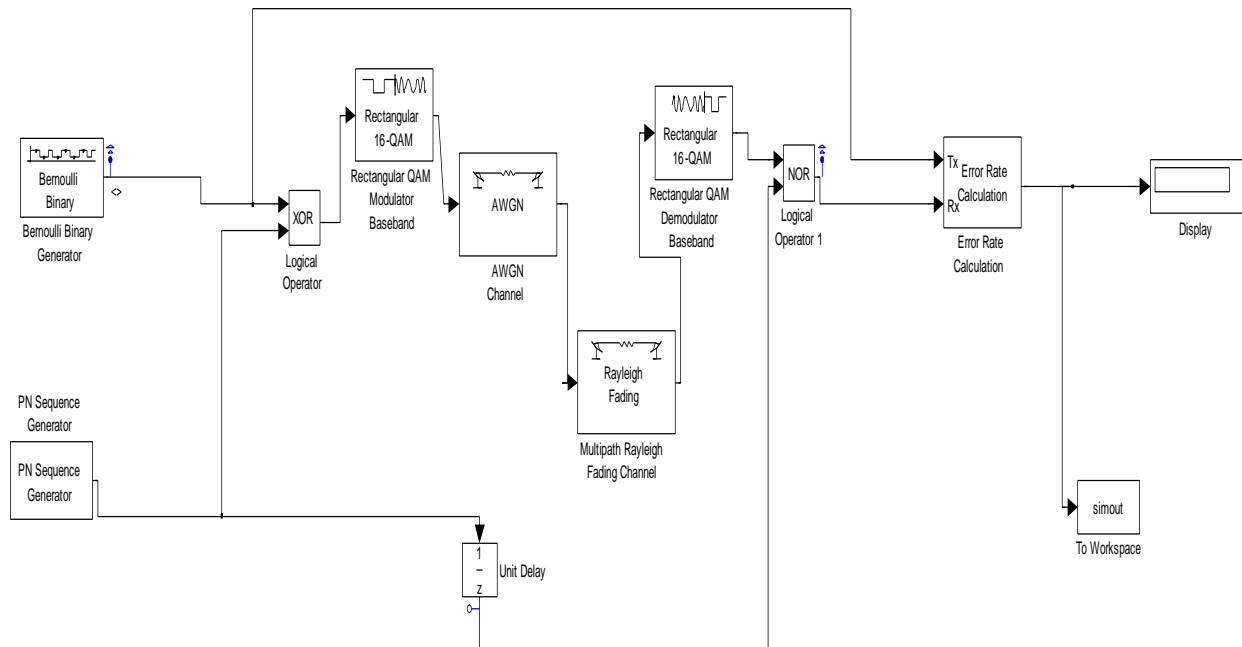


Figure 5.5: W-CDMA Model Using 16-QAM in AWGN and Multipath Raleigh Fading Channel

5.9 CHANNEL SPECIFICATION

Table 5.10 is used to initialize the parameters in the multipath Rayleigh fading block.

Table 5.10: parameter used in multipath Rayleigh fading channel

Parameter	Value
Maximum Doppler shift (h_z)	55.56/83.33/111.111
Sample time (s)	1/3840000
Delay vector (s)	20ray [0 2e -6] 30ray [0 2e-6 3e-6]
Normalize gain vector to 0 db overall gain box	Checked
Initial seed	40

a) Maximum Doppler shift (Hz). Relative motion between the transmitter and receiver causes Doppler shift in the signal frequency. The jacks PSD (power spectral density) determines the spectrum of the Rayleigh process. This implementation is based on the direct form simulator described in reference (1). Some wireless application, such as standard GSM (Global System for Mobile Communication systems, prefer to specify Doppler shifts in terms of the speed of the mobile. If the mobile moves at speed v making an angle θ of with the direct of wave motion, then Doppler's shift is

$$F_d = \frac{v f}{c} \cos \theta \dots \dots \dots (5.20)$$

Where f is the transmission carrier frequency and c is the speed of light. The Doppler frequency is the maximum Doppler shift arising from motion of the mobile.

In this Dissertation, to determine maximum Doppler shift for third generation systems, we assume that the transmission carrier frequency, $f=2\text{GHz}$. We assume mobile moves at three different speed, $v=60\text{km/hr}$, $v=90\text{km/hr}$ and $v=120\text{km/hr}$. Different speeds modeling the system in three different situations; in the middle of town, in the main road and in the highway. Angle θ set to 60 degree.

Based on the assumption above, the maximum Doppler shift for every speed value is:

When $v = 60\text{km/hr}$;

$$f_d = \frac{(60\text{km/hr} \times 2\text{GHz})}{30 \times 10^8 \text{ms}^{-1}} \cos 60^\circ \dots\dots\dots (5.20(a))$$

$$f_d = 55.56\text{Hz}$$

When $v = 90\text{km/hr}$;

$$f_d = \frac{(90\text{km/hr} \times 2\text{GHz})}{30 \times 10^8 \text{ms}^{-1}} \cos 60^\circ \dots\dots\dots 5.20(b)$$

$$f_d = 83.33\text{Hz}$$

When $v = 120\text{km/hr}$;

$$f_d = \frac{(120\text{km/hr} \times 2\text{GHz})}{30 \times 10^8 \text{ms}^{-1} \cos 600} \dots\dots\dots 5.20(\text{a})$$

$$f_d = 111.111\text{Hz}$$

- b) **Sample time** Equal to chip code rate, $T_c = 3840000\text{Hz}$
- c) **Delay Vector** is a vector that specified the propagation delay for each path. In this project, we assume the delays for 2 paths are 0 second and $2\text{e-}6$ second and the delays for 3 paths are 0 second, $2\text{e-}6$ second and $3\text{e-}6$ second.
- d) **Gain vector** that specified the gain for each path. The gains for 2 paths are 0 dB and -3 dB. The gains for 3 paths are 0 dB, -3 dB and 1 dB.
- e) **Normalize gain vector to 0 dB overall gain box.** Checking this box causes the block to scale the Gain vector parameter so that the channel's effective gain (considering all paths) is 0 decibels.

5.9.1 Performance Analysis for Phase 2

Same procedures are used to do the performance analysis for phase 2 as they are done in phase 1. Performance analysis for this system is based on the following conditions.

1. BER Versus SNR in AWGN and multipath Rayleigh fading channel with Doppler shift (60kmph, 90kmph and 120kmph) for QPSK modulation technique.

2. BER versus SNR in AWGN and multipath Rayleigh fading channel with Doppler shift (60kmph, 90kmph and 120kmph) for 16-Qam modulation scheme.

In summary, there are six procedures to be used on for simulation in phase 1 and phase 2 as they are shown as follows:

1. Bit Error Rate (BER) Versus Signal-to Noise Ration (SNR) in AWGN channel for QPSK modulation technique.
2. BER Versus SNR in AWGN channel for 16-QAM modulation scheme
3. BER versus SNR in AWGN and multipath Rayleigh fading channel with Doppler shift (60kmph, 90kmph and 120kmph) for QPSK modulation technique.
4. BER Versus SNR in AWGN and multipath Rayleigh fading channel with Doppler shift (60kmph, 90kmph and 120kmph) for 16-QAM modulation technique.
5. BER versus SNR to compare between AWGN channel and multipath Rayleigh fading channel for different number of user for QPSK modulation scheme.
6. BER versus SNR to compare between AWGN channel and multipath Rayleigh fading channel for different number of user for 16-QAM modulation Technique.

5.10 PERFORMANCE ANALYSIS ON WCDMA SYSTEM

Based on the data generated by computer simulation of W-CDMA models, relationship for multiple rays using QPSK and QAM modulation techniques between BER as a function of the following parameters are obtained. They are:

1. Bit error Rate (BER) versus Signal-to-Noise ratio (SNR) in AWGN channel for QPSK modulation technique.
2. BER versus SNR in AWGN channel for 16-QAM modulation scheme.
3. BER versus SNR in AWGN and multipath Rayleigh fading channel with Doppler shift (60kmph, 90kmph and 120kmph) for QPSK modulation technique
4. BER versus SNR in AWGN and multipath Rayleigh fading channel with Doppler shift (60kmph, 90kmph and 120kmph) for 16-QAM modulation scheme.
5. BER versus SNR to compare between AWGN channel and multipath Rayleigh fading channel for different number of user for QPSK modulation technique.
6. BER versus SNR to compare between AWGN channel and multipath Rayleigh fading channel for different number of user for 16-QAM modulation technique.

5.10.1 Performance Analysis of QPSK modulation technique of WCDMA in AWGN

Table 5.11: simulation result for evaluation on BER vs. SNR for 2-ray AWGN channel for 1 user when the number of data 200,000

Signal-to-Noise Ratio (E_bN_0)	No. of Error	Bit Error Rate (BER)
0	15615	7.807500e-002
1	11334	5.667000e-002
2	7520	3.760000e-002
3	4484	2.242000e-002
4	2489	2.244500e-002
5	1205	6.025000e-003
6	462	2.310000e-004
7	165	8.250000e004
8	39	1.950000e-004
9	2	1.000000e-005
10	1	5.000000e-006

In this simulation, the BERs are obtained by varying the values of E_bN_0 in the range of 0 to 10. The iteration is done 1000 times where total number of data transmitted is 200,0000. Matlab codes in appendix F1

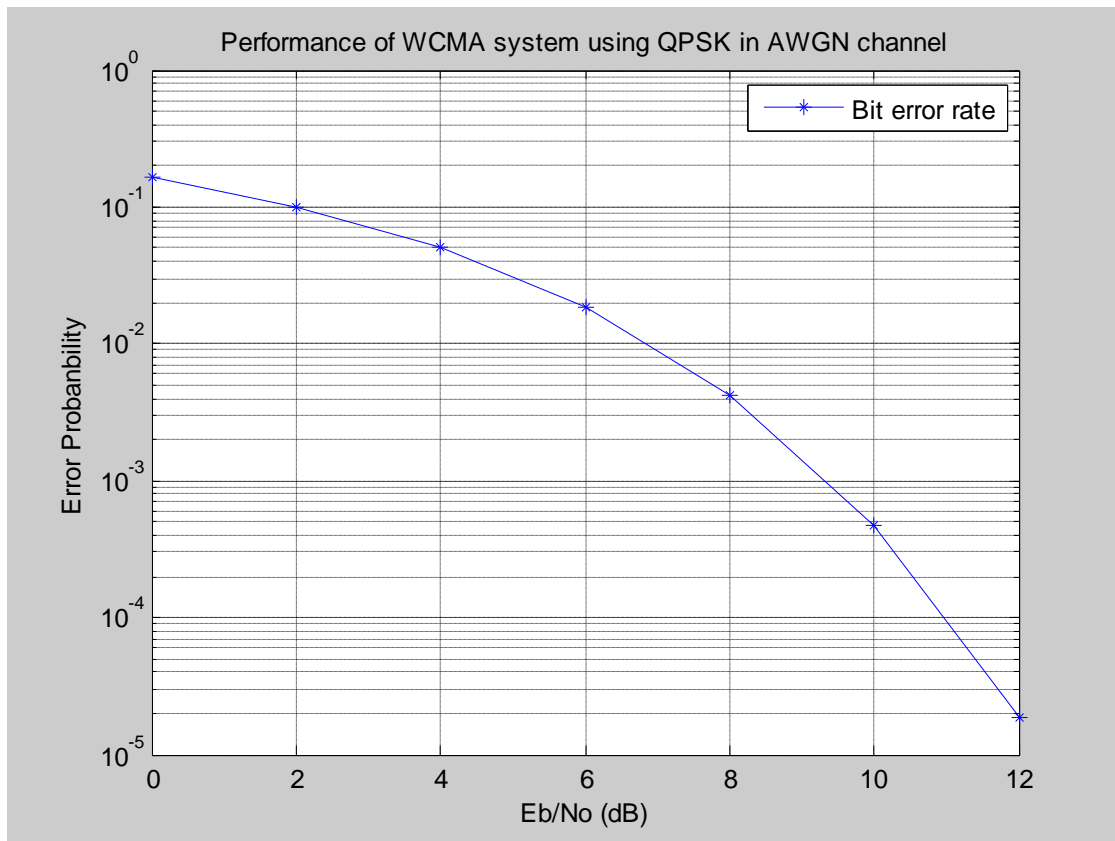


Figure 5.6. Performance of WCDMA system using QPSK in AWGN channel.

QPSK modulation technique has a better performance in AWGN at threshold of error probability of 10^{-3} , corresponding to 9,8dB

Table 5.12: simulation results for evaluation on BER vs. SNR for 2-ray multipath Rayleigh fading for 1 user when the number of data is 200,000 at 60 kmph , Matlab codes in appendix F2

Signal-to-Noise Ratio ($E_b N_0$)	No. of Error	Bit Error Rate (BER)
0	27889	1.394450e-001
2	20441	1.022050e-001
4	14529	7.264500e-002
6	9742	4.871000e-002
8	6494	3.247000e-002
10	4197	2.098500e-002
12	2926	1.463000e-003
14	1888	9.440000e-003
16	1261	6.305000e-003
18	916	4.580000e-003
20	614	3.070000e-003

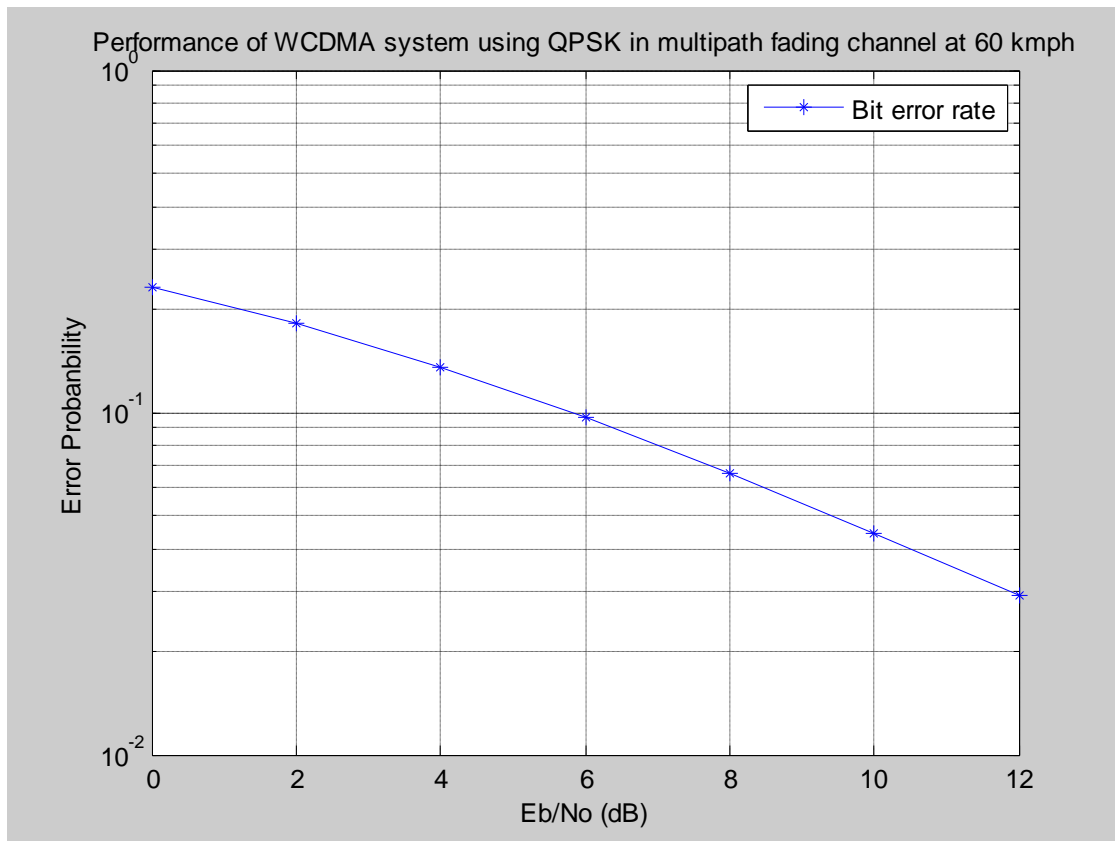


Figure 5.7: Performance of W-CDMA system using QPSK in Multipath fading channel at 60km, QPSK modulation technique has a better performance in multipath effect as the mobile speed at 60km/h

Table 5.13: simulation for evaluation on BER vs. SNR for 2-ray multipath Rayleigh fading channel for 1user when the number of data 200,000 at 90 kmph , Matlab codes in appendix F3

Signal-to-Noise Ratio (E_bN_0)	27464	Bit Error Rate (BER)
0	15615	1.373200e-001
2	20213	1.010650e-001
4	14046	7.023000e-002
6	9146	4.573000e-002
8	6147	3.073500e-002
10	3983	1.991500e-002
12	2649	1.324500e-002
14	1662	8.310000e-003
16	1059	5.295000e-003
18	618	3.405000e-003
20	415	2.075000e-003

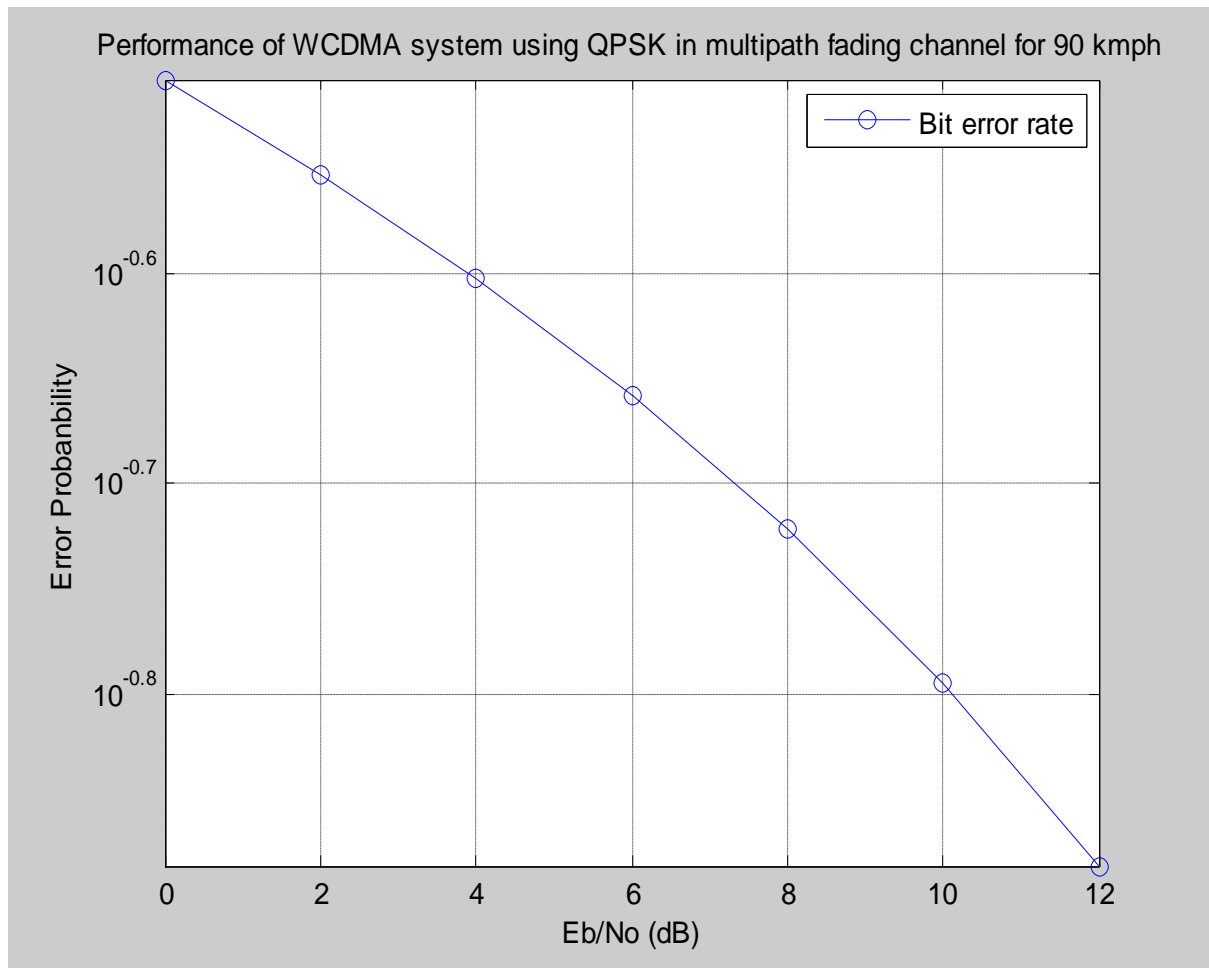


Figure 5.8: Performance of W-CDMA system using QPSK in Multipath fading channel at 90km. QPSK modulation technique has varied error probability as the speed of the mobile increases 90km/h.

**Table 5.15 simulation result for evaluation on BER vs. SNR 2-ray
Multipath Rayleigh fading channel for 1 user when the number of data
is 200,000 at 120 kmph , Matlab codes in appendix F4**

Signal-to-Noise Ratio ($E_b N_0$)	No. of Error	Bit Error Rate (BER)
0	27920	1.396000e-001
2	20820	1.041000e-001
4	14570	7.285000e-002
6	9998	4.999000e-002
8	6708	3.354000e-002
10	2889	2.218000e-002
12	2889	1.444500e-002
14	1878	9.390000e-002
16	1240	6.200000e-003
18	794	3.970000e-003
20	543	2.715000e-003

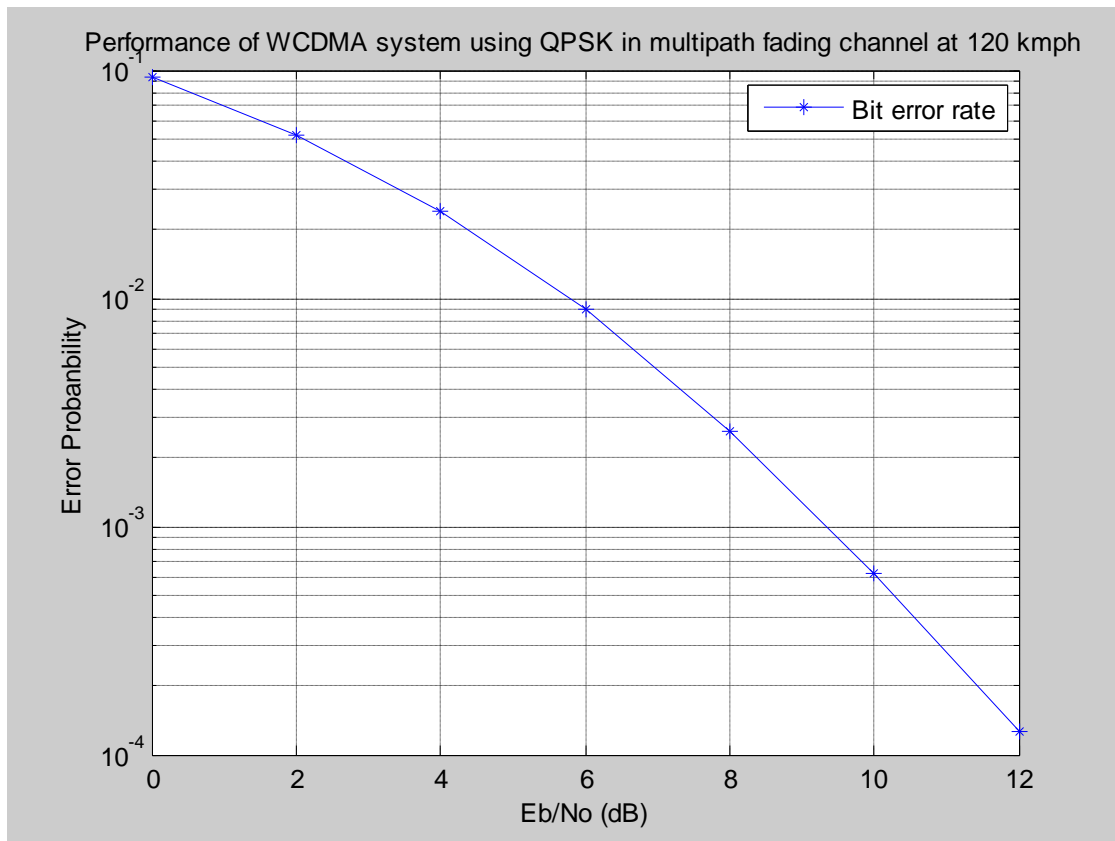


Figure 5.9: Performance of W-CDMA system using QPSK in Multipath fading channel at 120km

QPSK modulation technique has varied error probability as the speed of the mobile increases 120km/h.

5.10.2 Performance Analysis of 16-QAM modulation technique of W-CDMA in AWGN , Matlab codes in appendix F5

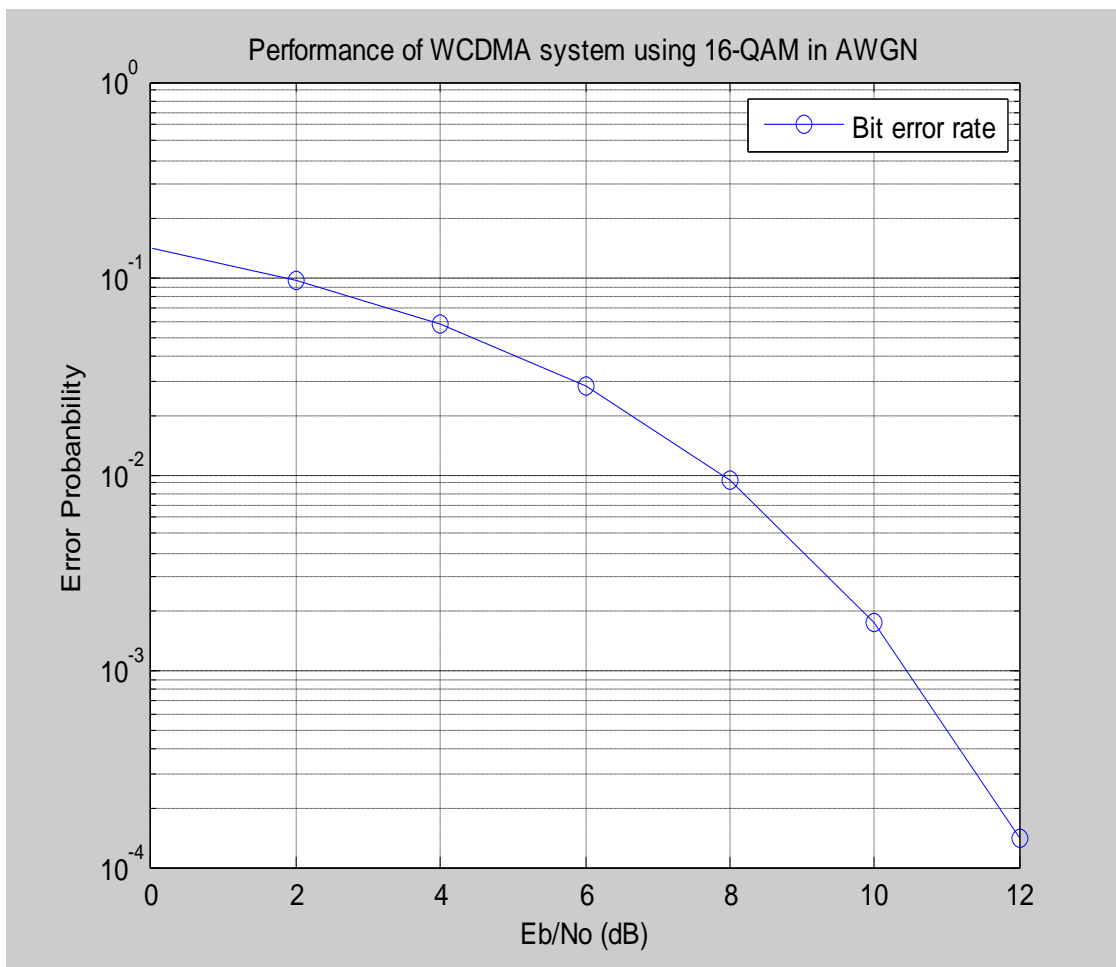


Figure 5.10: Performance of W-CDMA system using 16-QAM in AWGN

QAM modulation technique has more SNR in AWGN at threshold of error probability of 10^{-3} , corresponding to 10.2dB

5.10.3 Performance Analysis of W-CDMA system using 16QAM in AWGN and Multipath fading channel

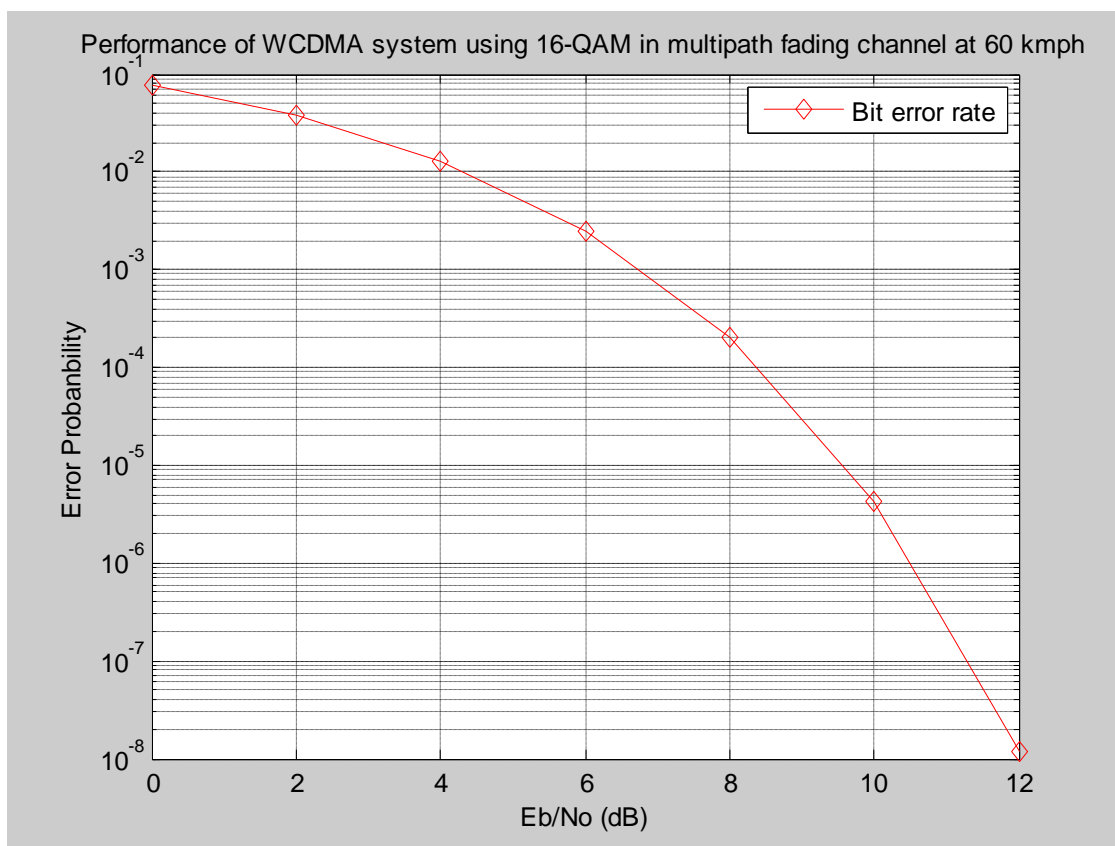


Figure 5.11: Performance of W-CDMA system using 16QAM in Multipath fading channel at 60kmph

QAM modulation technique has varied error probability as the speed of the mobile increases 60km/h.

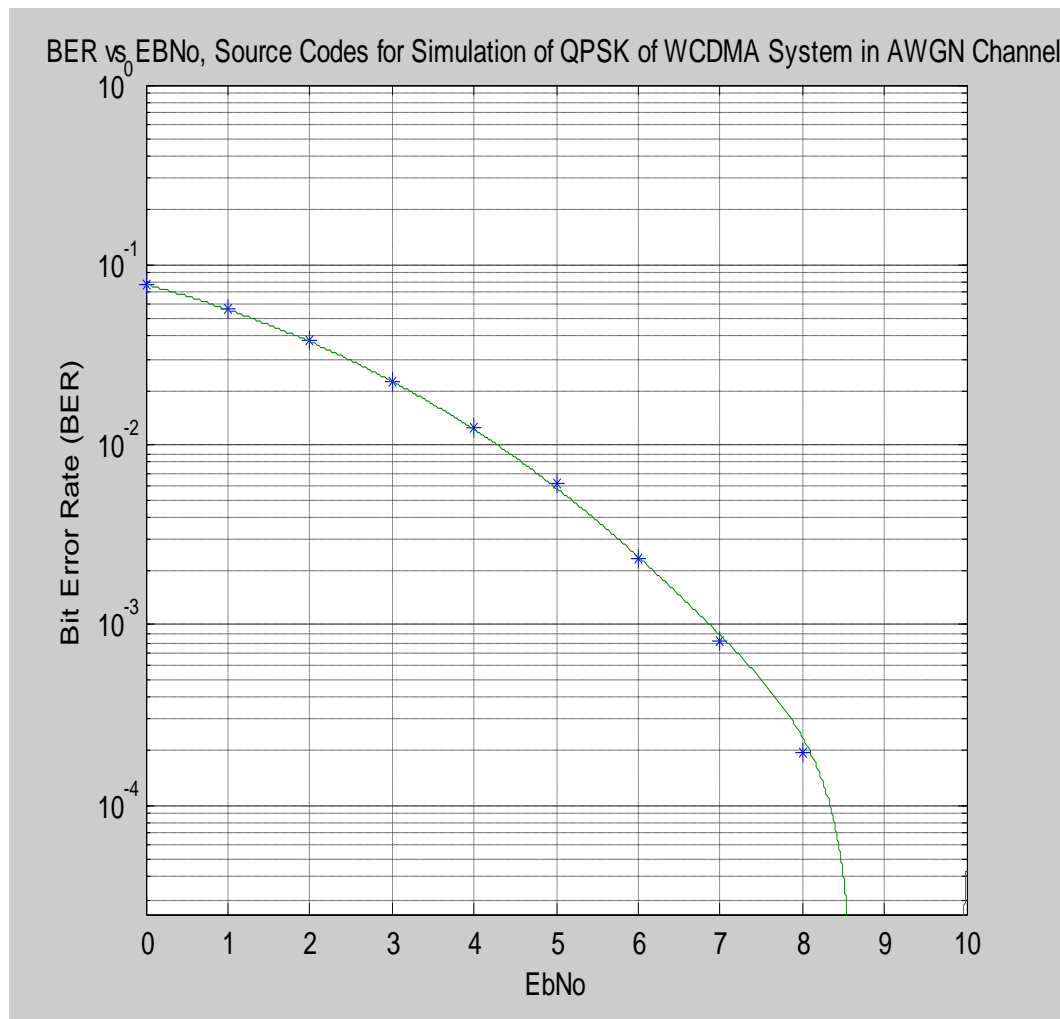


Figure 5.12: Performance of W-CDMA in 2 Rays of in AWGN channel for 1 user.

QPSK modulation technique has a better performance in AWGN at threshold of error probability of 10^{-3} , corresponding to 9,8dB for one user

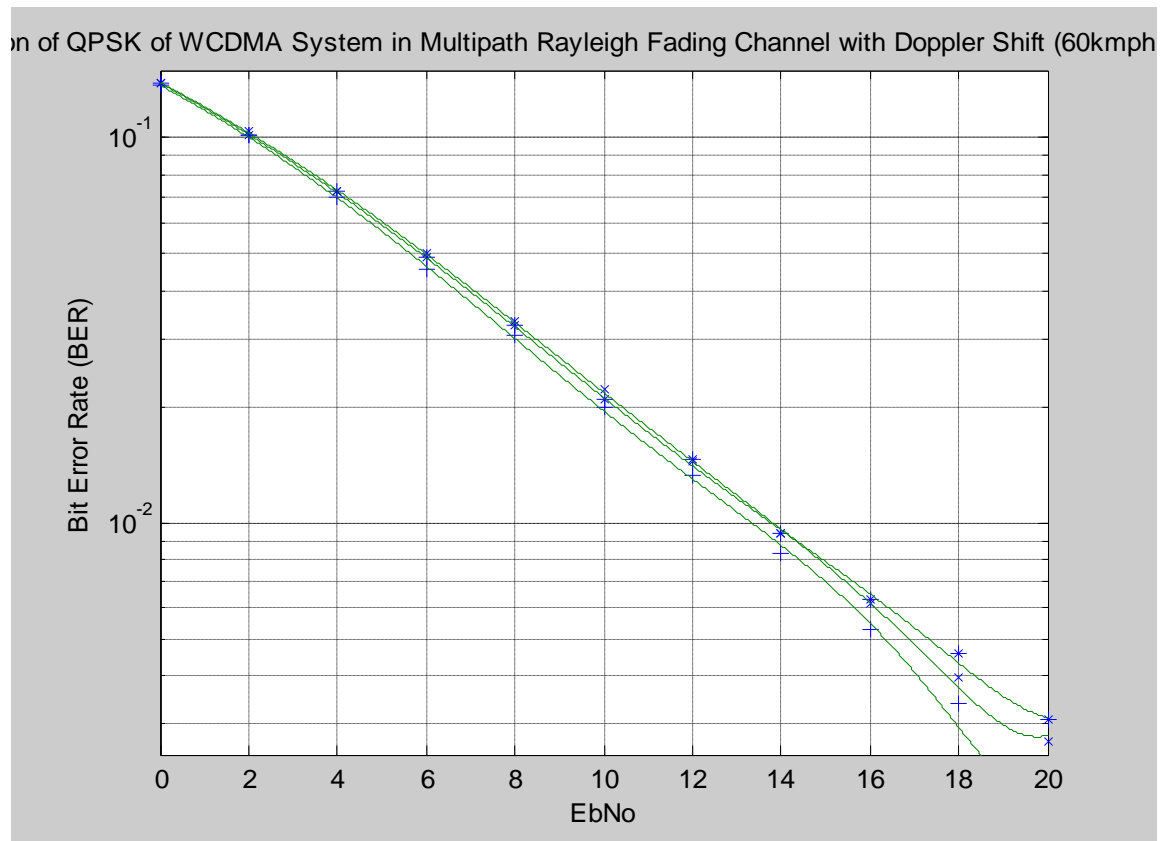


Figure 5.13: Performance of W-CDMA in 2 Rays in Multipath Rayleigh channels for 1 user for Doppler shift 60,90 and 120kmph.

Comparison of QPSK modulation technique at different speed 60km/h, 90km/h and 120km/h respectively, in multipath Rayleigh channel for one user, thus error increases as the speed of the mobile varies.

5.10.4 Performance Analysis comparison of QPSK modulation technique of WCDMA between AWGN and Rayleigh fading channel

Table 5.16: simulation result for evaluation on BER vs. SNR for 2-ray AWGN channel for 1 user when the number of data is 200,000

Signal-to-Noise Ratio ($E_b N_0$)	No. of Error	Bit Error Rate (BER)
0	15615	7.807500e-002
1	11334	5.667000e-002
2	7520	3.760000e-002
3	4484	2.242000e-002
4	2489	1.244500e-002
5	1205	6.025000e-003
6	462	2.310000e-003
7	165	2.350000e-004
8	39	1.950000e-004
9	2	1.000000e-005
10	1	5.000000e-006

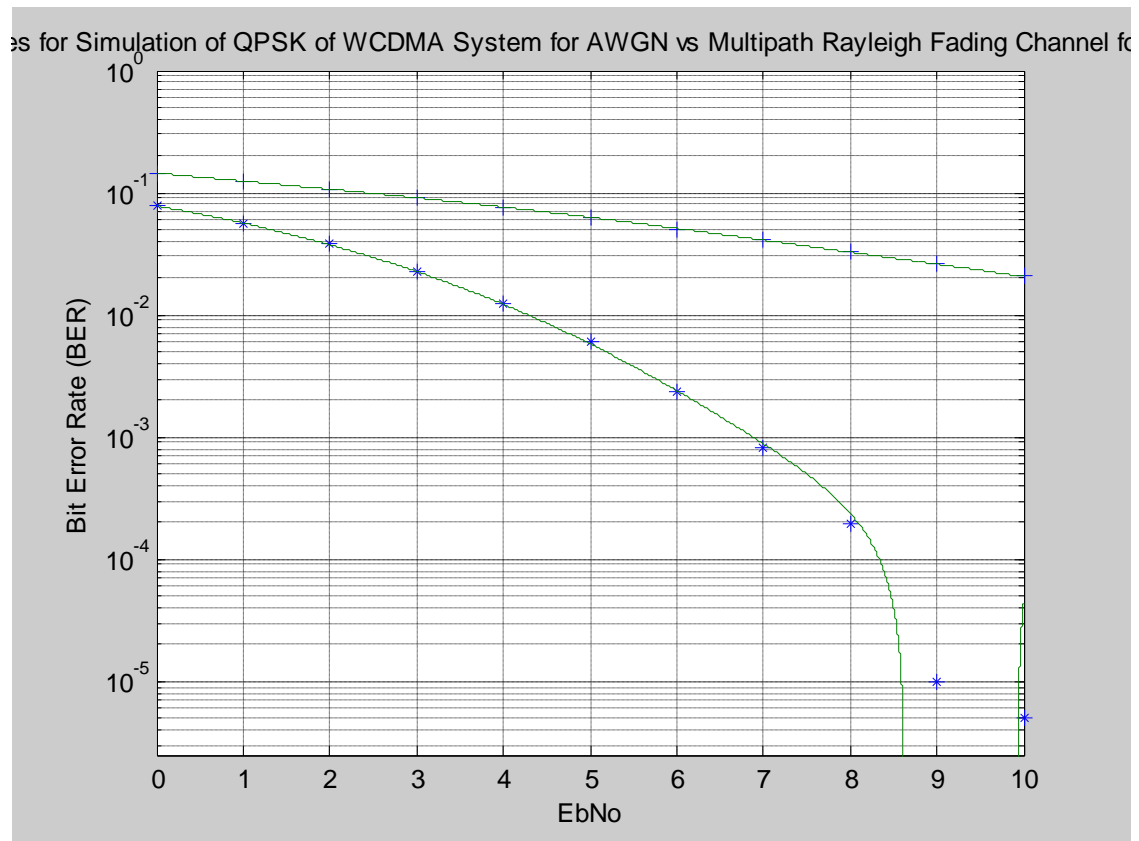


Figure 5.14: Performance comparison of W-CDMA in 2 Rays between AWGN and Multipath Rayleigh channel for 1 user.

QPSK modulation technique has a better performance in AWGN than in multipath Rayleigh channel for one user

Table 5.16: simulation result for evaluation on BER vs. SNR for 2-ray AWGN channel for 1 user when the number of data is 200,000

Signal-to-Noise Ratio ($E_b N_0$)	No. of Error	Bit Error Rate (BER)
0	28979	1.448950e-001
1	24809	1.240450e-001
2	21465	1.073250e-001
3	18128	9.064000e-002
4	15283	7.641500e-002
5	12601	6.300500e-002
6	10143	5.071500e-002
7	8285	4.42500e-002
8	6503	3.251500e-002
9	5194	2.597000e-002
10	4119	2.059500e-002

Table 5.17: simulation result for evaluation on BER vs. SNR for 2-ray AWGN channel for 5 users when the number of data is 200,000

Signal-to-Noise Ratio ($E_b N_0$)	No. of Error	Bit Error Rate (BER)
0	94680	9.468000e-002
2	56563	5.656300e-002
4	29383	2.938300e-002
6	13676	1.367600e-002
8	5393	5.393000e-003
10	1932	1.932000e-003
12	552	5.520000e-004
14	72	7.200000e-005
16	4	4.000000e-006
18	0	0
20	0	0

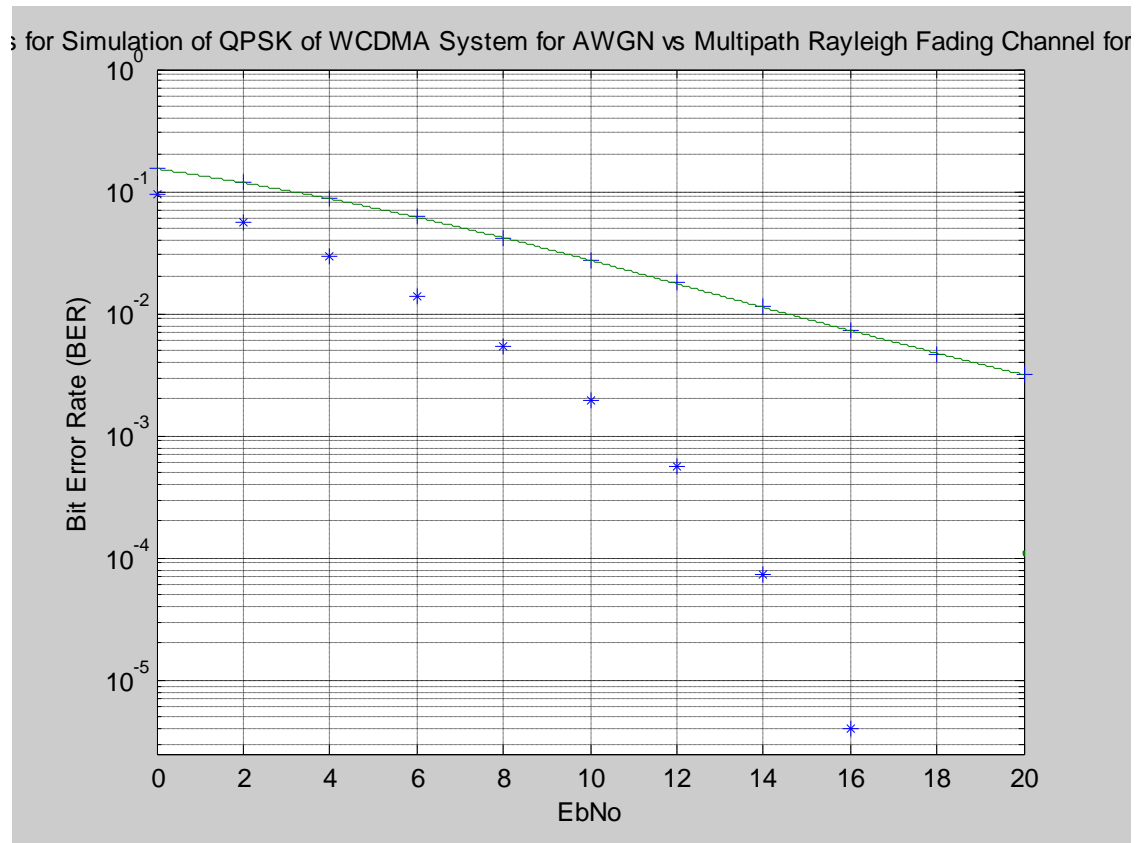


Figure 5.15: Performance comparison of W-CDMA in 2 Rays between AWGN and Multipath Rayleigh channel for 5 user.

QPSK modulation technique has a better performance in AWGN than in multipath Rayleigh channel for five users

Table 5.18: simulation result for evaluation on BER vs. SNR for 2-ray AWGN channel for 1 user when the number of data is 200,000

Signal-to-Noise Ratio ($E_b N_0$)	No. of Error	Bit Error Rate (BER)
0	153437	1.534370e-001
2	1188123	1.181230e-001
4	87273	8.727300e-002
6	61830	6.187500e-002
8	41875	4.187500e-002
10	27248	2.724800e-002
12	17799	1.779900e-002
14	11307	1.130700e-003
16	7314	7.314000e-003
18	4713	4.713000e-003
20	3210	3.210000e-003

5.10.5 Performance Analysis of 16-QAM modulation technique of WCDMA in AWGN

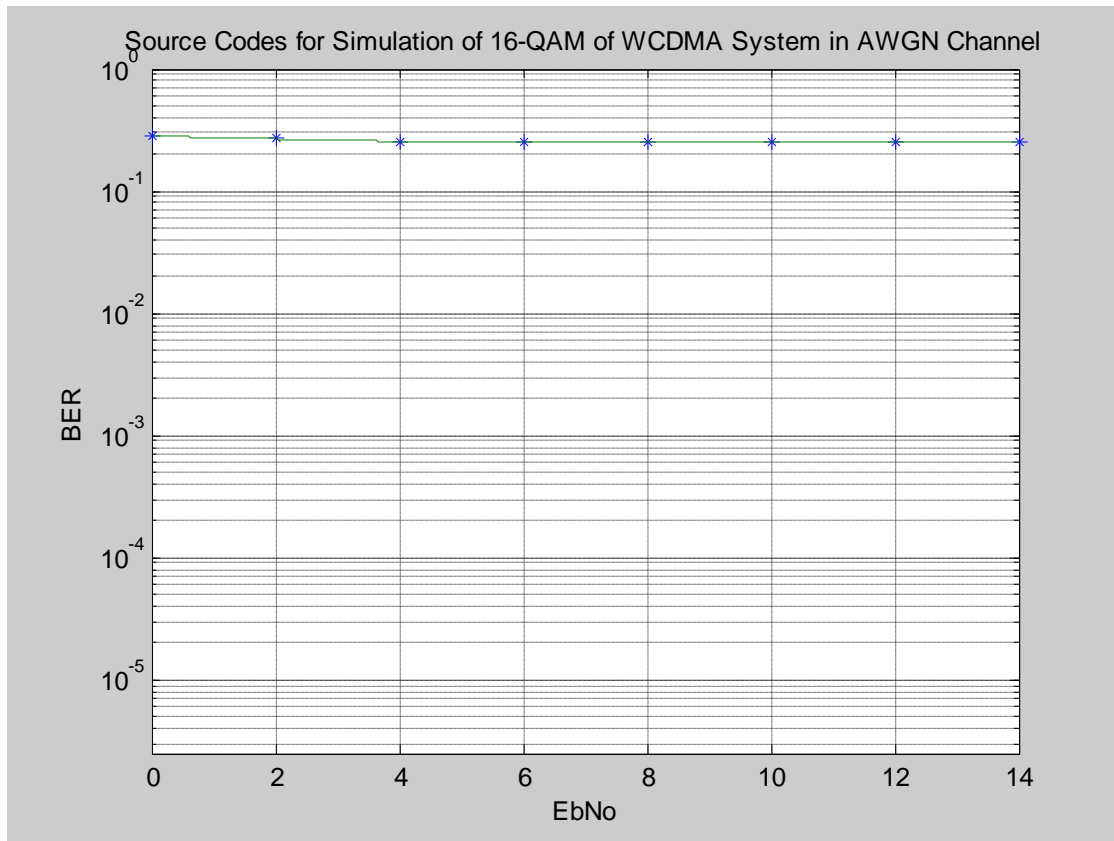


Figure 5.16: Performance Comparison of 16QAM in W-CDMA system in AWGN

QAM modulation technique performance in AWGN show abnormal result , basically due to the interference between adjacent carriers phase in the constellation of 16-ary QAM

- **DEDUCTIONS**

Both simulation using simulink and m-file shows that each QPSK and 16-QAM modulation technique in AWGN channel has good performance when it is compared under multipath Rayleigh channel. Also, the

performance of QPSK and 16-QAM degrades when the channel is subjected to multipath fading with increasing value of Doppler shift (Hz). In other words, it performs, poorly as the speed of mobile terminal is increased. Moreover, the system performs badly as the number user is increased. Comparison between QPSK and 16-QAM modulation schemes shows that 16-QAM performs very poorly in both AWGN and AWGN with multipath fading channel. The simulation of 16-QAM modulation technique using m files cannot be done because it is suspected that the variation of amplitude with phase caused in the constellation of 16-QAM signal. Thus, analysis for 16-QAM can only be done in Simulink

- The reason behind poor performance of 16-QAM of WCDMA system in multipath fading channel is basically due to the interference between adjacent carriers phase in the constellation of 16-ary QAM. A sound approach is needed to be used in 16-QAM of WCDMA system to ensure zero or minimal interference between adjacent carriers phase in the constellation of 16-QAM. It is suggested that error correction coding such as convolutional coding or turbo coding be used in this system to ensure better performance of 16-QAM modulation technique of WCDMA system. Also, it is possible to consider the use of a RAKE receiver or a smart antenna (MIMO) in this system to exploit the delayed signals generated in multipath fading channel. It is discovered, as well, that the performance of multiuser in the m file is limited to a maximum of 7 users. Thus, this system needs to be improved to simulate a greater number of users so that the performance of multiple access in W-CDMA can be studied more dynamically.

CHAPTER SIX

CONCLUSION

6.1. CONCLUSION

This work has shown the path loss models for Urban and Sub-urban Region of Imo state using two modulation techniques QAM and QPSK. The models were empirically developed by applying log-normal shadowing model on configured modulation techniques at different base station here QAM and QPSK were considered. It was shown that the efficient path loss model based on measurement for the two modulation techniques that should be adaptively deployed in Urban Area Category A, and Sub-Urban area Category B were found to be

❖ **PATHLOSS MODEL FOR QAM MODULATION in Urban CATEGORY A**

$$Lp\{d\} = 111 + 20.63\log_{10}(d/d_0)$$

➤ **PATHLOSS MODEL FOR QPSK MODULATION in Urban Category A**

$$Lp\{d\} = 106 + 14.94\log_{10}(d/d_0)$$

➤ **PATHLOSS MODEL FOR GMSK MODULATION IN URBAN**

$$Lp\{d\} = 103 + 21.104\log_{10}(d/d_0)$$

While that for Sub-Urban Category B

❖ **PATHLOSS MODEL FOR QAM MODULATION in Sub-Urban**

$$Lp\{d\} = 100.24 + 25\log_{10}(d/d_0)$$

➤ **PATHLOSS MODEL FOR QPSK MODULATION in Sub-Urban**

$$Lp\{d\} = 83.83 + 10.8\log_{10}(d/d_0)$$

Comparison Between these models and those predicted by hata, COST231 and free space have shown some variations. from these variations it shows that none of the aforementioned models can be fully be used as fixed model in Imo State due to

transmission impairment and environmental differences, hence, the need for adaptive modulation and modification.

The work also considered the performance of W-CDMA system in AWGN channel which shows that QPSK modulation technique has a better performance compared to 16-QAM. Furthermore, similar trend is found when the channel is subject to multipath Rayleigh fading with Doppler shift. The performance of QPSK and 16-QAM modulation technique in WCDMA system degrades as the mobility is increased from 60kmph to 120kmph for both QPSK and 16-QAM. However, QPSK shows better performance compared to that of 16-QAM in AWGN and multipath Rayleigh fading channel. In other words, 16-QAM suffers signal degradation and error proneness when the simulations are done in these channels. As the number of user is increased, the QPSK modulation technique performed poorly in WCDMA system. Unfortunately, the simulation for 16-QAM has failed to show the expected results. Therefore, it results in inconsistency of data or signal throughput causing an abnormal value of BER and eventually affecting the performance of WCDMA system. It is expected that 16-QAM will show performance degradation simulation similar like QPSK as the number of user is increased but with lower performance compared to that of QPSK. In general, the reason that causes poor performance of WCDMA system when the number of user increased is because the value of cross-correlation between the codes is not 0 and thus it causes interference.

Many studies and researches have shown that 16-QAM modulation technique is a primary candidate for high speed data transmission in 3G mobile communication. High speed downlink packed Access (HSDPA) is considered as a 3.5G where it has the capability to boost up the data rates of up to 10.7 Mbps using 16-QAM in a static environment. However, higher, data rate modulation schemes (e.g.16-QAM) suffers significant degradation in noise and multipath Rayleigh fading channel compared to

lower data rate modulation technique (e.g. QPSK). The errors are caused by interference between adjacent carriers phase in constellation of M-ary QAM. Larger value of M-ary AQM suffers more signal degradation. Thus, it is suggested that high data rate modulation technique such as 16-AQM needs an error correction coding such as convolutional coding or turbo coding so that the interference from the adjacent carrier phase in the constellation of 16-QAM be eliminated if not minimized.

6.2 CONTRIBUTION TO KNOWLEDGE

Presented here are empirically derived path loss model for microcellular wireless communication using adaptive modulation techniques for urban and Sub-Urban area of Imo State to maintain acceptable bit error rate to subscribers and can be used for radio planning and link budget analysis to achieve the following.

1. RF engineers can use the models obtained for radio planning and link budget analysis

2. Increase network capacity and improve user experience

3. To maintain efficient Quality of service (QOS) to the mobile users at acceptable bit error rate

4. To reduce operational and infrastructural cost for network operators

5. To Maintain constant link between subscribers on voice over internet protocols (VoIP) thus streaming of video , voice and conference call can be achieved with high speed.

6.3 SUGGESTION FOR FUTURE WORK

A more complete WCDMA system can be developed using the suggested method as they are explained as follows.

1. Generate binary data source for various data rates for various services offered by W-CDMA system in 3G environment. For example 144 kbps for suburban (indoor/outdoor), urban vehicular pedestrian, and 2 Mbps for indoor office.
2. Implement error correction scheme such as convolutional coding and turbo coding particularly with M-QAM modulation technique in WCDMA system. Higher order QAM modulation schemes are vulnerable to error. Therefore, error correction coding ensures higher chances of signal survivability in AWGN and multipath Rayleigh channel and thus enhances the performance of the system.
3. It is proposed that Rician fading is included in the channel in addition to AWGN and multipath Rayleigh fading channel. Then, comparison can be made between these channels.
4. Also, it is proposed that other sequence generator be employed to generate unique chip code and spread the bandwidth of WCDMA system such as Gold sequence Generator, and Kasami Sequence Generator beside the PN sequence. Then, comparison can be made to determine which one is having a better performance and good BER characteristics.
5. A complete uplink and downlink W-CDMA system can be implemented in the WCDMA system for a comprehensive study.
6. A RAKE receiver or a smart antenna (Multiple Input and Multiple Output) is suggested to be used in this system to exploit the delayed signals arrived at the antenna caused by multipath Rayleigh fading.

7. Newer version of MATLAB should be considered. This is due to the limitation of blocks in communication toolbox and block set. Even though the numbers of block in communication block set are many, more designs of block set using CDMA, especially W-CDMA technologies are needed in this thesis. This is to produce high accuracy and precision simulation model of W-CDMA system. Other alternative is to use high performance simulation software like Advanced Design System by Agilent Technologies.

REFERENCES

- [1] Proakis, G.J. *"Digital Communication" fourth Edition, McGraw-hill International Editions 2001.*
- [2] Gunnarsson, F. *"Power Control in Wireless Networks: characteristics and fundamentals, "in Wireless Communications Systems and Networks, M. Guizani, Ed. New York: Plenum Press, pp. 179-20 (2004).*
- [3] Virgillo, R. and Goodman, D. *'Prioritized Throughput Maximization via Rate and Power Control for 3g CDMA: The 2 Terminal Scenario', Brooklyn Polytechnic University (2002).*
- [4] Karalayali, M.K et al, *"Downlink throughput maximization in CDMA wireless Networks, "in Proc. Of IEEE Wireless Communication and Network Conference (2004).*
- [5] Simon Haykin, *"Cognitive Radio: Brain-Empowered Wireless Communications," IEEE journal on Selected Areas in Communications, Vol. 23, No.2, , pp 201-220 February 2005.*
- [6] S.T. Chung, A.J. Goldsmith, *"Degrees of Freedom in Adaptive Modulation: A Unified View," IEEE Trans. Commun., vol. 49, pp. 1561-1571, Sept. 2001.*
- [7] A. J. Goldsmith, S. G. Chua, *"Variable-Rate Variable-Power MQAM for Fading Channels," IEEE Trans. Communication., vol. 45, pp. 1218-1230, October 1997*
- [8] A. Goldsmith and P. Varaiya, *"Capacity of fading channels with channel side information," IEEE Trans. Inform. Theory, vol. 43, pp. 1986-1992, 1997*
- [9] A.J. Goldsmith, S.G. Chua, *"Adaptive Coded Modulation for Fading Channels," IEEE Trans. Commun., vol. 46, pp.595-602, May 1998*

- [10] K. J. Hole, H. Holm, G. E. Olien, "*Adaptive Multidimensional Coded Modulation over Flat Fading Channels*," *IEEE J. Select. Areas Commun.*, vol.18, pp. 1153-1158, July 2000
- [11] D. L. Goeckel, "Adaptive Coding for Time-Varying Channels Using Outdated Fading Estimates," *IEEE Trans. Communication.*, vol. 47, pp. 844-855, June 1999
- [12] S. Zhou, G. B. Giannakis, "*Adaptive Modulation for Multi antenna Transmissions with Channel Mean Feedback*", *IEEE Trans. Wireless Communication.*, vol.3, pp. 1626-1636, Sept. 2004
- [13] Goodman, d and Mandayam, N. "*Network assisted power control for wireless data*," *Mobile Network. And Appl.*, vol. 6, no. 5, pp. 409-418.
- [14] Sklar, B. *Digital Communications: Fundamentals and applications, fundamental and Applications – 2nd edition* (2001).
- [15] Viadya, N,H, and M.J, Miller; "*On-Demand TDMA Scheduling for Energy Conservation in Senior Networks*", *Technical Report* June 2004.
- [16] Garg, V, K *IS-95 CDMA and CDMA2000: Cellular/PCS Systems Implementation, Prentice Hall Communication Engineering and Emerging Technologies Series, T. Rappaport, Ed. New Jersey: Prentice Hal* (2000).
- [17] Akl, R and Parvez, A. '*Impact of Interference Model on capacity in CDMA cellular Networks*' *Proceedings of SCI 04. Communication and Network Systems, Technologies and Applications*, 3:404-408 (2004).
- [18] Julian Cheng, Norman, C. Beaulieu, "*Accurate DS-CDMA Bit-Error Probability calculation in Rayleigh fading*", *IEEE Transactions on Wireless Communications*, Vol 1, No. 1, January 2002.
- [19] Akl, R et.al '*Mobility-based CAC Algorithm for Arbitrary Traffic Distribution in CDMA Cellular System*' *IEEE Trans. Veh. Technol.*, 54:639-651 (2005).
- [20] Proakis, G.J. "*Digital Communication*" *fourth Edition, McGraw-hill International Editions* (2002).

- [21] CDMA Development Group, "CDG 1Q 2009 Subscribers Statistics, <http://www.cdg.org/worldwide/cdmaworldsubscriber.asp> (2009).
- [22] Jelitto, J. et al., "Dynamic Data and Transmit Power Adjustment in IEEE 802.11 wireless LAN," *Int. J. of Wireless Inf. New*, Vol. 12, no 3, pp. 123-145 (2005).
- [23] Lavery, R. J. "Throughput Optimization for Wireless data Transmission, M.S. Thesis, Polytechnic University, Brooklyn, N Y (2001).
- [24] Revi, K.V. "Comparison of Multi-Accessing Schemes for Mobile communication Systems," *IEEE Int. Conf. on Personal Wireless commum.* Pp. 152-156 (1994).
- [25] J. Litva, T. K. Lo, "Digital Beam forming in Wireless Communications," Artech House, Norwood, 1996
- [26] Huawei Technologies Co., Ltd, "Network Preliminary Proposal for Erbil CDMA WLL Project", 2003
- [27] Coperation, , "The Wireless Network Planning Report For Dalyasat Project", 2006.
- [28] Huawei Technologies Course Development Room, "RG0105 CDMA 1x Air Interface", March 2003
- [29] Julian Cheng, Norman, C. Beaulieu, "Accurate DS-CDMA Bit-Error Probability calculation in Rayleigh fading", *IEEE Transactions on Wireless Communications*, Vol 1, No. 1, January 2002.
- [30] Topny Ottoson, "Multi-rate Scheme and Multi-user Decoding in DS-CDMA Systems", *Thesis for degree of licentiate of Chalmers University of Technology*, Technical report no 2141, ISBN 91-7197-217-X, November 1995.
- [31] Y. Rosmansyah, P. Sweeney, R. Tafazolli, "Air-Interface Technique for Achieving High Data Rates for UMTS", *3G Mobile Communication Technologies*, Conference Publication No. 477, pp. 368-372, 26-28 March 2001.

- [32] A.S madhukumar, Francois Chin, *"An Efficient method for High-rate Data Transmission using Residue Number System based DS-CDMA"*, *IEEE*.
- [33] Rajak, A,R, *"The Performance of CDMA System with novel concatenated FEC Schemes in AWGN Chanel," AsianJ. Of Inf. Technol. Vol. 5, no. 10, pp. 1126-1130 2006.*
- [34] D. Cabric, Shridhar Mubaraq Mishra, Robert W. Brodersen, *"Implementation Issues in Spectrum Sensing for Cognitive radios"*, *Berkeley Wireless Research Centre, University of California, Berkeley..*
- [35] Volodymyr et.al *"Optimization in wireless CDMA Networks"*, *Report to IMA (2004).*
- [35] J. Proakis; *"Digital Communications," McGraw-Hill, 4 rd Edition, 2001.*
- [36] Ndubuisi.S., *Power system planning and Control Immaculate Publication, pp 15-18 (2002)*
- [37] <http://www.cs.tut.fi/kurssit/83080/CDMA.pdf> march 2011
- [38] D. Cabric, Shridhar Mubaraq Mishra, Robert W. Brodersen, *"Implementation Issues in Spectrum Sensing for Cognitive radios"*, *Berkeley Wireless Research Centre, University of California, Berkeley.*
- [39] Y. Ko and C. Tepedelenlioglu, *"Comparison of Adaptive Beamforming and Adaptive OSTBC with Outdated Channel Feedback," IEEE Conference Record of the Thirty-Eighth Asilomar Conference on Signals, Systems and Computers, vol. 1, 7-10, pp.1232 – 1236, Nov. 2004*
- [40] W. T. Webb, L. Hanzo, *"Modern QAM: Principles and Applications for Fixed and Wireless Channels," Pentech Press, London, 1994*
- [41] Nortel Network, , *"CDMA Technology Overview", February 2001*
- [42] Bernard Sklar, *"Rayleigh Fading channel in Mobile Digital Communication system part 1: Characterization", IEEE Communication Magazine, pp. 90-100,July 1997.*

- [43] T. J. Mouldsley, *"Throughput of High Speed Downlink packet Access for UMTS"*, Philips Research laboratories, 2002.
- [44] ZTE Corporation, *"Technical Specification of ZXC10 BSCB"*, Shenzhen P.R. China, 2006.
- [45] Dingli Communications Inc, *"Pilot Panorama User Guide"*, August 2004.
- [46] ZTE Cooperation, *"CDMA Principle"*, November 2006
- [47] Achim W., Kari S., Antti K., *" Remote Optimization of Antenna Subsystem Based on Radio Network Performance"*, Nokia Networks, 2001.
- [48] Y. H. Pan, K. Lataeif, Z. Cao, *"Dynamic Spatial Subchannel Allocation with Adaptive Beamforming for MIMO/OFDM Systems,"* IEEE Trans. Wireless Commun., vol. 3, pp. 2097-2107, Nov. 2004
- [49] T. Keller, L. Hanzo, *"Adaptive Modulation Techniques for Duplex OFDM Transmission,"* IEEE Trans. Vehicular Tech., vol. 49, pp.1893 – 1906, 2000
- [50] S. Catreux, V. Erceg, D. Gesbert, and R.W. Health, Jr., *"Adaptive Modulation and MIMO Coding for Broadband Wireless Data Networks,"* IEEE Communication Magazine, pp. 108-115, June 2002
- [51] S. Applebaum, *" Adaptive arrays,"* Technical Report SPL TR-66 001, Syracuse Univ. Rec., Corp. Report, 1965
- [52] B. Choi, L. Hanzo, *"Optimum Mode-Switching-Assisted Constant-Power Single and Multicarrier Adaptive Modulation,"* IEEE Trans. Vehicular Tech., vol. 52, pp. 536-560, May 2003.
- [53] Alpcan, T. et al. *"Power control for multicell CDMA wireless networks: by team optimization approach,"* in Proc. Of the Wiopt'05 workshop on modeling and optimization in mobile, Ad Hoc and Wireless Netw., pp-388 (2005).
- [54] http://www.ant.unibremen.de/teaching/atide/slides/part5_cd.ma.pdf

- [55] Medeisis ,and Kajackas “ *Use of the Universal Okumura Hata Propagation Prediction Model in Rural Area*” *Vehicular Technology Conference Proceedings, VTC Tokyo, Vol 3 pp 1818* (2000)
- [56] Siwiak, and Kazimierz, “ *Radio Propagation and Antenna for personal Communication*” *Artech House, Boston London* (1995).
- [57] <http://www.awe.communication.com/propagation/Rural/ho/index.htm>
- [58] *Proceedings of the world Congress on Engineering vol1 WCE London, UK 2008,*
- [60] Peticolas, W.L “ *Inelastic Light Scattering and the Raman effect* ” (1972)
- [61] Gupta V, Sharma. S.C and Bansal, M.C “ *Fringe Area Path loss Correction Factor for wireless communication* ” (2009)

APPENDIX A

APPENDIX A1

%%%%%%%%% PATHLOSS EXPONENT FORMULAR

%%%%%%%%%ENGR ALUMONA THEOPHILUS CREATED TODAY

%% =====
%% ALUMONA THEOPHILUS ECE DEPT UNIZIK
%%=====

%%%%%%%%% USING EQUATION

d = [0.1 0.2 0.3 0.4 0.5 0.6 0.7 0.8 0.9 1.0 1.1 1.2 1.3 1.4 1.5];%%
Reference distance in Km
LP = [107 109 111 114 116 118 119 121 122 124 126 127 128 131 137];%% Path
loss In dB
LP0 = 104;%%Ref Path Loss
g = sum(10*log10(d./do));
n = sum(LP-LP0)./g

APPENDIX A2

Configuration Interface of Classical Node Software showing Power Configuration ,QAM and QPSK Modulation Techniques and other parameters at the base station.

The screenshot displays the Classical Node Software Configuration Interface, which is divided into two main sections: 'Configure Radio Link - Browser' and 'Alarms and Status - Browser'.

Configure Radio Link - Browser

This section is divided into two columns, each representing a different radio link configuration.

Left Column (Pos 7):

- Terminal:** Terminal ID: 0065, Far End ID: 4288, Radio ID Check: ☒, Mode: 1+0.
- Capacity:** Enable XPSK: ☐, Adaptive Modulation: ☐, Channel Spacing (MHz): 28, Capacity - Modulation: 154 Mbit/s (v0) - 128-QAM, Number of E1s: 30, Packet Link Capacity (Config): 92.47 Mbit/s.
- RF:** Tx Freq. (MHz): 18629.00, Rx Freq. (MHz): 18637.00, Output Power Mode: Fixed (RTPC), Output Power (dBm): 17, Transmitter On: ☒.

Right Column (Pos 2):

- Terminal:** Terminal ID: 4288, Far End ID: 0065, Radio ID Check: ☒, Mode: 1+0.
- Capacity:** Enable XPSK: ☐, Adaptive Modulation: ☐, Channel Spacing (MHz): 28, Capacity - Modulation: 154 Mbit/s (v0) - 128-QAM, Number of E1s: 30, Packet Link Capacity (Config): 92.47 Mbit/s.
- RF:** Tx Freq. (MHz): 18637.00, Rx Freq. (MHz): 18629.00, Output Power Mode: Fixed (RTPC), Output Power (dBm): 17, Transmitter On: ☒.

Alarms and Status - Browser

This section displays the status of the radio terminals and provides options to manage traffic.

Near End Radio Terminal (Pos 7):

- Terminal ID: 0065, Transmitter On Ra1: ☒.
- Notifications On: ☒, Losses: Disabled.
- Restore Traffic:

Far End Radio Terminal (Pos 2):

- Name: URATTA, IP Address: 192.168.90.11, Terminal ID: 4288, Transmitter On Ra1: ☒.
- Notifications On: ☒, Losses: Disabled.
- Open Far End HSRL LINK Craft:
- Restore Traffic:

APPENDIX A3

Configuration Interface of Classical Node Software showing Power Configuration ,QPSK Modulation Techniques and other parameters at the base station.

Configure Radio Link

Near End Radio Terminal

Ra1
MMU2 C 1/6 (Pos 6)
RAU2 X 18/44 1/6.1

Terminal
Terminal ID 0065
Far End ID 4288
Radio ID Check ☒
Mode 1+0

Capacity
Capacity — Modulation 2x8 — C-QPSK

RF
Ra1
Tx Freq. (MHz) 18441.50
Rx Freq. (MHz) 18449.50
Output Power Mode Fixed (RTPC)
Output Power (dBm) 19
Transmitter On ☒

Far End Radio Terminal

Ra1
MMU2 C F6/1 (Pos 4)
RAU2 X 18/48 F6/L1.1

Terminal
Terminal ID 4288
Far End ID 0065
Radio ID Check ☒
Mode <Unknown>

Capacity
Capacity — Modulation 2x8 — C-QPSK

RF
Ra1
Tx Freq. (MHz) 18449.50
Rx Freq. (MHz) 18441.50
Output Power Mode Fixed (RTPC)
Output Power (dBm) 19
Transmitter On ☒

Advanced

Alarms and Status

Near End Radio Terminal

Pos 6
MMU2 C
RAU2 X 18/44
Tx 19
Rx -34.7
Transmitter On Ra1 ☒

Terminal ID 0065
Notifications On ☒
Loops Disabled
Restore Traffic

Far End Radio Terminal

Pos 4
RAU2 X 18/48
MMU2 C
Rx -34.7
Tx 19
Transmitter On Ra1 ☒

Name T-4288
Terminal ID 4288
Notifications On ☒
Loops Disabled
Open Far End MINE-LINK Craft
Restore Traffic

APPENDIX A4

Configuration of QAM and QPSK Modulation Techniques and other parameters at the base station



APPENDIX A5

Antenna Coupling and configuration at the base station



APPENDIX A6

Interface indicating the frequency band used,



APPENDIX A7

Configuration of the inverter section, to control the Generator, the battery bank and main power source from PHCN



APPENDIX A8

Antenna coupling completed ready to be mount to the mask



APPENDIX A9

Coupling the cable from the antenna to 2G and 3G radio



APPENDIX A10

Coupling of cable to 2G and 3G radios showing the signal arrestors



APPENDIX A11

3G interface showing the transmitter and receiver antenna interface



APPENDIX A 12

2G interface showing the transmitter and receiver antenna interface



APPENDIX A13

Testing of 3G radio completed and is working according to system specification.



APPENDIX A14

Testing of 2G radio completed and is working according to system specification.



APPENDIX A3

%%%%%%%%% SHADOW FACTOR AS DERIVED FROM EQUATION FOR URBAN

%%%%%%%%%ENGR ALUMONA THEOPHILUS CREATED TODAY

%% =====
%% ALUMONA THEOPHILUS ECE DEPT UNIZIK

```
LP = [107 109 111 114 116 118 119 121 122 124 126 127 128 131 137];%%  
pathloss in dB  
pr = [107 113 116 119 121 123 124 126 127 128 129 129 130 131 131];%%  
predicted pathloss  
b = (LP-pr).^2;  
c = sum(b)/15;  
d =sqrt(c)
```

APPENDIX B

APPENDIX B1

```
%% =====
%% ALUMONA THEOPHILUS LEONARD ECE DEPT UNIZIK
%% ===MATLAB PROGRAM TO COMPARE THE PATH LOSS OF MEASURED DATA OF QAM AND
%% QPSK WITH HATA MODEL CATEGORY A
%% =====
echo on
close all
%   distances measured in meters
d=[100:100:1500];
%   PATLOSS FOR QAM MODULATION

RSSI_1=[90 96 100 102 104 106 107 109 110 111 112 113 113 114 115];

%   PATLOSS FOR QPSK MODULATION

RSSI_2=[95 98 100 101 102 103 104 105 106 107 107 108 109 109 91];

%%%%%%PATLOSS FOR hata model
RSSI_3=[168 170 172 173 174 175 175 176 176 176 177 177 178 178 178];

plot(d,RSSI_1,'-gp');
hold on
grid on
xlabel('Distance in Meters')
ylabel('PATHLOSS (dB)')
plot(d,RSSI_2,'-b+');
plot(d,RSSI_3,'-r+');
title('PATHLOSS AGAINST DISTANCE')
legend('QAM MEASURED','QPSK MEASURED','HATA MODEL')
```

APPENDIX B2

```
%% =====
%% ALUMONA THEOPHILUS LEONARD ECE DEPT UNIZIK
%% ===MATLAB PROGRAM TO COMPARE THE PATH LOSS OF MEASURED DATA OF QAM AND
%% QPSK WITH COST 231 MODEL
%% =====
echo
on
close all
%   distances measured in meters
d=[100:100:1500];
%   PATLOSS FOR QAM MODULATION

RSSI_1=[ 90 96 100 102 104 106 107 109 110 111 112 113 113 114 115];
%   PATLOSS FOR QPSK MODULATION
RSSI_2=[ 91 95 98 100 101 102 103 104 105 106 107 107 108 109 109];
%%%%%%PATLOSS FOR hata model
RSSI_3=[ 173 176 178 179 180 181 82 183 184 184 184 185 185 185];

plot(d,RSSI_1,'-gp');
```

```

hold on
grid on
xlabel('Distance in Meters')
ylabel('PATHLOSS (dB)')
plot(d,RSSI_2,'-b+');
plot(d,RSSI_3,'-r+');
title('PATHLOSS AGAINST DISTANCE')
legend('16QAM MEASURED','QPSK MEASURED', 'COST 231 MODEL')

```

APPENDIX B3

```

%% =====
%% ALUMONA THEOPHILUS LEONARD ECE DEPT UNIZIK
%% ===MATLAB PROGRAM TO COMPARE THE PATH LOSS OF MEASURED DATA OF QAM AND
%% QPSK WITH FREE SPACE MODEL
%% =====

echo on
close all
% distances measured in meters
d=[100:100:1500];
% PATLOSS FOR QAM MODULATION

RSSI_1=[ 90 96 100 102 104 106 107 109 110 111 112 113 113 114 115];
% PATLOSS FOR QPSK MODULATION
RSSI_2=[ 91 95 98 100 101 102 103 104 105 106 107 107 108 109 109 ];

%%%%PATLOSS FOR hata model
RSSI_3=[ 79 85 88 91 93 95 96 97 98 99 100 101 102 103 ];
plot(d,RSSI_1,'-gp');
hold on
grid on
xlabel('Distance in Meters')
ylabel('PATHLOSS (dB)')
plot(d,RSSI_2,'-b+');
plot(d,RSSI_3,'-r+');
title('PATHLOSS AGAINST DISTANCE')
legend('16QAM MEASURED','QPSK MEASURED', 'FREE SPACE MODEL')

```

APPENDIX B4

```

%% =====
%% ALUMONA THEOPHILUS ECE DEPT UNIZIK
%% ===MATLAB PROGRAM TO COMPARE THE PATH LOSS OF MEASURED DATA OF QAM AND
%% QPSK WITH MODIFIED HATA MODEL FOR URBAN CATEGORY A
%% =====
%% =====

on
close all
% distances measured in meters
d=[100:100:1500];
% PATLOSS FOR QAM MODULATION

RSSI_1=[90 96 100 102 104 106 107 109 110 111 112 113 113 114 115];%
PATLOSS FOR QPSK MODULATION
RSSI_2=[[ 91 95 98 100 101 102 103 104 105 106 107 107 108 109 109 ]];
%%%%%%PATLOSS FOR hata model
RSSI_3=[99.81 101.81 103.81 104.81 105.81 106.81 106.81 107.81 107.81
107.81 108.81 108.81 109.81 109.81 109.81 ];
plot(d,RSSI_1,'-gp');
hold on
grid on
xlabel('Distance in Meters')
ylabel('PATHLOSS (dB)')
plot(d,RSSI_2,'-b+');
plot(d,RSSI_3,'-r+');
title('PATHLOSS AGAINST DISTANCE')
legend('16QAM MEASURED','QPSK MEASURED', 'MODIFIED HATA MODEL')

```

APPENDIX C

APPENDIX C1

```

%% =====
%% ALUMONA THEOPHILUS LEONARD ECE DEPT UNIZIK
%% ===MATLAB PROGRAM TO COMPARE THE PATH LOSS OF MEASURED DATA OF QAM AND
%% QPSK WITH HATA MODEL CATEGORY B
%% =====

```



```

%% =====
echo on
close all
%      distances measured in meters
d=[100:100:1500];
%      PATLOSS FOR QAM MODULATION

RSSI_1=[75 83 87 90 93 95 97 98 99 100 102 102 103 104 105];
%      PATLOSS FOR QPSK MODULATION
RSSI_2=[73 76 78 79 80 81 82 82 83 84 84 85 85 85 86];
%%%%%%PATLOSS FOR hata model
RSSI_3=[ 156 159 161 162 163 163 164 164 164 165 165 166 166 166 166 ];
plot(d,RSSI_1,'-gp');
hold on
grid on
xlabel('Distance in Meters')
ylabel('PATHLOSS (dB)')
plot(d,RSSI_2,'-b+');
plot(d,RSSI_3,'-r+');
title('PATHLOSS AGAINST DISTANCE')
legend('QAM MEASURED','QPSK MEASURED', 'HATA MODEL')

```

APPENDIX C2

```

%% =====
%% ALUMONA THEOPHILUS LEONARD ECE DEPT UNIZIK
%% ===MATLAB PROGRAM TO COMPARE THE PATH LOSS OF MEASURED DATA OF QAM AND
%% QPSK WITH HATA MODEL CATEGORY B
%% =====
%% =====
echo on
close all
%      distances measured in meters
d=[100:100:1500];
%      PATLOSS FOR QAM MODULATION

RSSI_1=[75 83 87 90 93 95 97 98 99 100 102 102 103 104 105 ];
%      PATLOSS FOR QPSK MODULATION
RSSI_2=[73 76 78 79 80 81 82 82 83 84 84 85 85 85 86];
%%%%%%PATLOSS FOR COST 231 model
RSSI_3=[175 178 180 181 182 183 183 184 185 185 185 186 186 186 187];
plot(d,RSSI_1,'-gp');
hold on
grid on
xlabel('Distance in Meters')
ylabel('PATHLOSS (dB)')
plot(d,RSSI_2,'-b+');
plot(d,RSSI_3,'-r+');
title('PATHLOSS AGAINST DISTANCE')
legend('QAM MEASURED','QPSK MEASURED', 'COST231 MODEL')

```

APPENDIX C3

```
%% =====
%% ALUMONA THEOPHILUS LEONARD ECE DEPT UNIZIK
%% ===MATLAB PROGRAM TO COMPARE THE PATH LOSS OF MEASURED DATA OF QAM AND
%% QPSK WITH HATA MODEL CATEGORY B
%% =====
%% =====

echo on
close all
% distances measured in meters
d=[100:100:1500];
% PATLOSS FOR QAM MODULATION

RSSI_1=[75 83 87 90 93 95 97 98 99 100 102 102 103 104 105];
% PATLOSS FOR QPSK MODULATION
RSSI_2=[73 76 78 79 80 81 82 82 83 84 84 85 85 85 86];
%%%%PATLOSS FOR FREE SPACE model
RSSI_3=[79 85 88 91 93 95 96 97 98 99 100 101 101 102 103];
plot(d,RSSI_1,'-gp');
hold on
grid on
xlabel('Distance in Meters')
ylabel('PATHLOSS (dB)')
plot(d,RSSI_2,'-b+');
plot(d,RSSI_3,'-r+');
title('PATHLOSS AGAINST DISTANCE')
legend('QAM MEASURED','QPSK MEASURED','FREE sapce MODEL')
```

APPENDIX C4

```
%% =====
%% ALUMONA THEOPHILUS ECE DEPT UNIZIK
%% ===MATLAB PROGRAM TO COMPARE THE PATH LOSS OF MEASURED DATA OF QAM AND
%% QPSK WITH MODIFIED HATA MODEL
%% =====
%% =====

close all
% distances measured in meters
d=[100:100:1500];
% PATLOSS FOR QAM MODULATION
RSSI_1=[75 83 87 90 93 95 97 98 99 100 102 102 103 104 105 ];
% PATLOSS FOR QPSK MODULATION
RSSI_2=[ 73 76 78 79 80 81 82 82 83 84 84 85 85 85 86 ];
%%%%PATLOSS FOR hata model
RSSI_3=[ 96.04 98.04 100.04 101.04 102.04 103.04 103.04 104.04 104.04104.04
105.04 105.04 106.04 106.04 106.04 ];
plot(d,RSSI_1,'-gp');
hold on
grid on
xlabel('Distance in Meters')
ylabel('PATHLOSS (dB)')
plot(d,RSSI_2,'-b+');
plot(d,RSSI_3,'-r+');
title('PATHLOSS AGAINST DISTANCE')
legend('QAM MEASURED','QPSK MEASURED','MODIFIED HATA MODEL for QPSK')
```


APPENDIX D

APPENDIX D1

```

%% =====
%% ALUMONA THEOPHILUS LEONARD ECE DEPT
%% =====MATLAB PROGRAM TO COMPARE THE RECEIVED SIGNAL STRENGTH AND BS=====
%% =====ANTENNA HEIGHT FOR THE VARIOUS EMPIRICAL PROPAGATION MODELS=====
%% =====
% Enter the operating frequency in MHz
f=2116.4;
% Enter the base station antenna height in meters
hb=20:2:38;
% Enter the distance between the transmitter and receiver in Km
d=10;
% Enter the mobile station antenna height in meters
hm=1.5;
F=2116.4;%operating frequency in MHz
% Enter the base station transmitter power in dBm
Pt=44.1;
% Enter the cable and connector losses in dB
A=3.5;
% Enter the correction factor in dB
ahm=(1.1*log(f)./log(10)-0.7)*hm-(1.56*log(f)./log(10)-0.8);
cf=3.2*(log(11.75*hm)./log(10))*(log(11.75*hm)./log(10))-4.97;
% Enter the Hata Okumura path loss model
PLokumura=69.55+26.16*log(f)./log(10)+(44.9-
6.55*log(hb)./log(10))*(log(d)./log(10))-13.82*log(hb)./log(10)-(ahm);
% Enter free space attenuation in dB
Afs=92.4+20*log(d)./log(10)+log(F)./log(10);
% Enter the basic median path loss in dB
Abm=20.41+9.83*log(d)./log(10)+7.894*log(F)./log(10)+9.56*(log(F)./log(10)).^
2;
% Enter the base station antenna gain factor in dB
Gt=log(hb/200)./log(10)*(13.958+5.8*log(d)./log(10)).^2;
% Enter the mobile station antenna gain factor in dB
Gr=(42.57+13.7*log(F)./log(10))*(log(hm)./log(10)-0.585);
% Enter the ECC-33 path loss model
PLECC33=Afs+Abm-Gt-Gr;
% Enter the COST-321 path loss model
PLCOST231=46.33+33.9*log(f)./log(10)-13.82*log(hb)./log(10)-ahm+(44.9-
6.55*log(hb)./log(10))*log(d)./log(10);
% The received signal strength using Hata Okumura model is calculated as
Prokumura=Pt+Gt+Gr-PLokumura-A;
% The received signal strength using ECC-33 model is calculated as
PrECC33=Pt+Gt+Gr-PLECC33-A;
% The received signal strength using COST-231 model is calculated as
PrCOST231=Pt+Gt+Gr-PLCOST231-A;
% Show the comparison between received signal strength and BS antenna
height for the various models
plot(hb,Prokumura,'-r*',hb,PrECC33,'-go',hb,PrCOST231,'-bp');
% Identify the models as Okumura Hata model,ECC-33 model and COST-231
% model
legend('Okumura Hata model','ECC-33 model','COST-231 model');
% label "Y-axis" as Received signal in dBm
ylabel('Received signal in dBm');
% Label "X-axis" as BS antenna height in m
xlabel('BS antenna height in m');

```

```
% Title the plot as the Received Signal Strength Vs BS antenna height for
the various path loss
% model
title('Received Signal Strength Vs BS antenna height for the various path
loss model');
grid on
```

APPENDIX D2

```
%% =====
%% ALUMONA THEOPHILUS ECE DEPT UNIZIK
%% ===MATLAB PROGRAM TO COMPARE THE PATH LOSS AND THE BASE STATION ANTENNA
%% ===HEIGHT FOR DIFFERENT PROPAGATION ENVIRONMENT=====
%% =====
'Enter the operating frequency in MHz';
f=2116.4;
'Enter the base station antenna height in meters';
hb=20:2:38;
'Enter the distance between the transmitter and receiver in Km';
d=10;
'Enter the mobile station antenna height in meters';
hm=1.5;
% The correction factor in dB for urban area is given as
j=2*((log(f*f/784)./log(10))-5.4);
cf1=3.2*(log((11.75*hm)./log(10)).^2)-4.97;
% The correction factor in dB for sub-urban area is given as
cf=3.2*(log(11.75*hm))*(log(11.75*hm))-4.97;
% The path loss the signal experienced in the urban area is given by the
model
Lpu=69.55+26.16*log(f)./log(10)+(44.9-
6.55*log(hb)./log(10))*(log(d)./log(10))-13.82*log(hb)./log(10)-(cf1)
% The path loss the signal experienced in sub-urban area is given by the
model
Lps_=69.55+26.16*log(f)./log(10)+(44.9-
6.55*log(hb)./log(10))*(log(d)./log(10))-13.82*log(hb)./log(10)-(cf)
Lps=Lps_-j;
% The path loss the signal experienced in the rural area is given by the
model
Lpr=Lpu-4.78*log(f*f)./log(10)+18.33*log(f)./log(10)-40.94;
% The path loss the signal experienced in free space is given by the model
Lpf=32.45+20*log(f)./log(10)+20*log(d)./log(10)+0*(log(hb)./log(10))
'Show the comparison between the path loss for the various environment and
the base station antenna height';
plot(hb,Lpf,'-m',hb,Lpr,'-go',hb,Lps,'-bh',hb,Lpu,'-rp')
'Label "Y-axis" as path loss in dB';
ylabel('pathloss in dB')
'Label "X-axis" as antenna height in m';
xlabel('Base station Antenna height in m')
% Title the plot as pathloss vs Base station Antenna height in different
propagation environment
title('pathloss vs Base station Antenna height in different propagation
environment')
'Identify them as free space, rural, sub-urban and urban';
legend('Free space','Rural','Sub-urban','Urban')
grid on
```

APPENDIX D3

```

%% =====
%% =====MATLAB PROGRAM TO COMPARE THE PATH LOSS FOR THE VARIOUS EMPIRICAL
%% =====PROPAGATION MODELS AND THE BS ANTENNA TILT=====
%% =====
'Enter the operating frequency in MHz';
f=2116.4;
'Enter the tilt angles in degree';
theta=0:0.2:7;
'Enter the base station antenna height in meters';
hb=30;
'Enter the mobile station antenna height in meters';
hm=1.5;
'The distance between the base station transmitter and mobile receiver in Km
is';
d=(hb-hm)./tan(theta);
F=2116.4;%Operating frequency in MHz
'Enter the correction factor in dB';
ahm=(1.1*log(f)./log(10)-0.7)*hm-(1.56*log(f)./log(10)-0.8);
cf=3.2*(log(11.75*hm)./log(10))*(log(11.75*hm)./log(10))-4.97;
'The Hata Okumura path loss model is';
PLokumura=69.55+26.16*log(f)./log(10)+(44.9-
6.55*log(hb)./log(10))*(log(d)./log(10))-13.82*log(hb)./log(10)-(ahm);
'Enter free space attenuation in dB';
Afs=92.4+20*log(d)./log(10)+log(F)./log(10);
'Enter the basic median path loss in dB';
Abm=20.41+9.83*log(d)./log(10)+7.894*log(F)./log(10)+9.56*(log(F)./log(10)).^
2;
'Enter the base station antenna gain factor in dB';
Gt=log(hb/200)./log(10)*(13.958+5.8*log(d)./log(10)).^2;
'Enter the mobile station antenna gain factor in dB';
Gr=(42.57+13.7*log(F)./log(10))*(log(hm)./log(10)-0.585);
'The ECC-33 path loss model is';
PLECC33=Afs+Abm-Gt-Gr;
'The COST-231 path loss model is';
PLCOST231=46.33+33.9*log(f)./log(10)-13.82*log(hb)./log(10)-ahm+(44.9-
6.55*log(hb)./log(10))*log(d)./log(10);
'Show the comparison between path loss for the various models and the tilt
angle';
plot(theta,PLokumura,'-bo',theta,PLECC33,'-g*',theta,PLCOST231,'-rp');
'Identify the models as Okumura Hata model,ECC-33 model and COST-231 model';
legend('Okumura Hata model','ECC-33 model','COST-231 model');
'label "Y-axis" as path loss in dB';
ylabel('Pathloss in dB');
'Label "X-axis" as Tilt angle in degree';
xlabel('Tilt angle in degree');
' Title it pathloss for various propagation model';
title('Comparison between path loss Vs Tilt angle');
grid on

```

APPENDIX D4

```
%% =====
%% ALUMONA THEOPHILUS LEONARD ECE DEPT UNIZIK
%% ===MATLAB PROGRAM TO COMPARE THE PATH LOSS AND THE BASE STATION ANTENNA=
%% ===HEIGHT FOR DIFFERENT EMPIRICAL PROPAGATION MODELS=====
%% =====
'BS antenna height ranging from 20m to 38m';
hb=[20 22 24 26 28 30 32 34 36 38];
% The path loss for each model from table 4.1
BSantennaheight=[165.23 164.87 549.78
    164.37 164.02 533.62
    163.60 163.25 518.87
    162.89 162.54 505.30
    162.23 161.88 492.74
    161.63 161.27 481.04
    161.06 160.70 470.10
    160.52 160.17 459.82
    160.02 159.66 450.13
    159.54 159.18 440.96];
% The bar chart representation is defined by the function
bar(hb,BSantennaheight,'grouped');
legend('Hata','COST-231','ECC-33');
ylabel('Path loss (dB)');
xlabel('BS antenna height (m)');
title('Effect of varying BS antenna height on path loss');
grid on
```

APPENDIX D5

```
%% =====
%% ALUMONA THEOPHILUS LEONARD
%% ===MATLAB PROGRAM TO COMPARE THE RECEIVED SIGNAL STRENGTH AND BS=====
%% ===TRANSMITTER POWER FOR THE VARIOUS EMPIRICAL PROPAGATION MODELS=====
%% =====
% Enter the operating frequency in MHz
f=2116.4;
% Enter the base station antenna height in meters
hb=30;
% Enter the distance between the transmitter and receiver in Km
d=10;
% Enter the mobile station antenna height in meters
hm=1.5;
F=2116.4;%operating frequency in MHz
% Enter the base station transmitter power in dBm
Pt=30:2:46;
% Enter the cable and connector losses in dB
A=3.5;
% Enter the correction factor in dB
ahm=(1.1*log(f)./log(10)-0.7)*hm-(1.56*log(f)./log(10)-0.8);
cf=3.2*(log(11.75*hm)./log(10))*(log(11.75*hm)./log(10))-4.97;
% Enter the Hata Okumura path loss model
```

```

PLokumura=69.55+26.16*log(f) ./log(10)+(44.9-
6.55*log(hb) ./log(10))*log(d) ./log(10)-13.82*log(hb) ./log(10)-(ahm);
% Enter free space attenuation in dB
Afs=92.4+20*log(d) ./log(10)+log(F) ./log(10);
% Enter the basic median path loss in dB
Abm=20.41+9.83*log(d) ./log(10)+7.894*log(F) ./log(10)+9.56*(log(F) ./log(10)).^
2;
% Enter the base station antenna gain factor in dB
Gt=log(hb/200) ./log(10)*(13.958+5.8*log(d) ./log(10)).^2;
% Enter the mobile station antenna gain factor in dB
Gr=(42.57+13.7*log(F) ./log(10))*(log(hm) ./log(10)-0.585);
% Enter the ECC-33 path loss model
PLECC33=Afs+Abm-Gt-Gr;
% Enter the COST-321 path loss model
PLCOST231=46.33+33.9*log(f) ./log(10)-13.82*log(hb) ./log(10)-ahm+(44.9-
6.55*log(hb) ./log(10))*log(d) ./log(10);
% The received signal strength using Hata Okumura model is calculated as
Prokumura=Pt+Gt+Gr-PLokumura-A;
% The received signal strength using ECC-33 model is calculated as
PrECC33=Pt+Gt+Gr-PLECC33-A;
% The received signal strength using COST-231 model is calculated as
PrCOST231=Pt+Gt+Gr-PLCOST231-A;
% Show the comparison between received signal strength and BS antenna
height for the various models
plot(Pt,Prokumura,'-r*',Pt,PrECC33,'-go',Pt,PrCOST231,'-bp');
% Identify the models as Okumura Hata model,ECC-33 model and COST-231
% model
legend('Okumura Hata model','ECC-33 model','COST-231 model');
% label "Y-axis" as Received signal in dBm
ylabel('Received signal in dBm');
% Label "X-axis" as BS transmitter power in dBm
xlabel('BS transmitter power in dBm');
% Title the plot as the Received Signal Strength Vs BS transmitter power
for the various path loss
% model
title('Received Signal Strength Vs BS transmitter power for the various path
loss model');
grid on

```

APPENDIX E

APPENDIX E1

```
%%
=====
=====
%% ALUMONA THEOPHILUS ECE DEPT UNIZIK
%% ===MATLAB PROGRAM TO COMPARE THE SNR OF MEASURED
DATA OF QAM, QPSK and GMSK MODULATION TECHNIQUE WITH
DISTANCE
%% =====
%%
=====
=====

close all
% distances measured in meters
d=[100:100:1500];
% snr FOR QAM MODULATION

RSSI_1=[ 16.73 16.54 16.34 16.03 15.81 15.57 15.45
15.20 15.06 14.78 14.49 14.32 14.17 13.64 12.33];
% SNR FOR QPSK MODULATION
RSSI_2=[16.99 16.87 16.54 16.24 16.03 16.24 15.81 15.69
15.57 15.45 15.45 15.06 14.93 14.78 14.48 ];
%%%%%snr FOR GMSK MODULATION
RSSI_3=[17.7 17.9 17.71 17.4 17.55 17.32 17.40 16.98
16.02 15.80 15.19 14. 13.0 11.76 12.30 ];
plot(d,RSSI_1,'-gp');
hold on
grid on
xlabel('Distance in Meters')
ylabel('SNR (dB)')
plot(d,RSSI_2,'-b+');
plot(d,RSSI_3,'-r+');
title('SNR AGAINST DISTANCE')
legend('MEASURED SNR QAM','MEASURED SNR QPSK',
'MEASURED SNR QPSK')
```

APPENDIX E2

```
%% ALUMONA THEOPHILUS ECE DEPT UNIZIK  
%% ===MATLAB PROGRAM TO COMPARE THE SNR OF MEASURED  
DATA OF QAM MODULATION TECHNIQUE WITH DISTANCE
```

```
d = [ 0.1 0.2 0.3 0.4 0.5 0.6 0.7 0.8 0.9 1.0 1.1 1.2 1.3 1.4 1.5];  
SNR = [17.72 17.57 17.17 17.17 16.54 16.13 16.13 16.03 15.81 15.58 14.93  
14.49 13.80 13.44 12.07];  
plot(d,SNR,'-r+')  
xlabel('distance'),ylabel('SNR')
```

APPENDIX E3

```
%% ALUMONA THEOPHILUS ECE DEPT UNIZIK  
%% ===MATLAB PROGRAM TO COMPARE THE SNR OF MEASURED  
DATA OF QPSK MODULATION TECHNIQUE WITH DISTANCE
```

```
d = [ 0.1 0.2 0.3 0.4 0.5 0.6 0.7 0.8 0.9 1.0 1.1 1.2 1.3 1.4 1.5];  
SNR = [18.64 18.52 18.45 18.39 18.33 18.33 18.23 18.20 18.07 18.00 17.64  
17.56 17.49 17.64 17.4 ];  
plot(d,SNR,'-b+')  
xlabel('distance'),ylabel('SNR')
```

APPENDIX F

APPENDIX 1

Figure 5.1 Performance of WCDMA system using QPSK in AWGN channel MATLAB CODES

```
EbNo = 0:2:12;
M = 4; % Use QPSK, so M = 4.
divorder = 60;
ber = berfading(EbNo, 'dpsk', M, divorder);
figure(41)
semilogy(EbNo, ber, 'b-*');
xlabel('Eb/No (dB)')
ylabel('Error Probanbility')
legend('Bit error rate')
title('Performance of WCMA system using QPSK in AWGN channel')
grid on
```


APPENDIX F2

Figure 5.2 Performance of W-CDMA system using QPSK in Multipath Fading channel at 60km MATLAB CODES

```
EbNo = 0:2:12;
M = 4; % Use QPSK, so M = 4.
divorder = 1;
ber = berfading(EbNo, 'dpsk', M, divorder);
figure(42)
semilogy(EbNo, ber, 'b-*');
xlabel('Eb/No (dB)')
ylabel('Error Probanbility')
legend('Bit error rate')
title('Performance of WCDMA system using QPSK in multipath fading channel at 60 kmph')
grid on
```

APPENDIX F3

Figure 5.3 Performance of W-CDMA system using QPSK in Multipath Fading channel at 90KMph

```
EbNo = 0:2:12;
M = 64; % Use QPSK, so M = 64.
divorder = 90;
ber = berfading(EbNo, 'dpsk', M, divorder);
figure(43)
semilogy(EbNo, ber, 'bo-');
xlabel('Eb/No (dB)')
ylabel('Error Probanbility')
legend('Bit error rate')
title('Performance of WCDMA system using QPSK in multipath fading channel for 90 kmph')
grid on
```

APPENDIX F4

Figure 5.4 Performance of W-CDMA system using QPSK in Multipath Fading channel at 120kmph

```
EbNo = 0:2:12;
M = 4; % Use QPSK, so M = 4.
divorder = 1;
ber = berfading(EbNo, 'oqpsk', M, divorder);
figure(44)
semilogy(EbNo, ber, 'b-*');
xlabel('Eb/No (dB)')
```

```

ylabel('Error Probanbility')
legend('Bit error rate')
title('Performance of WCDMA system using QPSK in multipath fading
channel at 120 kmph')
grid on

```

APPENDIX F5

Figure 5.5 Performance of W-CDMA system using 16QAM in AWGN

```

% Generate message signal of length >= M^L.
M = 16; % Alphabet size of modulation
L = 1; % Length of impulse response of channel
msg = [0:M-1 0]; % M-ary message sequence of length > M^L
% Modulate the message signal using baseband modulation.
modsig = qammod(msg,M); % Use 16-QAM.
Nsamp = 16;
modsig = rectpulse(modsig,Nsamp); % Use rectangular pulse shaping.
% Apply a transmit filter.
txsig = modsig; % No filter in this example
% Run txsig through a noiseless channel.
rxsig = txsig*exp(j*pi/180); % Static phase offset of 1 degree
% Use the semianalytic function.
num = ones(Nsamp,1)/Nsamp;
den = 1;
EbNo = [0:2:12]; % Range of Eb/No values under study
ber = semianalytic(txsig,rxsig,'qam',M,Nsamp,num,den,EbNo);
bertheory = berawgn(EbNo,'qam',M);
figure(45)
semilogy(EbNo,bertheory,'-bo');
title('Performance of WCDMA system using 16-QAM in AWGN');
legend('Bit error rate')
ylabel('Error Probanbility')
xlabel('Eb/No (dB)')
grid on

```

APPENDIX F6

Figure 5.6 Performance of W-CDMA system using 16QAM in Multipath Fading channel at 60kmph

```
EbNo = 0:2:12;
M = 16; % Use 16QAM,
divorder = 60;
ber = berfading(EbNo, 'oqpsk', M, divorder);
figure(46)
semilogy(EbNo, ber, 'rd-');
xlabel('Eb/No (dB)')
ylabel('Error Probanbility')
legend('Bit error rate')
title('Performance of WCDMA system using 16-QAM in multipath fading
channel at 60 kmph')
grid on
```

APPENDIX F7

Figure 5.7 Performance of W-CDMA in 2 Rays of in AWGN channel for 1 user. MATLAB CODES

```
x=[0 1 2 3 4 5 6 7 8 9 10];
y=[7.807500e-002 5.667000e-002 3.760000e-002 2.242000e-002 1.244500e-002
6.025000e-003 2.310000e-003 8.250000e-004 1.950000e-004 1.000000e-005
5.000000e-006];
n=5;
p=polyfit(x,y,n);
xi=linspace(0, 10, 100000);
yi=polyval(p, xi);
semilogy(x, y, '*', xi, yi, '-')
axis manual;
axis([0 10 0.000025 1]);
xlabel('EbNo');
ylabel('Bit Error Rate (BER)');
title('BER vs EBN0, Source Codes for Simulation of QPSK of WCDMA System
in AWGN Channel');
grid on
```

APPENDIX F8

MATLAB CODES for Performance Analysis of QPSK modulation technique of WCDMA in AWGN ,figure 5.8

```
coderate = 1/4; % Code rate
% Create a structure dspec with information about distance spectrum.
dspec.dfree = 10; % Minimum free distance of code
dspec.weight = [1 0 4 0 12 0 32 0 80 0 192 0 448 0 1024 ...
    0 2304 0 5120 0]; % Distance spectrum of code
EbNo = 3:0.5:12;

berbound = bercoding(EbNo,'conv','soft',coderate,dspec);
semilogy(EbNo,berbound) % Plot the results.
xlabel('E_b/N_0 (dB)'); ylabel('Error probability');
title('Performance of WCMA system using QPSK in AWGN channel');
grid on;
```

APPENDIX F9

Figure 6.9 Performance of W-CDMA in 2 Rays of in Multipath Rayleigh channels for 1 user for Doppler shift 60,90 and 120kmph

```
x=[0 2 4 6 8 10 12 14 16 18 20];
y=[1.394450e-001 1.022050e-001 7.264500e-002 4.871000e-002 3.247000e-002
2.098500e-002 1.463000e-002 9.440000e-003 6.305000e-003 4.580000e-003
3.070000e-003];
n=5;
p=polyfit(x,y,n);
xi=linspace(0, 20, 100000);
yi=polyval(p, xi);
semilogy(x, y, 'y', xi, yi, '-')
hold on;
x=[0 2 4 6 8 10 12 14 16 18 20];
y=[1.373200e-001 1.010650e-001 7.023000e-002 4.573000e-002 3.073500e-002
1.991500e-002 1.324500e-002 8.310000e-003 5.295000e-003 3.405000e-003
2.075000e-003];
n=5;
p=polyfit(x,y,n);
x90=linspace(0, 20, 100000);
y90=polyval(p, x90);
semilogy(x, y, 'b', x90, y90, '-')
hold on;
x=[0 2 4 6 8 10 12 14 16 18 20];
y=[1.396000e-001 1.041000e-001 7.285000e-002 4.999000e-002 3.354000e-002
2.218000e-002 1.444500e-002 9.390000e-003 6.200000e-003 3.970000e-003
2.715000e-003];
n=5;
p=polyfit(x,y,n);
x120=linspace(0, 20, 100000);
y120=polyval(p, x120);
semilogy(x, y, 'r', x120, y120, '-')
axis manual;
```

```

axis([0 20 0.0025 0.15]);
xlabel('EbNo');
ylabel('Bit Error Rate (BER)');
title('Codes for Simulation of QPSK of WCDMA System in Multipath
Rayleigh Fading Channel with Doppler Shift (60kmph, 90kmph & 120kmph)');
grid on

```

APPENDIX F10

Figure 5.10 Performance of W-CDMA in 2 Rays of in AWGN channel for 1 user. MATLABCODES

```

x=[0 1 2 3 4 5 6 7 8 9 10];
y=[7.807500e-002 5.667000e-002 3.760000e-002 2.242000e-002 1.244500e-002
6.025000e-003 2.310000e-003 8.250000e-004 1.950000e-004 1.000000e-005
5.000000e-006];
n=5;
p=polyfit(x,y,n);
xi=linspace(0, 10, 100000);
yi=polyval(p, xi);
semilogy(x, y, '*', xi, yi, '-')
axis manual;
axis([0 10 0.000025 1]);
xlabel('EbNo');
ylabel('Bit Error Rate (BER)');
title('BER vs EBN0, Source Codes for Simulation of QPSK of WCDMA System
in AWGN Channel');
grid on

```

APPENDIX F11

Figure 5.11 Performance comparison of W-CDMA in 2 Rays between AWGN and Multipath Rayleigh channel for 1 user

```

x=[0 1 2 3 4 5 6 7 8 9 10];
y=[7.807500e-002 5.667000e-002 3.760000e-002 2.242000e-002 1.244500e-002
6.025000e-003 2.310000e-003 8.250000e-004 1.950000e-004 1.000000e-005
5.000000e-006];
n=5;
p=polyfit(x,y,n);
xAWGNuser1=linspace(0, 10, 100000);
yAWGNuser1=polyval(p, xAWGNuser1);
semilogy(x, y, '*', xAWGNuser1, yAWGNuser1, '-')
hold on;
x=[0 1 2 3 4 5 6 7 8 9 10];
y=[1.448950e-001 1.240450e-001 1.073250e-001 9.064000e-002 7.641500e-002
6.300500e-002 5.071500e-002 4.142500e-002 3.251500e-002 2.597000e-002
2.059500e-002];
n=5;
p=polyfit(x,y,n);
xRayleighUser1=linspace(0, 10, 100000);
yRayleighUser1=polyval(p, xRayleighUser1);
semilogy(x, y, '+', xRayleighUser1, yRayleighUser1, '-')

```

```

axis manual;
axis([0 10 0.0000025 1]);
xlabel('EbNo');
ylabel('Bit Error Rate (BER)');
title('Source Codes for Simulation of QPSK of WCDMA System for AWGN vs
Multipath Rayleigh Fading Channel for a Single User');
grid on

```

APPENDIX F12

Figure 5.12 Performance comparison of W-CDMA in 2 Rays between AWGN and Multipath Rayleigh channel for 5 user

```

x=[0 2 4 6 8 10 12 14 16 18 20];
y=[9.468000e-002 5.656300e-002 2.938300e-002 1.367600e-002 5.393000e-003
1.932000e-003 5.520000e-004 7.200000e-005 4.000000e-006 0.000000e+000
0.000000e+000];
n=5;
p=polyfit(x,y,n);
xAWGNUser5=linspace(0, 20, 1);
yAWGNUser5=polyval(p, xAWGNUser5);
semilogy(x, y, '*', xAWGNUser5, yAWGNUser5, '-')
hold on;
x=[0 2 4 6 8 10 12 14 16 18 20];
y=[1.534370e-001 1.181230e-001 8.727300e-002 6.183000e-002 4.187500e-002
2.724800e-002 1.779900e-002 1.130700e-002 7.314000e-003 4.713000e-003
3.210000e-003];
n=5;
p=polyfit(x,y,n);
xRayleighUser5=linspace(0, 20, 100000);
yRayleighUser5=polyval(p, xRayleighUser5);
semilogy(x, y, '+', xRayleighUser5, yRayleighUser5, '-')
axis manual;
axis([0 20 0.0000025 1]);
xlabel('EbNo');
ylabel('Bit Error Rate (BER)');
title('Source Codes for Simulation of QPSK of WCDMA System for AWGN vs
Multipath Rayleigh Fading Channel for a Five (5) Users');
grid on

```

APPENDIX F13

Figure 5.13 Performance Comparison of 16QAM in W-CDMA system in AWGN

```
x=[0 2 4 6 8 10 12 14];
y=[2.819550e-001 2.674925e-001 2.555000e-001 2.496600e-001 2.480425e-001
2.489800e-001 2.500000e-001 2.502500e-001];
n=5;
p=polyfit(x,y,n);
xi=linspace(0, 14, 100000);
yi=polyval(p, xi);
semilogy(x, y, '*', xi, yi, '-')
axis manual;
axis([0 14 0.0000025 1]);
xlabel('EbNo');
ylabel('BER');
title('Source Codes for Simulation of 16-QAM of WCDMA System in AWGN
Channel');
grid on
```